DISSERTATION

THE VULNERABILITY OF PERMAFROST CARBON TO DECOMPOSITION AFTER THAW: EXPLORING CHEMICAL AND MICROBIAL CONTROLS

Submitted by

Jessica G. Ernakovich

Graduate Degree Program in Ecology

In partial fulfillment of the requirements

For the Degree of Doctor of Philosophy

Colorado State University

Fort Collins, Colorado

Summer 2014

Doctoral Committee:

Advisor: Matthew Wallenstein
Co-Advisor: Ken Reardon

Rich Conant
Mary Stromberger

ABSTRACT

THE VULNERABILITY OF PERMAFROST CARBON TO DECOMPOSITION AFTER THAW: EXPLORING CHEMICAL AND MICROBIAL CONTROLS

Climate change has increased temperatures at northern latitudes, resulting in a longer growing season, shifts in aboveground species composition, and extinctions in tundra ecosystems. The cryosphere is also shrinking, observed by the decline in sea ice, melting of glaciers, and thawing of permafrost (permanently frozen soil). Experts estimate that 47-61% of permafrost could be lost by 2100. Nearly a quarter of the Northern Hemisphere is underlain by permafrost and it contains almost 1700 Pg of organic carbon (C), twice as much as the atmosphere and nearly 200 times as much C as humans emit yearly from the burning of fossil fuels. The previously frozen C stored in permafrost is vulnerable to decomposition following thaw, which could increase greenhouse gas (GHG) emissions leading to a potential C-climate feedback. However the complexity and interactions of the mechanisms controlling the rate of GHG emissions from thawing permafrost make them difficult to predict.

Decomposition of soil organic matter is not merely the first order decay of a homogenous carbon pool, but rather a function of the microbial community, where different microorganisms specialize on carbon with different chemistry. Relatively little is known about the chemical composition of permafrost organic matter or the activity and diversity of the microbial community. The aims of my dissertation were to contribute knowledge to some of these unknowns, specifically: the chemical make-up of the organic matter in permafrost, the factors that structure the microbial community composition and diversity, how permafrost microbial function responds to a changing temperature regime, and the mechanisms that control CO_2 and

CH_4 production when permafrost thaws. I studied permafrost soils from Sagwon Hills, Alaska with the objective of exploring the complex interactions between microbial communities and soil organic matter chemistry, and the resulting production of greenhouse gases.

I assessed the chemical composition of permafrost using Fourier transformed mid-infrared spectroscopy (MidIR), and compared it to the chemistry of the seasonally thawed active layer soils. I found that the there is more chemically labile C in the organic component of the active layer than the top of the permafrost (0-5 cm below the maximum active layer thaw), which in turn has more labile C than the mineral active layer and deeper permafrost. All the soils have evidence of processed material, but the compounds are different between the organic active layer and the permafrost and mineral active layer soils. This type of detailed chemical analysis of permafrost soils could decrease the uncertainty of the role of permafrost in the global carbon cycle by increasing our understanding of the availability of these carbon compounds to decomposition.

I assessed the abiotic factors that drive community assembly in permafrost and active layer soils by analyzing the bacterial community composition and diversity using analysis of the 16S rRNA gene. I found that diversity was higher in the active layer than the permafrost, even in the mineral active layer, which has similar pH and carbon content as the permafrost. The community structure was also different between the active layer and the permafrost. The organic and mineral active layers were most similar to each other, and the permafrost soils were similar. Relationships between richness and structure with depth and soil C content suggest that both environmental filtering and historical community legacy dictate the current permafrost community structure. This work showed that permafrost is a fundamentally different

environment than the active layer, and therefore it harbors a microbial community distinct from the active layer.

I characterized the functional diversity of permafrost and active layer microbial communities by assessing substrate-use richness, substrate preference, growth rate and substrate specific growth rate using 31 substrates with an EcoPlate^{TM} (Biolog, Inc.) assay at three incubation temperatures (1, 10, and 20 °C). I used a kinetic approach, wherein the microbial response to each substrate was modeled with a modified logistic growth function. Growth rates of permafrost microbial communities were less than or equal to the organic active layer at every temperature, including the 1 °C incubation temperature. All communities increased their growth rates with temperature, indicating that the highest incubation temperature (20 °C) was below their temperature optima. The organic active layer used more substrates than the permafrost and mineral active layer microbial communities at every temperature, and the number of substrates used increased with temperature for the permafrost and mineral active layer. These results indicate that permafrost microbial communities may not respond rapidly to changes in the permafrost temperature regime immediately following thaw.

In my final dissertation chapter, I investigated the mechanisms controlling CO_2 and CH_4 production from thawed permafrost with a laboratory incubation under oxic and anoxic conditions at 1 and 15 °C. While CO_2 production was greater than CH_4 production under all treatments, I observed that CH_4 production was much more variable than anaerobic CO_2 production, which is well supported in the literature. CH_4 production is the terminal step in the anaerobic conversion of fresh detritus to gas, and can be inhibited by the activity of anaerobes higher on the redox ladder or substrate limited. Using a combination of biogeochemical tools, carbon chemistry analysis and statistical modeling, I found evidence for both limitations to

methanogenesis. I propose that the variability in CH_4 can be attributed to the many processes required by a consortium of anaerobic microorganisms to enable methanogenesis, and that this complexity needs to be considered in estimating CH_4 production rates.

In summary, my dissertation work suggested that GHG production at temperatures close to 0 °C, which are field relevant immediately following thaw, can be substantial (up to 1%; anoxic: 0.08-1.06%; oxic: 0.13-0.63%). Thus, the constraints on aerobic and anaerobic decomposition are important for understanding the mechanisms controlling the potential positive C-climate feedback due to permafrost thaw. My work suggests that the microbial community likely limits CO_2 production rather than by the chemical recalcitrance of the organic matter, because the organic matter in the top of the permafrost was chemically labile and readily decomposable at higher temperatures, while the functional diversity of the microbial community was low. I identified that both a historical and environmental filter reduced the permafrost microbial taxonomic diversity, which could explain the low functional diversity and thus the low GHG production. The process of CH_4 production appears to have additional complexity, and to be controlled by the consortium of anaerobic microorganisms that gain more energy from their metabolism than methanogens, but that also supply the substrates needed for methanogenesis. This work exemplifies the complex interactions between permafrost microbiology and chemistry that contribute to the production of GHG production from permafrost. Our current tools to predict GHG production from permafrost thaw do not include these types of controls, and continued research in this area will enable better predictions of the C-climate feedback from thawing permafrost. Future work should test these mechanisms in more sites, with different timescales, and with the explicit aim to include these mechanisms in models of permafrost C loss.

ACKNOWLEDGEMENTS

I have many people to thank for their help along my path. First, my advisor Matt Wallenstein helped me to think in a new way. When I started this program, I barely knew what biogeochemistry was, but he believed in me anyway and I am grateful for that. From the start, Matt was good at asking questions that pushed me and made me feel that he valued my answer. His laidback nature allowed me the time to explore new avenues on my own, but he always was very committed to helping me flesh out my ideas, whether on paper for a fellowship proposal or over an Americano on the way to the ski hill. Ken Reardon stepped in as my co-advisor early in my program, and he always kept me true to my roots as a chemist and ensured that I explained concepts in a tangible way rather than using euphemisms or other tools that are commonly used when a concept is not fully understood.

I am also grateful to my other committee members, Rich Conant and Mary Stromberger. Rich invited me to participate in many side projects, including reading his grant proposals and doing parts of small experiments. I appreciated these opportunities to expand my science greatly. Mary taught a class that I took my first semester, and much of my fundamental understanding of microbiology can be attributed to her teaching. In addition, she entrusted a couple of lectures a year to me for that course; developing my ideas into a framework for teaching was very helpful. Although not an official committee member, Francisco Calderon helped me significantly, not only in the collection of the data for chapters 2 and 5 of my dissertation, but also in the development of my ideas.

There are a few graduate students who helped me greatly in my learning progression at CSU. My first lab mate, Meg Steinweg, was not only the person who taught me how to do much of the microbial work that I did, but she also allowed me to bounce ideas off of her for every

experiment, even after she had graduated. Sarah Evans, another lab mate, was always pushing the boundaries and always made me think. My current officemate, Shinichi Asao always forced me to clarify my thinking. He was direct and told me when he didn't think my idea was interesting or novel, which made me dig deeper and write better manuscripts. Lastly, Kelly Hopping and I worked for years on a manuscript outside of our dissertation work, and her commitment to the project will forever mold my perception of a wonderful co-author and collaborator.

I would also like to thank the entire "Belowground" lab group, who meet weekly to discuss each other's science and always provide thoughtful and helpful comments. People spoke their minds, and the criticism was very constructive. I would especially like to thank Francesca Cotrufo, Claudia Boot and Ed Hall, whose consistently insightful comments made me push my work to a different level. I would also like to note that NREL is a unique place to be a graduate student. I appreciate being respected as a peer by the senior scientists. I believe this had made me hold my own opinions in higher regard and be a better scientist.

Of course, the sampling, lab work, and analysis were not done alone. Thank you to Shawna McMahon for sampling with me in the field. It was hard work for two of us to collect all this permafrost, but we had a blast. Thank you to the EcoCore Analytical Services team, specifically Dan Reuss and Colin Pinney for their help setting up my final incubation with the octopus of hoses and regulators for flushing the incubation jars. Thanks to Guy Beresford, who helped me during my early struggles in proteomics and pushed me to learn the proper methods of molecular biology. Thank you to two friends who generously gave their personal time to help me in the lab: Barbara Fricks and Kirstin Holfelder, the latter of whom also built me a database to manage the data for chapter 4. By giving their time, they also gave their support. Thank you to

Paul Brewer for your help with the collection of the gas data. And thanks to Jenny Rocca and Akihiro Koyama for help in the analysis of the diversity data. Thank you to the 15 undergraduates who worked on my project over the years, but specifically to Alisa Challenger and Claire Freeman. Thank you to Ann Hess in the CSU Statistics Laboratory for many consultations about my statistics and help building code to run many of the models used in chapters 4 and 5.

Thank you to the National Science Foundation, who funded this work through a fellowship (Graduate Research Fellowship Program) and a "Dissertation Improvement Grant," as well as award number 0733074, and to the Department of Energy, who funded this work through Global Change Education Program. Thank you to the Graduate Degree Program in Ecology for molding me as an ecologist through seminars and classes. Many thanks to Jeri Morgan for helping me navigate through the process.

Lastly, I would like to sincerely thank all my family and friends, who supported me emotionally through this process. Mom and Dad- your untiring commitment to personal growth inspired me to be my best self. I appreciate that I always know that you support me, and the time you gave me to help take care of Clark was amazing. And to Drew- I know this was a long haul, but you always approached it with grace. Thank you for your unwavering support— knowing you were behind me always made me feel strong.

TABLE OF CONTENTS

Chapter 1: Introduction

Permafrost soils contain roughly twice the amount of carbon (C) as is stored in the atmosphere, just within the frozen component, with additional C stored in the organic component closest to the surface (Kuhry et al., 2009; Schuur et al., 2008; Tarnocai et al., 2009). Although permafrost thaw and formation is a naturally dynamic process, increasing temperatures in the Arctic have increased permafrost degradation in recent years and decades (Nelson et al., 2002; Osterkamp and Romanovsky, 1999; Romanovsky et al., 2010; 2012; Shiklomanov et al., 2013; Vaughan et al., 2013). It was once presumed that these vast stores of organic matter would be protected from mineralization because there was no active or viable microbial community, and that the microbes within permafrost were ancient relics. However, both culture studies and molecular investigations into the microorganisms within permafrost have revealed that these microbes are active and poised to become part of modern biogeochemical cycles (Rivkina et al., 2004). In addition, mineralization rates of permafrost organic matter indicate that the organic matter is highly labile (Lee et al., 2012; Waldrop et al., 2010).

The field of permafrost biogeochemistry has changed rapidly during the course of my Ph.D. studies. As I began asking these questions, the literature was filled mostly with results about microbial physiology from culture studies from two great Russian scientists, Elizaveta Rivkina and David Gilichinsky, with a few emerging studies of the microbial community (Shi et al., 1997). Concurrently, our ability to perform whole community sequencing has rapidly advanced our understanding of the genetic diversity and in some cases even the potential functional diversity of the microbial communities within these frozen soils (Mackelprang et al., 2011; Mondav et al., 2014; Tuorto et al., 2014).

A handful of incubation studies (Dutta et al., 2006; Zimov et al., 2006) were the only estimates of the potential C release from permafrost, and these have now been joined by an increasing number (i.e. Knoblauch et al., 2013; Lee et al., 2012; Waldrop et al., 2010 and synthesized by Schädel et al., 2014; Treat et al., 2014). However, the majority of the incubation studies to investigate the lability of the potential C pool in permafrost-affected soils only manipulate the active layer and not the permafrost itself (Schädel et al., 2014; Treat et al., 2014). Thus, estimates of C lability and future C release are really only based on a small number of studies (i.e. Dutta et al., 2006; Knoblauch et al., 2013; Lee et al., 2012; Waldrop et al., 2010). In addition, these incubations do not always represent a realistic field condition, which is acceptable if the objective is to push the system and explore the decomposability of organic matter, but if the intention is to inform models for potential C loss, they may provide overestimates. Lastly, decomposition of permafrost C can occur via aerobic or anaerobic pathways, depending on water inundation after permafrost thaw. There are even fewer studies that have investigated the potential CH_4 release from permafrost and the mechanisms controlling it (i.e. Knoblauch et al., 2013; Lee et al., 2012; and see Treat et al., 2014 for a synthesis).

Therefore, I set out to answer these four questions:

(1) What is the chemical make-up of the organic matter in permafrost, and how is it similar or different from the soils in the seasonally thawed active layer?

(2) Do abiotic factors structure the permafrost and the active layer microbial communities similarly?

(3) How will microbial community function respond to a changing temperature regime?

(4) When permafrost thaws, what mechanisms control whether CO_2 or CH_4 is produced?

In the following chapters, I investigate these questions through a mixture of natural history and manipulative approaches in permafrost collected at Sagwon Hills, Alaska.

References

Dutta, K., Schuur, E.A.G., Neff, J.C., Zimov, S.A., 2006. Potential carbon release from permafrost soils of Northeastern Siberia. Glob Change Biol 12, 2336–2351. doi:10.1111/j.1365-2486.2006.01259.x

Knoblauch, C., Beer, C., Sosnin, A., Wagner, D., Pfeiffer, E.-M., 2013. Predicting long-term carbon mineralization and trace gas production from thawing permafrost of Northeast Siberia. Glob Change Biol 19, 1160–1172. doi:10.1111/gcb.12116

Kuhry, P., Ping, C.-L., Schuur, E.A.G., Tarnocai, C., Zimov, S., 2009. Report from the International Permafrost Association: carbon pools in permafrost regions. Permafrost Periglac. Process. 20, 229–234. doi:10.1002/ppp.648

Lee, H., Schuur, E.A.G., Inglett, K.S., Lavoie, M., Chanton, J.P., 2012. The rate of permafrost carbon release under aerobic and anaerobic conditions and its potential effects on climate. Glob Change Biol 18, 515–527. doi:10.1111/j.1365-2486.2011.02519.x

Mackelprang, R., Waldrop, M.P., DeAngelis, K.M., David, M.M., Chavarria, K.L., Blazewicz, S.J., Rubin, E.M., Jansson, J.K., 2011. Metagenomic analysis of a permafrost microbial community reveals a rapid response to thaw. Nature 480, 368–371. doi:10.1038/nature10576

Mondav, R., Ben J Woodcroft, Kim, E.-H., McCalley, C.K., Hodgkins, S.B., Crill, P.M., Chanton, J., Hurst, G.B., VerBerkmoes, N.C., Saleska, S.R., Hugenholtz, P., Rich, V.I., Tyson, G.W., 2014. Discovery of a novel methanogen prevalent in thawing permafrost. Nature Communications 5, 1–7. doi:10.1038/ncomms4212

Nelson, F.E., Anisimov, O.A., Shiklomanov, N.I., 2002. Climate change and hazard zonation in the circum-Arctic permafrost regions. Natural Hazards 26, 203–225.

Osterkamp, T.E., Romanovsky, V.E., 1999. Evidence for warming and thawing of discontinuous permafrost in Alaska. Permafrost Periglac. Process. 10, 17–37.

Rivkina, E., Laurinavichius, K., McGrath, J., Tiedje, J., Shcherbakova, V., Gilichinsky, D., 2004. Microbial life in permafrost. Advances in Space Research 33, 1215–1221. doi:10.1016/j.asr.2003.06.024

Romanovsky, V.E., Smith, S.L., Christiansen, H.H., 2010. Permafrost thermal state in the polar Northern Hemisphere during the international polar year 2007-2009: a synthesis. Permafrost Periglac. Process. 21, 106–116. doi:10.1002/ppp.689

Romanovsky, V.E., Smith, S.L., Christiansen, H.H., Shiklomanov, N.I., Streletskiy, D.A., Drozdov, D.S., Oberman, N.G., Kholodov, A.L., Marchenko, S.S., 2012. Permafrost, in: Jeffries, M.O., Richter-Menge, J.A., Overland, J.E. (Eds.), Arctic Report Card 2012.

Schädel, C., Schuur, E.A.G., Bracho, R., Elberling, B., Knoblauch, C., Lee, H., Luo, Y., Shaver, G.R., Turetsky, M.R., 2014. Circumpolar assessment of permafrost C quality and its vulnerability over time using long-term incubation data. Glob Change Biol 20, 641–652. doi:10.1111/gcb.12417

Schuur, E.A., Bockheim, J., Canadell, J.G., Euskirchen, E., Field, C.B., Goryachkin, S.V., Hagemann, S., Kuhry, P., Lafleur, P.M., Lee, H., 2008. Vulnerability of permafrost carbon to climate change: Implications for the global carbon cycle. BioScience 58, 701–714.

Shi, T., Reeves, R.H., Gilichinsky, D.A., Friedmann, E.I., 1997. Characterization of viable bacteria from Siberian permafrost by 16S rDNA sequencing. Microb Ecol 33, 169–179.

Shiklomanov, N.I., Streletskiy, D.A., Little, J.D., Nelson, F.E., 2013. Isotropic thaw subsidence in undisturbed permafrost landscapes. Geophys. Res. Lett. 40, 6356–6361. doi:10.1002/2013GL058295

Tarnocai, C., Canadell, J.G., Schuur, E.A.G., Kuhry, P., Mazhitova, G., Zimov, S., 2009. Soil organic carbon pools in the northern circumpolar permafrost region. Global Biogeochem. Cycles 23, GB2023. doi:10.1029/2008GB003327

Treat, C., Natali, S., Ernakovich, J., Iversen, C., Lupascu, M., McGuire, A.D., Norby, R., Chowdhury, T.R., Richter, A., Santruckova, H., Schadel, C., Schuur, T., Sloan, V., Turetsky, M., Waldrop, M., 2014. Controls on CH4 and CO2 production from permafrost soil carbon under saturated conditions. Glob Change Biol.

Tuorto, S.J., Darias, P., McGuinness, L.R., Panikov, N., Zhang, T., HÃggblom, M.M., Kerkhof, L.J., 2014. Bacterial genome replication at subzero temperatures in permafrost 8, 139–149. doi:10.1038/ismej.2013.140

Vaughan, D.G., Comiso, J.C., Allison, I., Carrasco, J., Kaser, G., Kwok, R., Mote, P., Murray, T., Paul, F., Ren, J., Rignot, E., Solomina, O., Steffen, K., Zhang, T., 2013. Observations: Cryosphere (No. 5). Cambridge University Press, Cambridge, United Kingdom and New York, NY, USA.

Waldrop, M.P., Wickland, K.P., White, R.I., Berhe, A.A., Harden, J.W., Romanovsky, V.E., 2010. Molecular investigations into a globally important carbon pool: permafrost-protected carbon in Alaskan soils. Glob Change Biol 16, 2543–2554. doi:10.1111/j.1365-2486.2009.02141.x

Zimov, S.A., Davydov, S.P., Zimova, G.M., Davydova, A.I., Schuur, E.A.G., Dutta, K., Chapin, F.S., III, 2006. Permafrost carbon: Stock and decomposability of a globally significant carbon pool. Geophys. Res. Lett. 33, L20502. doi:10.1029/2006GL027484

Chapter 2: The Chemical Properties of Alaskan Permafrost and Seasonally Thawed Soils

Introduction

Sixteen percent of the terrestrial northern hemisphere is underlain by permafrost (Kuhry et al., 2009), which contains four times more C than the global vegetation and twice as much as the atmosphere (Kuhry et al., 2009; Lee et al., 2012; Schuur et al., 2008; Tarnocai et al., 2009). Permafrost temperatures are rising (Hinzman et al., 2005; Osterkamp and Romanovsky, 1999; Romanovsky et al., 2012), and permafrost degradation and thaw have already been observed (ACIA, 2004; Osterkamp and Romanovsky, 1999). As permafrost thaws and drains, this C may be decomposed and released to the atmosphere as carbon dioxide (CO_2) and methane (CH_4), resulting in a positive feedback with climate warming.

The vulnerability of soil organic matter (SOM) to decomposition is dependent on complex interactions between the constituents of the soil ecosystem, including physical, chemical, and biological components in soils (Schmidt et al., 2011). Thus, organic matter (OM) chemistry plays a central role in determining decomposability, and it is important that we better understand the chemical complexity of the organic compounds stored in permafrost soils. The chemistry of OM affects the temperature sensitivity of decomposition (Conant et al., 2008; Davidson and Janssens, 2006), and microbial taxa tend to specialize on metabolizing specific substrates (Goldfarb et al., 2011; Jones et al., 2009; Wallenstein et al., 2007). Thus, a catalog of the types of C compounds will help us improve predictions of C release from permafrost soils.

Incubation studies and chemical analyses indicate that the C in permafrost can decompose quickly. Incubations have shown that permafrost OM has equal (Lee et al., 2012) or greater (Waldrop et al., 2010) lability than OM from the overlying, seasonally-thawed active

layer soils. In addition, Waldrop *et al.* (2010) observed that permafrost SOM was more labile than active layer SOM in three permafrost soils, based on nuclear magnetic resonance (NMR) and on the yield of dissolved organic carbon (DOC) and total dissolved nitrogen (TDN) during decomposition.

Soil carbon to nitrogen (C/N) ratios have been a useful predictor of decomposability in a variety of soils. It is generally accepted that lower C/N ratios indicate that soils have undergone greater microbial processing, and are therefore less labile (Chapin et al., 2002). Permafrost C/N ratios are lower than or equal to the C/N ratios of organic-rich, active layer soils (Lee et al., 2012; Waldrop et al., 2010), which would indicate that permafrost SOM is more decomposed. The results from bulk soil C/N analysis contradict results from incubations, DOC and TDN yield, and NMR studies, which all indicate that permafrost SOM is more labile than active layer SOM. This suggests that standard soil metrics, such as C/N, are not sufficient indicators of permafrost SOM chemistry.

Fourier transformed mid-infrared spectroscopy (MidIR) enables the analysis of the functional groups that make up SOM as well as soil minerals without chemical extraction (Baes and Bloom, 1989; Bornemann et al., 2010; Haberhauer and Gerzabek, 1999; Janik et al., 2007; Nguyen et al., 1991), and can be used as a semi-quantitative tool to detect differences in C or N functional groups in SOM (Calderón et al., 2013). The high OM content of the permafrost and overlying active layer soils may result in relatively low interference of mineral absorbance bands on the spectral interpretation of organic bands. In addition, oxidation of the SOM followed by subtraction of the resultant mineral spectrum from the corresponding whole-soil spectrum can be used to resolve OM spectral features from the mineral bands (Cox et al., 2000; Sarkhot et al., 2007), but cautious interpretation is required because artifacts of degradation of clay minerals

can occur after heating soils (Reeves, 2012). Using the whole-soil spectra and those acquired through spectral subtraction in tandem can increase the ability to interpret changes in SOM chemistry with MidIR. The degree of decomposition in SOM can also be assessed using a ratio of two MidIR regions that represent functional groups indicative of chemically labile and recalcitrant compounds (Artz et al., 2006; Calderón et al., 2006; Haberhauer et al., 2000; 1998). Analysis of the vibrational response of SOM to MidIR radiation by probing the spectra in these ways, therefore, provides valuable information into the functional characteristics of the chemical constituents of SOM.

The objective of this study was to catalogue the functional groups that comprise permafrost SOM and compare them to the active layer. I hypothesized that the permafrost contains an organic C molecular signature consistent with chemical preservation due to continuously frozen temperatures and likely anoxic conditions. Additionally, I hypothesized that the organic horizon of the active layer contains a mixture of SOM from recently added plant residue and more decomposed SOM. MidIR was carried out on bulk permafrost and active layer soils (henceforth called “whole-soil”), and then on the mineral component following OM removal using two methods— ashing at high temperature or chemical oxidation— to be able to characterize the organic component through spectral subtraction. Additionally, I investigated the efficacy of OM removal during ashing and chemical oxidation to evaluate the use of spectral subtraction as a tool for Arctic soils and other C rich soils. This in-depth understanding of the similarities and differences between the chemical make-up of permafrost and active layer SOM will decrease the uncertainty of the role of permafrost in the global C cycle.

Materials and Methods

Description of the study site and soil sampling

Organic active layer (OAL), mineral active layer (MAL), and permafrost soils were collected from Sagwon Hills, Alaska (N 69° 25' 32.190" W 148° 41' 38.731", 288 m above sea level). The soils were collected from under moist acidic tundra vegetation and are classified as Ruptic Histic Aquiturbels (Borden et al., 2010). The permafrost at Sagwon Hills is of loess origin over gravel deposits (Borden et al., 2010). Cores were collected from 15 plots representative of the site and covering 150 m^2. The seasonally thawed active layer had a depth of 26.8 $\pm$ 1.3 cm in August of 2009, and consisted of an organic and mineral horizon with evidence of cryoturbation (Fig. 2.1 a). The organic horizon of mildly decomposed plant material (peat) with many fine roots was between 5 and 14 cm in depth. The remainder of the active layer was visibly gleyed mineral soil with no additional horizonation. In two plots, a buried organic horizon was visible. In these cases, samples were taken from the mineral soil not in the buried organic horizon. At each plot, the active layer was removed and placed on a tarp as a monolith (Fig. 2.1 a). OAL and MAL soils were sampled from the monolith from the center of their respective depths (OAL: ~2 cm, MAL: ~10 cm). Permafrost soils were obtained as cores using a Tanaka auger fitted with a Sipre soil coring bit (Jon's Machine Shop, Fairbanks, Alaska) (Fig. 2.1b). Permafrost cores were collected to between 30-47 cm below the thaw depth, where glacial till restricted deeper sampling.

The samples were stored on dry ice in the field, at -20 °C during my eight day collection period at Toolik Biological Field Station, and then brought back to the Colorado State University EcoCore laboratory on dry ice where they were stored at -10 °C during processing and storage.

Soil sample processing

Permafrost cores were processed in a walk-in -10°C freezer. First, they were scraped under aseptic conditions to remove any possible field contamination from sub-surface water flow or active layer plant material. Permafrost samples were then separated into approximately 5 cm increments (Fig. 2.1 b), however if there was a natural fracture point at an ice lens within 2 cm of the 5cm fracture point, that point was chosen. Finally, homogenization of the permafrost and organic and mineral active layer soils was carried out on frozen soil by crushing the soils with a hammer while double wrapped in sterile plastic bags inside canvas bags to resemble soils homogenized with a 2 mm sieve. The samples were dried at 55°C for 36 hours, ground with a mortar and pestle, and stored in 20mL glass scintillation vials until analysis. For OAL, n=12; MAL, n=9; permafrost 0-5 cm (below the maximum active layer thaw depth), n=15; 6-10 cm, n=15; 11-15 cm, n=15; 16-20 cm, n=14; 21-25 cm, n=12; 26-30 cm, n=8; 31-35 cm, n=4; 36-40 cm, n=2. The number of replicates varied as a function of active layer samples lost during processing and inability to collect deep cores at some sites.

MidIR spectra were collected on both whole-soil samples and samples after removal of the OM by ashing or hypochlorite treatment. To remove the OM with ashing, 4g samples were placed in crucibles in a furnace at 550°C for 3h. Removal of SOM with hypochlorite was based on the method first described by Anderson (1961). Briefly, 4 g soil were thoroughly mixed with sodium hypochlorite (25 mL 6% w/w, pH 9.5) and incubated in a hot-water bath to allow oxidation (15 min, 80°C). Solutions were centrifuged (15 min at 1081 RCF) and the supernatant discarded. This was repeated twice for a total of three treatments. Soils were then washed twice with ddH2O (20 mL, 15 min at 1081 RCF), allowed to air-dry, and briefly re-ground to

homogenize air-dried crusting. Total C loss was measured with a C/N Analyzer (ECS 4010 Costech Analyzer).

Chemical Analysis

Soil C and N

The dried and ground soils (0.10 - 0.21g, depending on C content) were analyzed for total C and N content using a LECO Tru-SPEC elemental analyzer (Leco Corp., St. Joseph, MI). Due to the high SOM content of the OAL soils, a C and N standard of mixed grass was used. For mineral soils with relatively less OM, an agricultural soil standard from Sidney, Nebraska was used.

MidIR

All dried and ground soil samples (both whole soils and after ashing) were scanned undiluted (neat) in the mid-infrared region on a Digilab FTS 7000 Fourier transform spectrometer (Varian, Inc., Palo Alto, CA) with a deuterated, Peltier-cooled, triglycine sulfate detector and potassium bromide beam splitter. The spectrometer was fitted with a Pike AutoDIFF diffuse reflectance accessory (Pike Technologies, Madison, WI) and potassium bromide was used as background. Data was obtained as pseudo-absorbance (log [1/Reflectance]). Spectra were collected at 4 cm^{-1} resolution, with 64 co-added scans per spectrum from 4000 to 400 cm^{-1}. Duplicate scans of each sample were performed and included in the multivariate analyses. All spectral averages were calculated using GRAMS/AI software, Version 9 (Thermo Galactic, Salem, NH). All of the soils were scanned before and after ashing, and before and after oxidation with sodium hypochlorite oxidation method.

Statistical Analyses

Soil C and N

Differences between the means of the C content, N content, and C to N ratio of each depth increment was determined using an analysis of variance (ANOVA) with a mixed model (PROC MIXED, SAS version 9.2, Cary, NC, USA) with a Tukey Honestly Significant Difference (HSD) multiple comparison adjustment ($p<0.05$). The model included depth as a fixed effect, and each core was treated as a random effect. The data were log transformed to satisfy the ANOVA model assumptions of equal variance.

MidIR

The sample set of "whole-soils" consisted of 106 samples, which included the OAL, MAL, and all permafrost depths. There were also 106 ashed samples to correspond with each of the whole-soil samples, as well as a subset of hypochlorite-oxidized samples. Spectral differences between the depths were determined by Principle Components Analysis (PCA) using the *PLS Plus*/IQ software in GRAMS/AI Ver. 9 (Thermo Galactic, Salem. NH). All spectra were mean-centered and were pre-treated with multiplicative scatter correction before the PCA analyses. The PCA scores were used for dimensionality reduction, while the component loadings were used to indicate which spectral bands explained the distribution of the sample scores along the principle components. The spectral subtractions of ashed or oxidized spectra from whole-soil sample spectra were carried out with GRAMS/AI software. Correlations of whole-soil and ashed or oxidized spectra with soil C and N were performed in GRAMS/AI. Because of the distribution of C contents in the sample set including OAL soils (Fig. 2.2), I performed a multivariate

analysis of the mineral samples in absence of the OAL to increase the resolution between the MAL and permafrost soils.

Spectral band ratios

Ratios of spectral regions (in 50 x 10^6 cm^{-1} or 2nm increments) were analyzed in order to determine if an "index of decomposition" (Artz 2006) exists in these soils. I explored ratios proposed by Artz et al. (2006), Haberhauer et al. (1998) and Calderón et al. (2006). Differences by depth were determined using an ANOVA with a mixed effect model (PROC MIXED, SAS version 9.2, Cary, NC, USA) with a Tukey Honestly Significant Difference (HSD) multiple comparison adjustment ($p<0.05$).

Results

Soil C Content

The soils analyzed for this study had a wide range of C contents, from less than 30 g C kg dry weight $soil^{-1}$ (dws) in the deepest permafrost to more than 450 mg C g dws^{-1} in the OAL soils to (Fig. 2.2 a). The OAL soils had nearly three times the amount of C compared to the mineral active layer (MAL) soils and soils collected from the top of the permafrost (Fig. 2.2 a). Carbon content varied between permafrost soils depending on how far they were from the maximum active layer thaw boundary. The permafrost layers within the top 15 cm had greater C content than the deeper permafrost layers (Fig. 2.2 a). The deepest permafrost layers (16-40 cm) had less C than all the layers above them, and this was significantly different (alpha<0.05) from the OAL soil and the top of the permafrost (0-15 cm), but not from the MAL soil.

Soil N Content

The N content ranged from 1 mg N g dws^{-1} in the deepest permafrost samples to nearly 19 mg N g dws^{-1} in the OAL. Similar to soil C content, the OAL soil had considerably more N than any of the mineral layers, including the MAL soil and all the permafrost layers (Fig. 2.2 b). The MAL and the top 25 cm of the permafrost had similar total N, while the deepest permafrost layers collected (26-40 cm) had less N. There was a gradual decline in soil N content in the permafrost soil profile starting at the 16-20 cm core, which became significant at the deepest depth (36-40 cm).

Soil C/N Ratios

The C/N ratio of the OAL soil (27.4 $\pm$ 0.8) was greater than the MAL and permafrost layers (Fig. 2c). The MAL had the lowest mean C/N (16.6 $\pm$ 0.9), however it was not significantly different from the C/N for the permafrost layers. The deepest permafrost layer (36-40 cm) had greater C/N (21.9 $\pm$ 1.2) than the shallower permafrost layers, but this difference was not significant.

Active layer and permafrost average spectra

Given the statistical difference in soil C between the 0-15 cm permafrost (which is henceforth called the "top of the permafrost") and 16-40 cm permafrost (which is called "deeper permafrost) (Fig. 2.2 a), spectral averages for the whole-soil spectra were calculated for these layers, as well as for the OAL and MAL (Fig. 2.3). The absorbance at 3620 cm^{-1} indicated a greater clay content in the permafrost and MAL samples (Table 2.1) than the OAL soils. The greater absorbance at the 3400 cm^{-1} OH/NH region (Table 2.1) in the OAL may be due to root

growth and recent addition of light fraction plant material (Calderón et al., 2011 a). Greater absorbance at 2930-2850 cm^{-1} and 1470-1370 cm^{-1} in the OAL samples indicated higher amounts of aliphatic CH bonds in this soil (Table 2.1). These bands are associated with high SOM content, and are also known to decrease during OM decomposition (Huang et al., 2006; Janik et al., 2007). The spectral features between 2000-1770 cm^{-1} and the inversion band between 1226-1070 cm^{-1} suggest that the permafrost samples had greater quartz absorbance than the OAL soils, as expected from the lower C content. All soils had a feature at 1730 cm^{-1}, which is a band for aromatic C=C found in resistant soil C fractions and lignin (Calderón et al., 2011b; Cox et al., 2000), but could also include C=O absorbance from a variety of functional groups (Table 2.1). The OAL had a peak at 1655-1615 cm^{-1}, whereas the rest of the layers had a peak at 1610 cm^{-1} (Fig. 2.3). This difference suggested that the OAL had increased influence of amide I absorbance, but the rest of the layers had relatively more aromatic C=C absorbance (Table 2.1). This assertion was supported by the greater absorbance of amide III (shoulder at 1320-1220 cm^{-1}) in the OAL and the aromatic C-H bending region (from 950-750 cm^{-1}). The MAL and the shallower permafrost had a shoulder at 1370 cm^{-1} that is absent in the 16-40 cm permafrost (Fig. 2.3). This region contains bands for phenolic and carboxylate C-O stretching, C-H, N-H, C-N and O-H deformation, and my results showed it to be sensitive to the decreased C and N content of the deeper permafrost (Fig. 2.2 a and b). The deeper permafrost had a peak at 1420 cm^{-1} that was not as abundant in the top of the permafrost, suggestive of polysaccharide CH_2, protein CH_2, C-H or C-O (Table 2.1). Due to the relative abundance of other peaks representing these compounds, 1420 cm^{-1} was likely due to aliphatics or carbohydrates.

Principle Components Analysis of the whole-soil (no oxidation) spectra

Principle components analysis (PCA) of the whole-soil spectra showed separation of the OAL soils from the permafrost and MAL along the first component (Fig. 2.4 a). Permafrost and MAL soils had low component 1 scores, while OAL soils had larger component 1 scores (Fig. 2.4 b). Component 1 loadings showed that the samples from the permafrost and MAL soils absorbed at the sand and clay bands more than the OAL soils (Fig. 2.4 b), which was consistent with the average spectral data (Fig. 2.3). Component 1 loadings also showed that the OAL soils are distinguished by absorbance of the organic bands at 3400 cm^{-1}, 2850-2930 cm^{-1}, 1740 cm^{-1}, 1225 cm^{-1}, and 1093 cm^{-1}, which indicated that OAL soils have greater concentrations of OH/NH, aliphatics, carbonyls, amide III, and esters (Table 2.1) than the permafrost and MAL soils. The permafrost and the MAL soils were partially separated along the third component (Fig. 2.4 a). Loadings indicated that the MAL soils absorbed more than the permafrost at 2850-2930 cm^{-1} (aliphatic CH bonds), 1740 cm^{-1} (aromatic material), and 1045 cm^{-1} (carbonyl bonds). The presence of aliphatic and carbonyl bonds suggest that the MAL soils contain more easily degradable, lower mean residence time C than the permafrost. The permafrost absorbed more than the MAL soils at 3630 cm^{-1}, and a broad area between 1554-1412 cm^{-1}. These results suggested that the permafrost soils contain greater clay content than the MAL soils. However, the absorbance at 1045 cm^{-1} in MAL soils could be due to clay absorbance.

Analysis of soil OM through spectral subtraction: comparison of organic removal techniques

In order to identify organic features of the spectra in the permafrost and active layer samples in the absence of the mineral background (Fig. 2.5), I assessed two OM removal techniques— oxidation with heat (ashing) and chemical oxidation (hypochlorite treatment).

Comparing the spectra after ashing and chemical oxidation showed the bias introduced by incomplete hypochlorite oxidation of the organic material in the OAL spectra and the artifacts from the heating of clays in the ashing treatment (Fig. 2.6). Proportionally more C was left unoxidized in the OAL relative to the other layers due to the large amount of initial C content, however total C removal was greater than other studies (Siregar et al., 2005). The hypochlorite oxidation C removal ranged from 78.9 percent in the OAL samples to 91 percent in the MAL samples. The hypochlorite-treated OAL soils retained the aliphatic CH band at 2850-2930, the amide I band at 1655, and the band at 1330 cm^{-1} for carboxylate C-O (Table 2.1). The subtractions produced from the hypochlorite oxidation of permafrost and MAL produced better spectra than for the OAL, likely because they have lower OM content and thus did not suffer from incomplete oxidation of the organic material. The high temperature used to ash the soils caused deformation (rounding) of the clay peak at 3620 cm^{-1}, which was not observed after the hypochlorite oxidation (Figs. 7 and 8). Both ashing and subtraction enhanced the band near 2515 cm^{-1} in the deeper permafrost (16-40 cm), which is typically attributed to carbonates. However, due to the low pH of these soils, this diffuse "shoulder" was likely due to O-H of H-bonded carboxylic acids (Piccolo et al., 1992) that remained after oxidation. The silicate inversion band at 1225-1075 cm^{-1} was enhanced with both types of OM removal, but especially in the ashed treatment. The peak at 810 cm^{-1}, representing pure silica (Calderón et al., 2011a), was apparent in the soils after both oxidation treatments. After spectral subtraction, the hypochlorite treated OAL showed a negative peak at 3620 cm^{-1}, possibly due to washing off of clays (Fig. 2.7). Despite the potential for artifacts due to clay heating in the ashing procedure, the inadequate removal of OM from these soils in the hypochlorite oxidation indicated that the ashing technique was the better tool in these OM-rich soils. However, comparisons between the resultant spectra

from the two methods allowed me to identify regions in the ashed spectra (in addition to those proposed by Reeves et al. 2012) that posed additional challenges to interpretation (e.g. 3630, 1415, 1331,1225-1075 and 810 cm^{-1}).

Analysis of soil OM after spectral subtraction (post-ashing of soil)

The spectral subtractions of ashed soils from whole-soils showed that active layer and permafrost soils differed in the amount and type of OM (Fig. 2.5). The OAL soil had greater absorbance at 3400, 2850-2930, 1730, 1600 and 1350 cm^{-1} than the MAL soil or permafrost. The spectral assignments of 3400, 2850-2930, and 1730 were described previously (Table 2.1). The compounds that absorbed at 1350 cm^{-1} may indicate more labile C, as it was found previously to be greater in the particulate organic matter (POM) fraction than the silt-size fraction (Calderón et al., 2011b), and was also in greater abundance in shallow soils than in deeper soils (Calderón et al., 2011a). Given its POM origins and ester C-O assignment, 1350 cm^{-1} could also reflect C-O bonds of polymers in litter, such as lignin, the presence of which was confirmed by the absorbance of the lignin C-O bond in the OAL at 1190-1000 cm^{-1}. Thus, 1350 cm^{-1} may have been representative of relatively non-decomposed, low mean residence time OM.

The samples from the permafrost and MAL had peaks not found in the OAL, such as 1510 cm^{-1} and 1420 cm^{-1}. Both lignin and amides absorb at 1510 cm^{-1} (Movasaghi et al., 2008; Reeves, 1993). The band at 1420 cm^{-1} can be due to the presence of many functional groups, including C-O bonds and phenolic C-O, the bending of C-H bonds observable in aliphatics, polysaccharides, aromatic compounds, and protein (Calderón et al., 2013; 2011b; Movasaghi et al., 2008), and O-H deformation. Absorbance at 1424 cm^{-1} was found to increase during

decomposition (Chen et al., 2010), indicating that the 1420 peak I observed may be composed of material chemically resistant to decomposition.

Correlation of spectral bands and sample C and N content

The spectral data and the C and N content were highly correlated (R>0.8) for the regions between 3520-3240, 2850-2930, 1760-1650 and 1270-1047 cm^{-1} (Fig. 2.8, top panel), organic regions including the OH/NH stretch, aliphatics, proteins and amides, and carbohydrates (Table 2.1). The band at 1230 cm^{-1} can indicate the presence of highly processed C with a high mean residence time and is characteristic of the clay-associated OM (Calderón et al., 2011b), but it can also be a clay mineral band. Because a high correlation to C or N content was not observed with the 3620 cm^{-1} clay band, the 1230 cm^{-1} region was likely due to the absorbance of organic material rather than the clay mineral. Negative correlations were found with mineral bands near 3620, 1970-1870, and 805 cm^{-1}. Bands associated with proteins at 1650 and 1550 cm^{-1} had slightly larger R scores for the correlation with percent N compared to the correlation with percent C. The region between 1390-1545 cm^{-1}, traditionally thought to be within the MidIR organic fingerprint region, was less correlated to total soil C than would be expected from the various organic assignments in this region (Table 2.1).

Correlations of the organic spectral components obtained through subtraction of the ashed spectra from the whole-soil (unashed) spectra with percent C and percent N (Fig. 2.8, bottom panel) followed a similar pattern to the correlations using the whole-soil (unashed) spectra (Fig. 2.8, top panel). The only exception was that the correlation with total N is greater than the correlation with total C between 2200 to 3400 cm^{-1}.

PCA of the MAL and permafrost samples

The MidIR spectral properties of the permafrost samples were different from the MAL samples (Fig. 2.9 a). The top of the permafrost (0-15 cm) and deeper permafrost (16-40 cm) layers were separated along Component 1. Loadings indicate that the soils from the top of the permafrost had more absorbance at 3400, 2850-2930, 1690-1740, and 1240 cm^{-1}, and the deeper permafrost had more absorbance of 3620, 2515, 1795, 1487 and 810 cm^{-1}. The co-occurrence of 1795 and 810 cm^{-1} indicated that the deeper permafrost has greater amounts of silicates, which was confirmed by the high loadings for clay at 3620. Component 2 loadings showed that the MAL samples were characterized by absorbance at 1320 and 2850-2930 cm^{-1} and less absorbance at 2515 and 1480 cm^{-1} (Fig. 2.9 b) than the permafrost soils.

Spectral band ratios

The trends of the spectral band ratios fell into four major categories: (1) the ratios decreased with depth except for the top of the permafrost, which fell between the OAL and the MAL; (2) the ratios decreased with depth with the exception of the MAL samples, which had the lowest ratios; (3) there was no predictable trend with depth; and (4) the ratios decreased with depth with no exceptions (Table 2.2). The ratio of 2930 to 1734, 1653, 1600, and 1510 cm^{-1} fell into the first category (Table 2.2). The ratios of 1734 to 897 and 3400 to 1510 cm^{-1}also showed the same pattern. The ratios of 3400 to 1653 and 1600, and 1600 and 1653 to 897 cm^{-1} fell into the second scenario. Similarly, although this trend was not predictable by depth, the MAL soils were the most depleted in1510 cm^{-1} relative to 897. I found no trend for the ratios 1734 to 1600 or 1510 and 1653 to 1600 or 1510. One ratio (1600 to 1510) fit into the fourth type of result.

Discussion

Analysis of chemical make-up of permafrost and active layer soils

Arctic soils, including organic, mineral and permafrost soil horizons, contain large amounts of C and N, which could be relatively non-decomposed due to energetic constraints on decomposition, including frozen conditions in permafrost (Sannel and Kuhry, 2009; Schirrmeister et al., 2011; White et al., 2004). Generally in the active layer, the organic horizon is composed of OM that is considerably less decomposed than in the mineral, active layer soils (White et al. 2004). Therefore, I expected to observe a chemical signature indicative of newly added plant residues in the active layer, especially in the OAL. Organic matter present in the active layer also undergoes decomposition, albeit slowly due to low summer temperatures and anoxia (Hobbie et al., 2000), so I expected to also observe a chemical signature of more decomposed SOM than in the permafrost. In the permafrost, I expected to observe fresh, preserved OM through the depth profile. MidIR spectroscopy can be used to identify organic functional groups in soils. Due to the reactivity of different functional groups, inferences can be made about the lability of the constituents of SOM and whether they are newly added compounds or whether they have undergone microbial processing (e.g.(Artz et al., 2006; Calderón et al., 2011b; Haberhauer et al., 1998). Overall, I found that all the soil depths contained signatures of labile OM, but that there was considerably more in the OAL than the permafrost and MAL soils. All the soils also contained spectral features indicative of previously processed and resistant materials, indicating that decomposition had occurred in all these soils including permafrost. Relative to the deeper permafrost, the top of the permafrost contained a greater amount of several organic C functional groups— including OH/NH, aliphatics, carboxylates, esters and amides— which would likely be labile to decomposition.

In this study, I observed that the OAL soils at Sagwon Hills have much greater C and N content than the mineral soils, including both the MAL and permafrost. Soil C content was greater in the top 15 cm of the permafrost than in permafrost found 16-40 cm from the maximum active layer thaw depth. Nitrogen also showed this trend, although the results were not statistically significant. These C and N results are consistent with the values found by Lee et al. (2012) for sites in a similar geographic region, but C content is roughly ten times greater than those of Siberian mineral permafrost (Schirrmeister et al., 2011).

C/N ratios indicate the degree of microbial processing that has occurred in soils, with high C/N indicating less decomposed material and lower C/N indicating previous microbial processing. The C/N values in this study were similar to those from other permafrost samples on the North Slope of Alaska (Lee et al., 2012), but were greater than those observed in Siberian coastal permafrost by Schirrmeister et al. (2011). Like Lee et al. (2012), I found the C/N ratio of the OAL was greater than the MAL and permafrost soils, which were similar. This suggests that mineralization of OM in permafrost has occurred, either before the permafrost was formed or suggests that decomposition occurs despite the frozen conditions in permafrost. Schirrmeister et al. (2011) postulated that permafrost C content and C/N ratios are dependent on how much non-decomposed OM was incorporated at the time of permafrost formation. In addition, end products of decomposition (such as CO_2 and CH_4) have been observed, indicating that decomposition can, indeed, occur *in situ* despite the frozen conditions (Michaelson et al., 2011; Rivkina et al., 1998; 2004). Thus, the lower C/N ratios of the permafrost likely are due to both mechanisms.

The whole-soil spectra and the “organic component” obtained through spectral subtractions show that the OAL and permafrost samples differ in their amount of OM, but generally have similar types of organic functional groups. For both the spectral averaging and the

PCA of the whole-soil spectra, the permafrost depths were grouped corresponding to the significant difference in soil C content. Calderón et al. (2011b) found that bands with absorbance at 3400, 2870-2930, 1223 cm^{-1} are indicative of low mean residence time OM, decreasing rapidly upon incubation. The absorbance in these regions in both the whole-soil (unoxidized) spectra and the "organic spectra" was greater for the OAL soil than the MAL and permafrost soils, confirming that the OAL had greater OM content and more non-decomposed organic materials. The permafrost soils did, however, absorb in these regions confirming that they also contain non-decomposed material.

Analysis of the MidIR spectral properties of the soils in absence of the OAL illuminated differences between permafrost and the MAL, as well as differences between the permafrost depths. Compounds of mixed reactivity separate the MAL from the permafrost, indicating that the MAL contained both chemically labile and recalcitrant compounds. The top of the permafrost contained more organic compounds labile to decomposition (OH/NH, aliphatics, carboxylates, esters and amides) than deeper permafrost. The presence of these compounds in greater abundance in the top of the permafrost suggests that these compounds are depleted in the deeper permafrost during decomposition. Assuming the controls on decomposition are the same in the top and the deeper permafrost, decomposition must also then occur in the top of the permafrost. Therefore, the greater amount of these labile organic compounds in the top of the permafrost suggests that fresh OM is introduced to the permafrost. This could occur through cryoturbation, diffusion of less processed DOM carried over the permafrost via subsurface flow, or through syngenetic permafrost formation where the bottom of the MAL, which is possibly richer with DOM than the middle of the MAL where I sampled, is incorporated into the permafrost during

cold years. This could also be a relic of previous depth trends of decomposition before glaciation and retreat resulted in stores of OM as permafrost.

This was also supported by the analysis of band ratios, which can show small changes in the OM pool that cannot be detected by PCA or bands alone. Previous studies have explored these ratios as 'indices of decomposition' (Artz et al., 2006; Haberhauer et al., 1998) to identify which bands decrease or accumulate over the course of incubation or with depth (Table 2.2). Given my initial hypothesis, I expected that ratios of labile to recalcitrant OM would decrease with depth in the active layer. Due to preservation of OM in permafrost, I expected the ratios to remain constant through the permafrost depths and that they would be greater than the MAL, but lower than the OAL, as the OAL soils have continuing new OM inputs. Most of the ratios of labile to recalcitrant bands fit into two scenarios: (1) OAL>top of permafrost>MAL>deeper permafrost and (2) OAL>top of permafrost >deeper permafrost>MAL. Both of these scenarios confirm that the OM in the OAL has the most labile material relative to the other layers, and that the MAL has less than at least the top of the permafrost. However, the relative abundance of labile compounds to recalcitrant compounds was not the same through the permafrost and was greater for the top of the permafrost than deeper permafrost.

The spectra of the OAL and permafrost soils also showed evidence of processed material. 1730 and 1600 cm^{-1} are regions found to persist in soils or increase during decomposition (Calderón et al., 2011b; 2006; Haberhauer et al., 1998), and thus likely represent chemically recalcitrant compounds such as humic compounds (Cox et al., 2000). However, absorbance at 1730 cm^{-1} is merely indicative of C=O bonds, which can be found in many different types of molecules, such as esters and ketones, but also in aromatic compounds, such as phenols. The OAL has absorbance at 1730 cm^{-1} and it is clear from the whole-soil spectra and PCA loadings

that the presence of this material contributes to the differences between the OAL, MAL, and permafrost soils. Spectral subtractions indicated that the MAL and top of the permafrost also have some absorbance at 1730 cm^{-1}, and loadings from the PCA where the OAL was omitted indicate that 1730 cm^{-1} is more abundant in the MAL than the permafrost layers, indicating a larger amount of decomposition in the active layer. The band at 1600 cm^{-1} has been observed to increase during incubation (Calderón et al., 2011b) and has been identified as aromatic C=C, phenolics (Bornemann et al., 2010; Nuopponen et al., 2006) or carboxylates (Artz et al., 2006; Haberhauer et al., 1998). In the whole-soil spectra, the two permafrost layers had a distinct peak at 1600 cm^{-1}, whereas the OAL absorbance declined. However, after spectral subtraction, none of the spectra appeared to have absorbance at 1600 cm^{-1}. When 1600 and 1510 cm^{-1} are both present in soils, this can lend support to the presence of more aromatic material such as lignin (Calderón et al., 2011b; Reeves, 1993). However, 1510 is due to compounds with different chemistries and reactivities— either amide II or C=C (Movasaghi et al., 2008). Haberhauer et al. (1998) found that this region is correlated to total soil C and that absorbance in this region decreases from litter to mineral soil, indicating that compounds that absorb at 1510 are labile to decomposition, and Reeves (1993) found that while absorbance at 1510 is mainly due to lignin, N remaining after extraction can cause a broadening in this region. Spectral subtraction showed that the top of the permafrost had the highest absorbance in this region, followed by deeper permafrost and MAL soils. This indicated that the top of the permafrost had the least decomposition of compounds that absorb in this region (e.g. lignin or amide II). Alternatively, the similar trend between the 1600 and 1510 cm^{-1} could indicate that the permafrost had accumulated more processed, resistant material than the OAL.

MidIR as a tool to investigate the properties of OM in high C content soils

Not only can soil properties, such as C content, N content, and C/N ratios be predicted by mid-infrared spectroscopy and regression tools (Viscarra Rossel et al., 2006) and references within), but spectroscopy also provides a measure of the "quality" and chemical composition of OM stored in soils (Calderón et al., 2011b) beyond the information extracted out of bulk C, N and C/N measurements. The high (R>0.8) and positive correlation of C and N content with the organic bands at 3400 cm^{-1}, 2850-2930 cm^{-1}, 1740-1700 cm^{-1}, 1650 cm^{-1}, 1550 cm^{-1}, 1230 cm^{-1}, and 1100 cm^{-1} confirmed that MidIR can be used to understand basic SOM properties. All these bands are observed in diverse soils, with relatively labile C absorbing at 3400 and 2850-2930 cm^{-1} and compounds of varied decomposability absorbing in the "fingerprint region" between 1750-1100 cm^{-1} (Calderón et al., 2011b).

Soils contain both organic and mineral components, both of which absorb in the MidIR region. The organic component of soils is the biologically active portion, so MidIR analysis of the organic component would inform our understanding of the relative reactivities of the SOM in active layer and permafrost soils. Unfortunately, extractions to isolate the organic material in soils are wrought with challenges, as most of these extractions require strong bases, acids, or organic solvents, each of which can change the chemical make-up of the organic material. The organic component of soils can be analyzed using MidIR regions with minimal overlap of organic and mineral absorbances (Reeves, 2012) or through spectral subtraction (Calderón et al., 2011b). Subtracting a MidIR spectrum of the mineral component from the whole-soil spectrum produces a spectrum representative of the organic component of each soil (Calderón et al., 2011b; Parikh et al., 2013). I obtained mineral spectra through two methods for removing the organic component—oxidation with heat (ashing) and chemical oxidation with hypochlorite.

Upon heating, clays can deform, causing changes to the spectra that could be misleading after spectral subtraction (Reeves, 2012). Nevertheless, bands between 1750–1600 cm^{-1} and 3000–2800 cm^{-1} are thought to be free of these artifacts (Reeves, 2012). In hypochlorite oxidation, clay deformation can be avoided because samples are not heated. Therefore, I expected hypochlorite oxidation to produce results with less changes due to mineral deformation. However, chemical oxidation did not fully remove the organic component of the OAL. Although clays were less affected by the hypochlorite treatment than in the ashing treatment, the incomplete and variable oxidation of organic material in the hypochlorite treatment makes the ashing a more effective treatment for these soils with high C content.

To analyze the spectra after ashing without clay heating artifacts, I used the comparison of the ashing and hypochlorite treatments to identify regions with clay heating interference. Reeves et al. (2012) found that 1750–1600 cm^{-1} and 3000–2800 cm^{-1} are regions with minimal mineral interference, indicating that these regions are best to interpret. Additionally, I found that the 3500-3000, 2800-1700, and 1580-1360 cm^{-1} regions have little mineral interference.

High correlations between total C and N with spectral regions at 3400, 2850-2930, 2200, 1730, 1650, 1550 cm^{-1} and 1360-1100 cm^{-1} in the spectra of the organic component obtained through spectral subtraction confirms that these bands are indeed due to absorbance of organic material. These correlations are similar to those of the whole-soils.

Conclusions

In my inventory of the chemical composition of permafrost and active layer SOM, I expected to find that permafrost contains less decomposed material than the active layer, which I expected to contain a mixture of both new and decomposed material. I found that the OAL,

MAL, and two permafrost layers contained many similar chemical functional groups, but in different amounts. The different soil depths also have MidIR regions that differentiate them.

Both the top of permafrost and the OAL contained compounds considered to be chemically labile, but also show evidence of decomposition. The top of the permafrost often contains more similar types of compounds to the OAL than the MAL, indicating that compounds have either been preserved in the top of the permafrost or introduced (e.g. through cryoturbation, diffusion, syngenetic permafrost formation), confirming previous findings in incubation studies showing that permafrost OM is more or equally able to be decomposed as the OM in the organic, active layer soils.

All the soils show evidence of prior decomposition, which I did not expect in the permafrost soils. This indicates that either these soils underwent decomposition prior to becoming permanently frozen, or that permafrost OM decomposes, even if very slowly, by heterotrophic microbes capable of metabolic activity well below freezing (Drotz et al., 2010; McMahon et al., 2009) or through abiotic mechanisms, such as oxidation of phenols to quinones resulting from catalysis by metal oxides (Sollins et al., 1996). Additionally, the C/N ratios in the permafrost are lower than the OAL, and although this is consistent with previous reports, it is in contrast to the concept that permafrost OM is more labile than active layer OM and to the results of this study. Previous reports also found incongruent results between potential permafrost lability, as indicated by NMR, and C/N ratios (Lee et al., 2012; Waldrop et al., 2010), suggesting the C/N ratios may not be an adequate index of SOM decomposition in high C content soils.

The MAL and the deeper permafrost often absorb in similar MidIR regions and had similar ratios of labile to recalcitrant compounds. Multivariate analysis of the spectral properties of the mineral soils (MAL and permafrost layers) in the absence of OAL showed that the

presence of labile organic compounds contributed to differences between the top of the permafrost and deeper permafrost. These results add to a growing understanding of the chemical composition of OM in permafrost. Future incubation studies on these soils will shed further light on the reactivity and decomposability of these chemical structures in soils.

Tables

Table 2.1. Putative assignments for the bands relevant to this study. Note that mid infrared absorption bands occur over a range, and that there are overtone and combination bands from several different functional groups that may overlap with these frequencies. δ is bending, and ν is stretching.

wn (cm^{-1})	Assignment
3660-3620	ν O-H in clays [b]
3400	νO-H and ν N-H [a]
2930-2845	νC-H [a]
2515	Carbonates
2200-2000	Overtones of ν –COH[d]
2000-1770	Quartz overtones [b]
1740-1700	ν C=O bond stretching in carboxylic acids and/or esters, ring ν C=C
1670-1600	Amide I, or phenyl ring ν C=C [a]
1590-1570	Ring ν C=C of phenyl [a]
1560-1480	Amide II band ν C-N and δ C-N-H [a, c]. Also δ CH in phenyl rings
1530	ν C=N, or ν C=C [a]
1450-1400	C-O single bond absorbance, δ CH [c]
1450-1370	δ(CH_2) in polysaccharides and proteins [a]. Also, N-H, and ν C-N [c]
1330	Carboxylate C-O [f], ν C-N in amides, δ(CH) in phenyls and polysaccharides [a]
1320-1220	Amide III band [a]
1170-1060	ν C-O in carbohydrates, nucleic acids, proteins [a]
1050	δ C-O in carbohydrates [a]
810	silica[e]

a- Movasaghi et al., 2008
b- Nguyen et al., 1991
c- Haberhauer and Gerzabek, 1999
d- Janik et al., 2007
e- Calderon et al., 2011b
f- Tatzber et al., 2007
g- Anderson, 1961

Table 2.2. Means of the ratios of two band regions for each soil depth. The "Chemical Assignment" is from the original citation, and in most cases, I used the ratio of the two bands that the original citation chose, except for those marked with a †. Different letters indicate statistically significant differences at $\alpha < 0.05$ after using a Tukey HSD multiple testing adjustment.

				Soil Depth			
Chemical assignment	Ratio	OAL	MAL	Perm 0-15 cm	Perm 16-30 cm	Perm 31-45 cm	Trend with depth
carbohydrate: carboxylate[Δ]	1030/1600	1.02a	1.04a	0.96b	0.96b	1.01a	
aromatics or carboxylates: aliphatics[ø]	1630/2920	1.31a	1.60b	1.57b	1.80c	1.82c	
aromatics or carboxylates: lignin 2[ø]	1630/1510	1.14a	1.08b	1.07b	1.02c	0.97d	
C–H bonds: esterified carbohydrates[∂]	2930/1734†	0.93a	0.86bc	0.88b	0.83c	0.83c	
C–H bonds: amides in proteins[∂]	2930/1653†	0.78a	0.64bd	0.66b	0.59cd	0.58d	
C–H bonds: lignin 1[∂]	2930/1600†	0.78a	0.60bd	0.62b	0.54c	0.54d	
C–H bonds: lignin 2[∂]	2930/1510†	0.88a	0.66b	0.67b	0.56c	0.53c	
C–H bonds: cellulose[∂]	2930/897†	1.01a	0.65bc	0.71b	0.62c	0.60c	
Amines, –OH: amides in proteins[∂]	3400/1653	0.87a	0.73b	0.77c	0.75b	0.75b	
Amines, –OH: lignin 1[∂]	3400/1600	0.88a	0.68bcd	0.73b	0.69cd	0.69bd	
Amines, –OH: lignin 2[∂]	3400/1510	0.98a	0.74bc	0.78b	0.72c	0.68c	
Carbohydrates: amides in proteins[∂]	1734/1653	0.84a	0.75b	0.75b	0.70c	0.70c	
Carbohydrates: lignin 1[∂]	1734/1600	0.84a	0.70b	0.70b	0.65c	0.64c	
Carbohydrates: lignin 2[∂]	1734/1510	0.94a	0.77b	0.76b	0.68c	0.64c	
Carbohydrates: cellulose[∂]	1734/897	1.09a	0.76bc	0.81b	0.74c	0.72c	
Amides in proteins: lignin 1[∂]	1653/1600	1.01a	0.94bc	0.94b	0.92c	0.92c	
Amides in proteins: lignin 2[∂]	1653/1510	1.13a	1.02b	1.02b	0.96c	0.91d	
Amides in proteins: cellulose[∂]	1653/897	1.30a	1.01b	1.08c	1.05bc	1.03b	
Lignin 1: lignin 2[∂]	1600/1510	1.12a	1.09ab	1.08b	1.04c	0.99d	
Lignin 1: cellulose[∂]	1600/897	1.29a	1.08b	1.15c	1.14cd	1.12bd	
Lignin 2: cellulose[∂]	1510/897	1.15a	0.99b	1.06c	1.09d	1.13ad	

† Calderon et al. used the 2870 cm^{-1} for C-H; I used 2930 cm^{-1} due to maximum of the C-H band in my study
Δ- Artz et al., 2006
ø- Haberhauer et al., 1998
∂- Calderon et al., 2006

Figures

(a) (b)

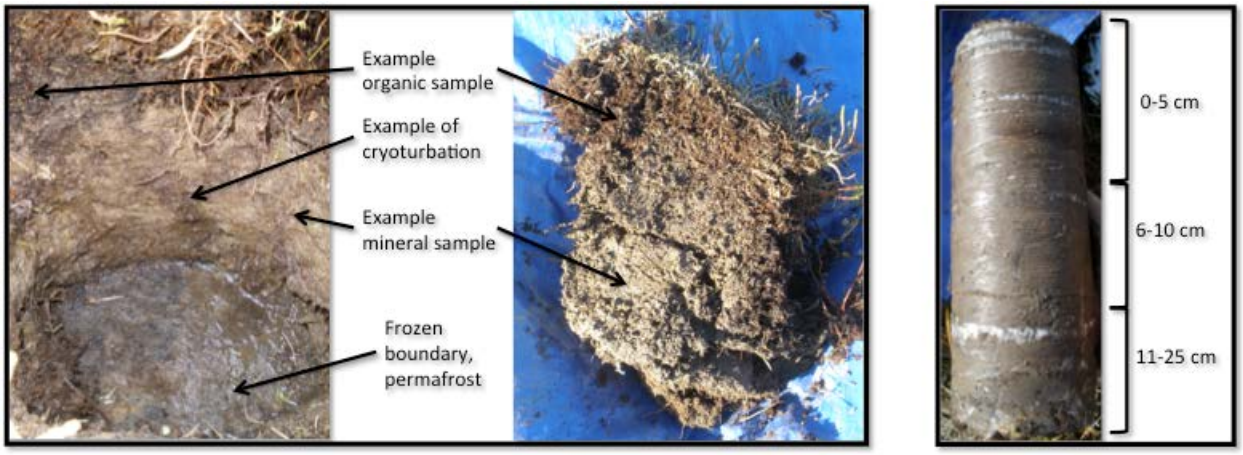

Figure 2.1. (a) Example soil pit from Sagwon Hills, Alaska showing soil sampling depths and portraying cryoturbation. (b) Permafrost core showing how samples were divided.

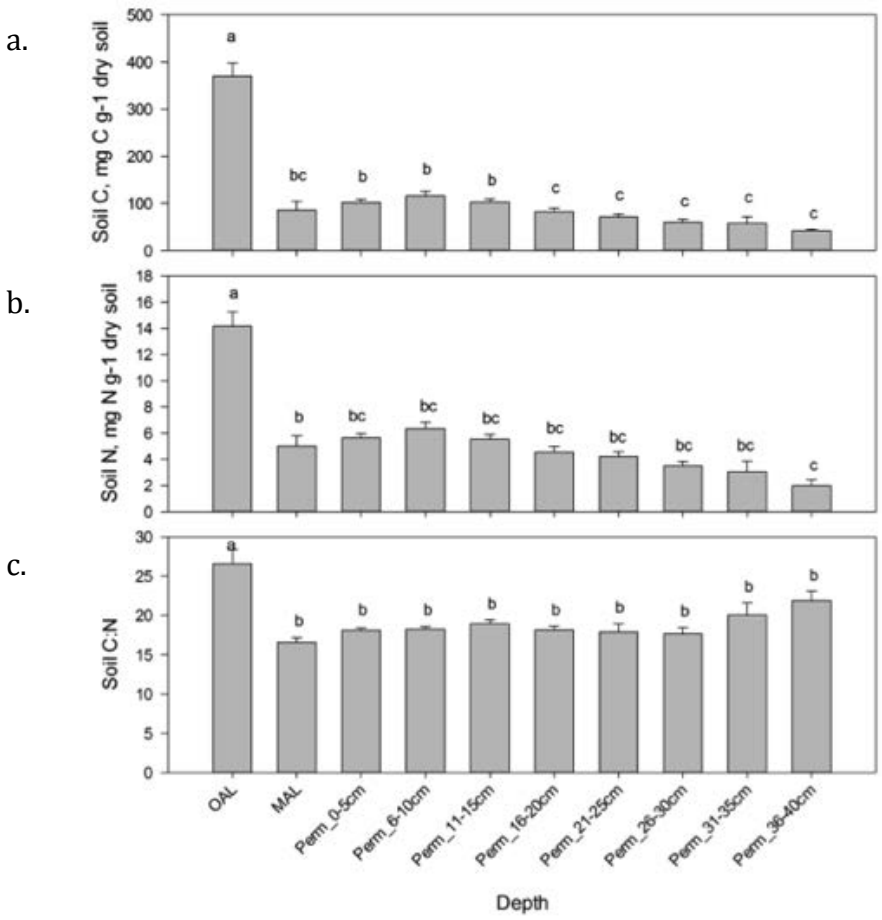

Figure 2.2. Total C content (a), N content (b), and C to N ratios (c) of the permafrost (perm) and active layer (AL) samples. Different letters indicate significant differences in the means of the log-transformed data after using the Tukey HSD multiple comparison adjustment ($p < 0.05$). The total number of samples was 106; OAL n= 12; MAL n= 9; Perm 0-5 cm n= 15; Perm 6-10 cm n= 15; Perm 11-15 cm n= 15; Perm 16-20 cm n= 14; Perm 21-25 cm n= 12; Perm 26-30 cm n= 8; Perm 31-35 cm n= 4; Perm 36-40 cm n= 2.

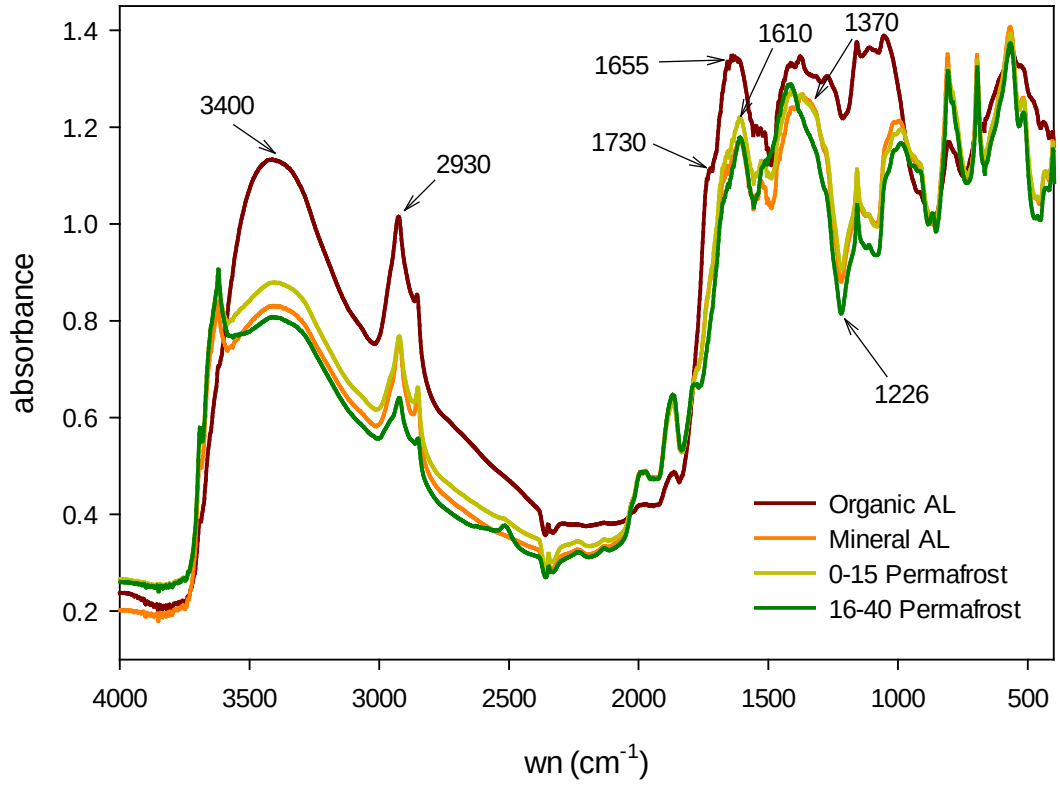

Figure 2.3. Average Fourier transform mid infrared diffuse reflectance spectra (neat, not ashed) of the active layer and the permafrost samples. Layers were selected according the statistical mean separation test in Fig. 2.

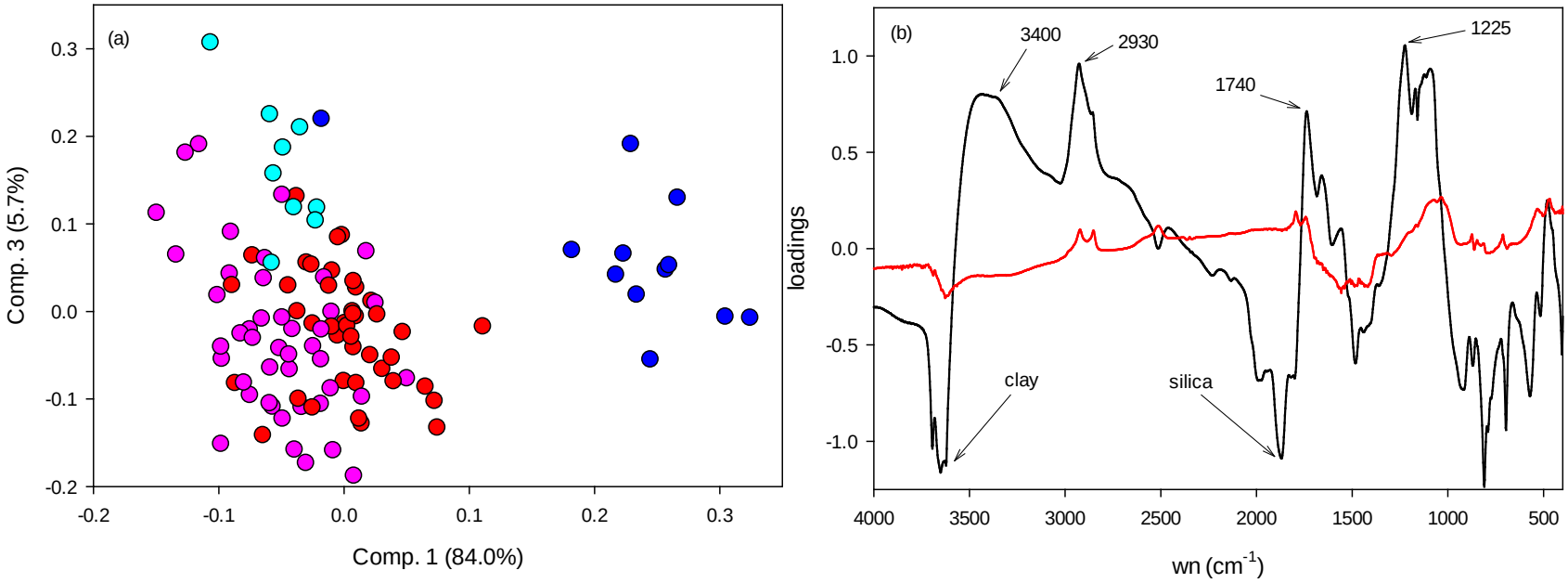

Figure 2.4. (a) Principle Components Analysis (PCA) of whole-soil MidIR spectra from OAL (dark blue), MAL (teal), permafrost 0-15 cm below the maximum active layer depth (pink), and permafrost 16^{+} cm (red). The percent variance explained by each component is in parenthesis. (b) PCA component 1 loadings (black line) show the regions that differences between the OAL and other soils can be attributed to. PCA component 3 loadings (red line) show regions that result in a separation of the MAL from permafrost soils.

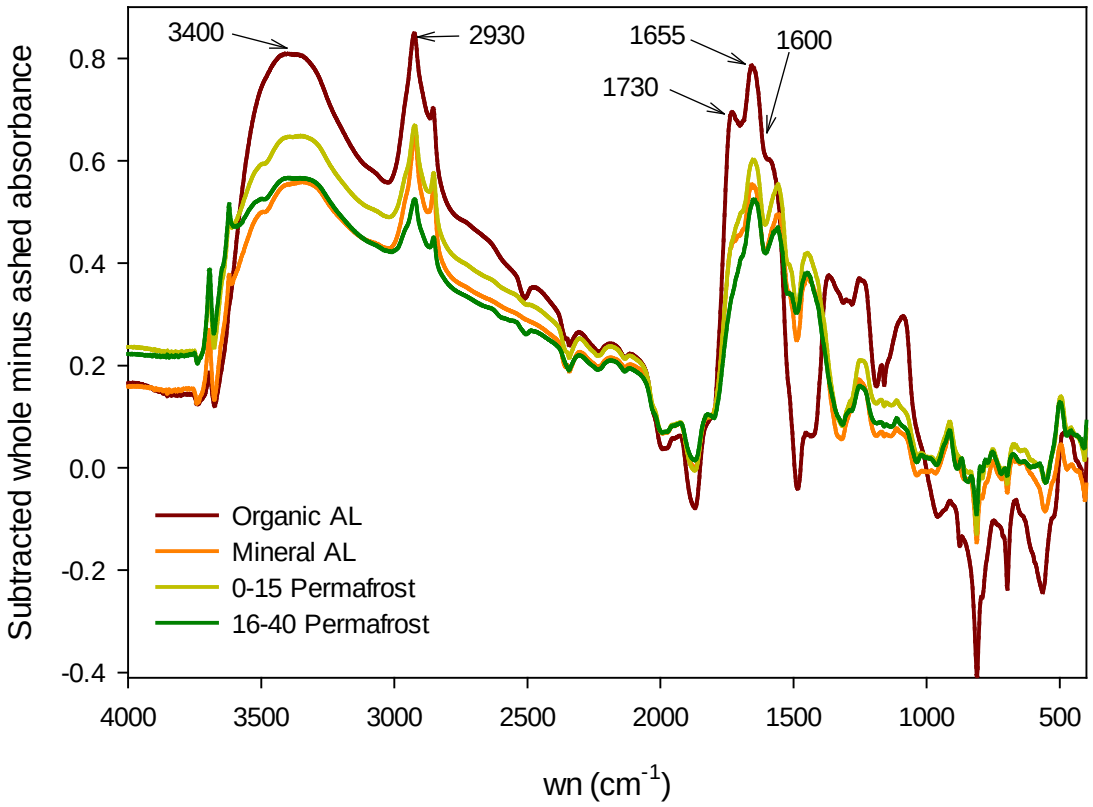

Figure 2.5. Average of the whole minus ashed spectral subtractions of the permafrost and active layer. Layers were selected according the statistical mean separations in Fig. 2.

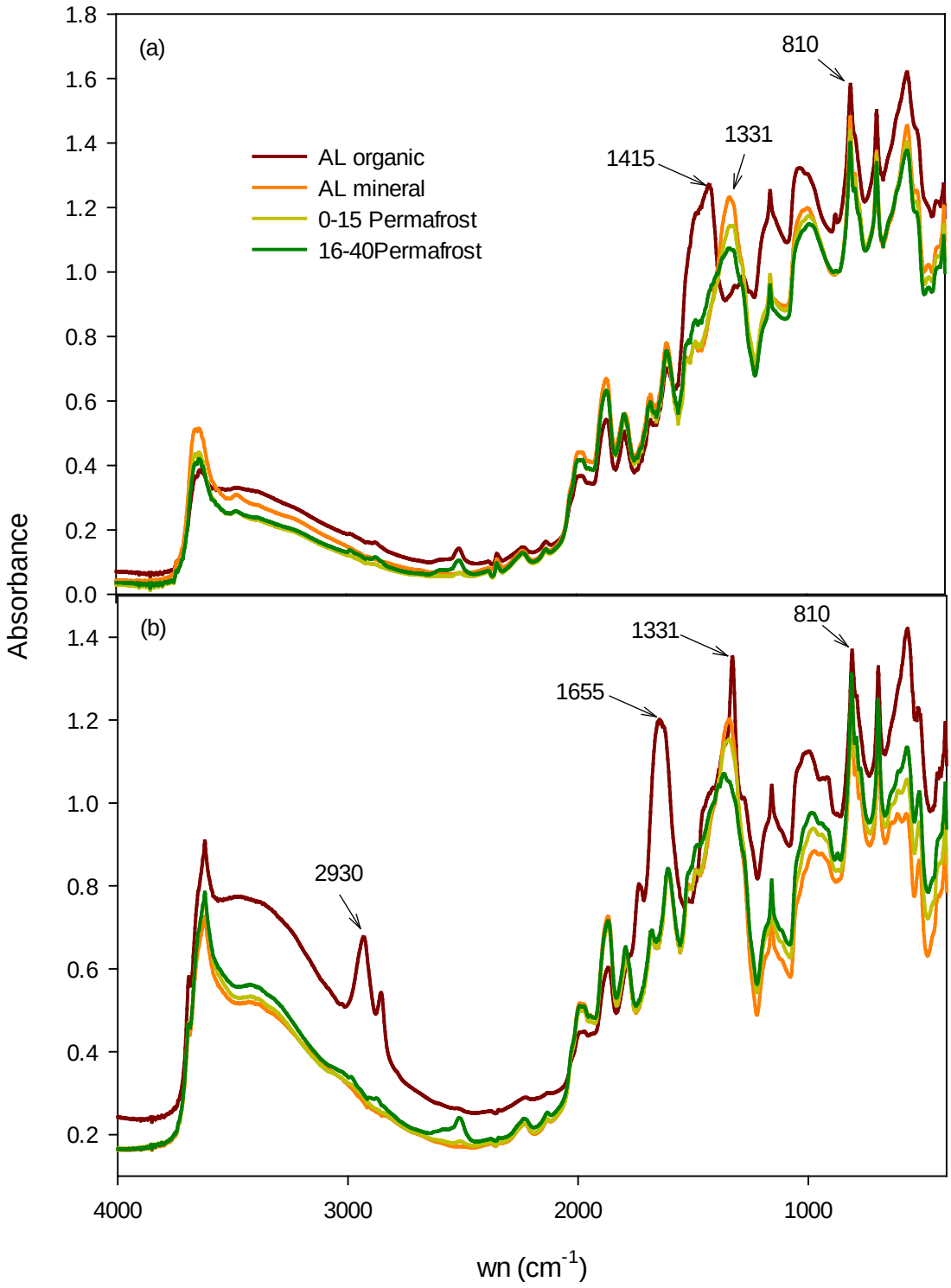

Figure 2.6. Mid-IR spectra of the active layer and the permafrost ashed soils (a), and hypochlorite oxidized soils (b).

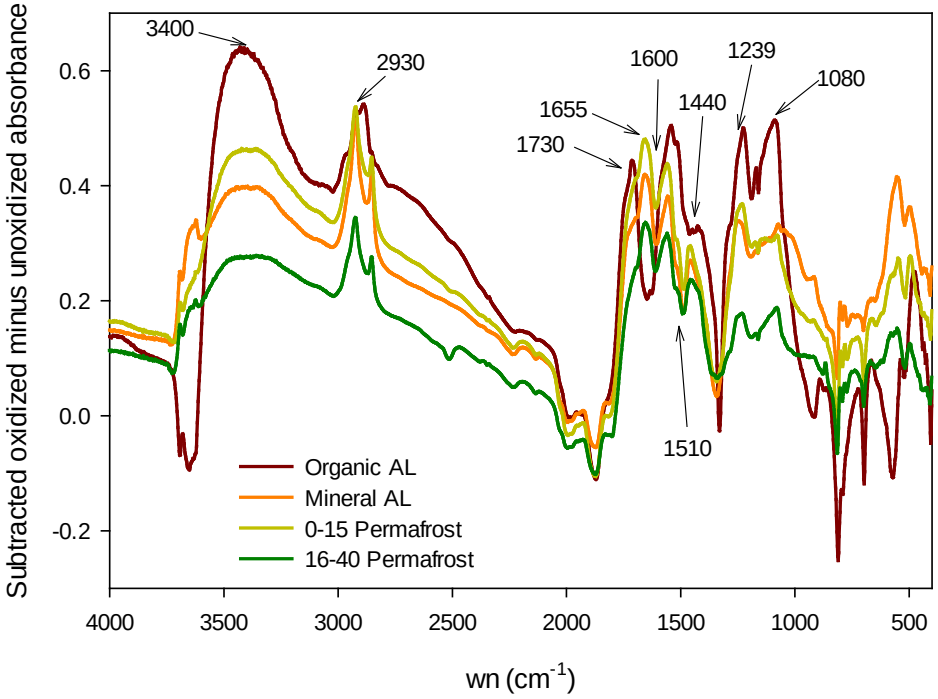

Figure 2.7. Average of the whole-soil minus hypochlorite oxidized spectral subtractions of the permafrost and active layer. Layers were selected according the statistical mean separation test in Fig. 2.2.

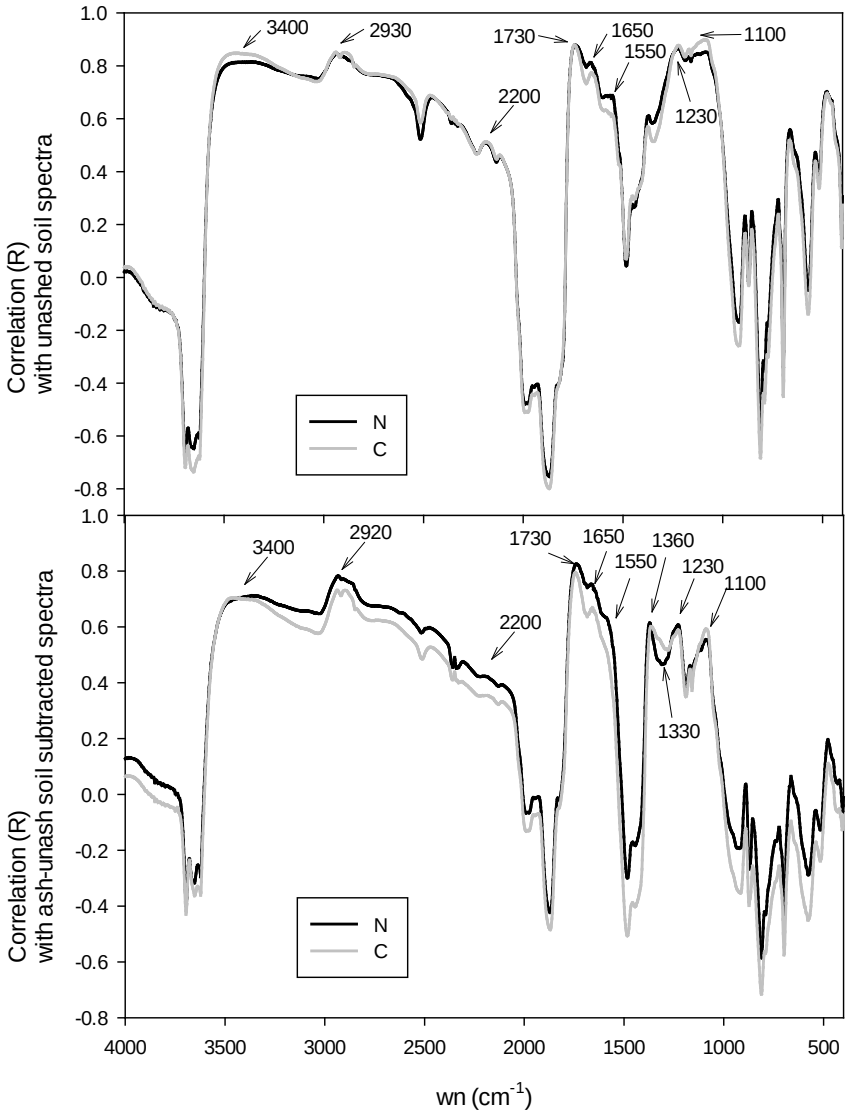

Figure 2.8. Correlation coefficient (R) for the MidIR spectral data correlation between percent N and percent C. The top panel shows correlations with the whole-soil (unashed) and % C and % N. The bottom panel shows correlations with the whole-soil minus ashed spectral subtractions and % C and % N. n=106.

(a) (b)

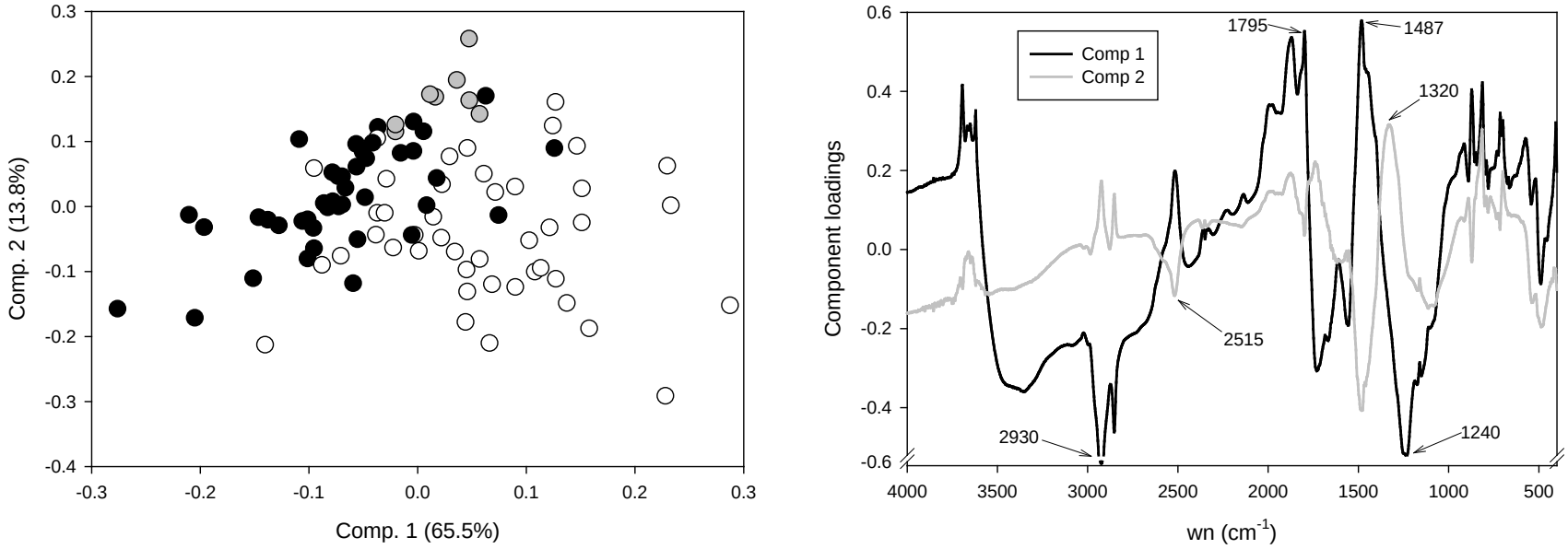

Figure 2.9. (a) PCA of the whole-soil MidIR spectral components from the mineral soils, excluding the OAL samples. The top of the permafrost (0-15 cm) are in black symbols; deeper permafrost (16-47.5 cm) are in white symbols; active mineral active layer samples have grey symbols. The percent variance explained by each component is in parentheses. (b) Component loadings for the Principal Components Analysis shown in (a).

References

ACIA, 2004. Impacts of a Warming Arctic: Arctic Climate Impact Assessment. Impacts of a Warming Arctic-Arctic Climate Impact Assessment, by Arctic Climate Impact Assessment, pp. 144. ISBN 0521617782. Cambridge, UK: Cambridge University Press, December 2004.

Anderson, J.U., 1961. An improved pretreatment for mineralogical analysis of samples containing organic matter. Clays and Clay Minerals 10, 380–388.

Artz, R.R.E., Chapman, S.J., Campbell, C.D., 2006. Substrate utilisation profiles of microbial communities in peat are depth dependent and correlate with whole soil FTIR profiles. Soil Biology and Biochemistry 38, 2958–2962. doi:10.1016/j.soilbio.2006.04.017

Baes, A.U., Bloom, P.R., 1989. Diffuse reflectance and transmission Fourier transform infrared (DRIFT) spectroscopy of humic and fulvic acids. Soil Science Society of America Journal 53, 695–700.

Borden, P.W., Ping, C.-L., McCarthy, P.J., Naidu, S., 2010. Clay Mineralogy in Arctic Tundra Gelisols, Northern Alaska. Soil Science Society of America Journal 74, 580. doi:10.2136/sssaj2009.0187

Bornemann, L., Welp, G., Amelung, W., 2010. Particulate Organic Matter at the Field Scale: Rapid Acquisition Using Mid-Infrared Spectroscopy. Soil Science Society of America Journal 74, 1147. doi:10.2136/sssaj2009.0195

Calderón, F., Haddix, M., Conant, R., Magrini-Bair, K., Paul, E., 2013. Diffuse-Reflectance Fourier-Transform Mid-Infrared Spectroscopy as a Method of Characterizing Changes in Soil Organic Matter. Soil Science Society of America Journal 77, 1591. doi:10.2136/sssaj2013.04.0131

Calderón, F.J., McCarty, G.W., Reeves, J.B., III, 2006. Pyrolisis-MS and FT-IR analysis of fresh and decomposed dairy manure. Journal of Analytical and Applied Pyrolysis 76, 14–23. doi:10.1016/j.jaap.2005.06.009

Calderón, F.J., Mikha, M.M., Vigil, M.F., Nielsen, D.C., Benjamin, J.G., Reeves, J.B., III, 2011a. Diffuse-Reflectance Mid-infrared Spectral Properties of Soils under Alternative Crop Rotations in a Semi-arid Climate. Communications in Soil Science and Plant Analysis 42, 2143–2159. doi:10.1080/00103624.2011.596243

Calderón, F.J., Reeves, J.B., Collins, H.P., Paul, E.A., 2011b. Chemical Differences in Soil Organic Matter Fractions Determined by Diffuse-Reflectance Mid-Infrared Spectroscopy. Soil Science Society of America Journal 75, 568. doi:10.2136/sssaj2009.0375

Chapin, F.S., Matson, P.A., Mooney, H.A., 2002. Principles of terrestrial ecosystem ecology.

Chen, H.-L., Zhou, J.-M., Xiao, B.-H., 2010. Characterization of dissolved organic matter derived from rice straw at different stages of decay. J Soils Sediments 10, 915–922. doi:10.1007/s11368-010-0210-x

Conant, R.T., Drijber, R.A., Haddix, M.L., Parton, W.J., Paul, E.A., Plante, A.F., Six, J., Steinweg, J.M., 2008. Sensitivity of organic matter decomposition to warming varies with its quality. Glob Change Biol 14, 868–877. doi:10.1111/j.1365-2486.2008.01541.x

Cox, R.J., Peterson, H.L., Young, J., Cusik, C., Espinoza, E.O., 2000. The forensic analysis of soil organic by FTIR. Forensic Sci. Int. 108, 107–116.

Davidson, E.A., Janssens, I.A., 2006. Temperature sensitivity of soil carbon decomposition and feedbacks to climate change. Nature 440, 165–173. doi:10.1038/nature04514

Drotz, S.H., Sparrman, T., Nilsson, M.B., Schleucher, J., Oquist, M.G., 2010. Both catabolic and anabolic heterotrophic microbial activity proceed in frozen soils. Proc. Natl. Acad. Sci. U.S.A. 107, 21046–21051. doi:10.1073/pnas.1008885107

Goldfarb, K.C., Karaoz, U., Hanson, C.A., Santee, C.A., Bradford, M.A., Treseder, K.K., Wallenstein, M.D., Brodie, E.L., 2011. Differential growth responses of soil bacterial taxa to carbon substrates of varying chemical recalcitrance. Front. Microbio. 2, 94. doi:10.3389/fmicb.2011.00094

Haberhauer, G., Feigl, B., Gerzabek, M.H., Cerri, C., 2000. FT-IR spectroscopy of organic matter in tropical soils: changes induced through deforestation. Applied Spectroscopy 54, 221–224.

Haberhauer, G., Gerzabek, M.H., 1999. Drift and transmission FT-IR spectroscopy of forest soils: an approach to determine decomposition processes of forest litter. Vibrational Spectroscopy 19, 413–417.

Haberhauer, G., Rafferty, B., Strebl, F., Gerzabek, M.H., 1998. Comparison of the composition of forest soil litter derived from three different sites at various decompositional stages using FTIR spectroscopy. Geoderma 83, 331–342.

Hinzman, L.D., Bettez, N.D., Bolton, W.R., Chapin, F.S., Dyurgerov, M.B., Fastie, C.L., Griffith, B., Hollister, R.D., Hope, A., Huntington, H.P., Jensen, A.M., Jia, G.J., Jorgenson, T., Kane, D.L., Klein, D.R., Kofinas, G., Lynch, A.H., Lloyd, A.H., McGuire, A.D., Nelson, F.E., Oechel, W.C., Osterkamp, T.E., Racine, C.H., Romanovsky, V.E., Stone, R.S., Stow, D.A., Sturm, M., Tweedie, C.E., Vourlitis, G.L., Walker, M.D., Walker, D.A., Webber, P.J., Welker, J.M., Winker, K.S., Yoshikawa, K., 2005. Evidence and Implications of Recent Climate Change in Northern Alaska and Other Arctic Regions. Climatic Change 72, 251–298. doi:10.1007/s10584-005-5352-2

Hobbie, S.E., Schimel, J.P., Trumbore, S.E., Randerson, J.R., 2000. Controls over carbon storage and turnover in high-latitude soils. Glob Change Biol 6, 196–210.

Huang, W.E., Hopper, D., Goodacre, R., Beckmann, M., Singer, A., Draper, J., 2006. Rapid characterization of microbial biodegradation pathways by FT-IR spectroscopy. Journal of Microbiological Methods 67, 273–280. doi:10.1016/j.mimet.2006.04.009

Janik, L.J., Merry, R.H., Forrester, S.T., Lanyon, D.M., Rawson, A., 2007. Rapid Prediction of Soil Water Retention using Mid Infrared Spectroscopy. Soil Science Society of America Journal 71, 507. doi:10.2136/sssaj2005.0391

Jones, S.E., Newton, R.J., McMahon, K.D., 2009. Evidence for structuring of bacterial community composition by organic carbon source in temperate lakes. Environmental Microbiology 11, 2463–2472. doi:10.1111/j.1462-2920.2009.01977.x

Kuhry, P., Ping, C.-L., Schuur, E.A.G., Tarnocai, C., Zimov, S., 2009. Report from the International Permafrost Association: carbon pools in permafrost regions. Permafrost Periglac. Process. 20, 229–234. doi:10.1002/ppp.648

Lee, H., Schuur, E.A.G., Inglett, K.S., Lavoie, M., Chanton, J.P., 2012. The rate of permafrost carbon release under aerobic and anaerobic conditions and its potential effects on climate. Glob Change Biol 18, 515–527. doi:10.1111/j.1365-2486.2011.02519.x

McMahon, S.K., Wallenstein, M.D., Schimel, J.P., 2009. Microbial growth in Arctic tundra soil at −2°C. Environmental Microbiology Reports 1, 162–166. doi:10.1111/j.1758-2229.2009.00025.x

Michaelson, G.J., Ping, C.L., Jorgenson, M.T., 2011. Methane and carbon dioxide content in eroding permafrost soils along the Beaufort Sea coast, Alaska. J. Geophys. Res. 116, G01022. doi:10.1029/2010JG001387
Movasaghi, Z., Rehman, S., Rehman, I.U., 2008. Fourier Transform Infrared (FTIR) Spectroscopy of Biological Tissues. Applied Spectroscopy Reviews 43, 134–179. doi:10.1080/05704920701829043
Nguyen, T.T., Janik, L.J., Raupach, M., 1991. Diffuse reflectance infrared Fourier transform (DRIFT) spectroscopy in soil studies. Soil Research 29, 49–67.
Nuopponen, M.H., Birch, G.M., Sykes, R.J., Lee, S.J., Stewart, D., 2006. Estimation of Wood Density and Chemical Composition by Means of Diffuse Reflectance Mid-Infrared Fourier Transform (DRIFT-MIR) Spectroscopy. J. Agric. Food Chem. 54, 34–40. doi:10.1021/jf051066m
Osterkamp, T.E., Romanovsky, V.E., 1999. Evidence for warming and thawing of discontinuous permafrost in Alaska. Permafrost Periglac. Process. 10, 17–37.
Parikh, S.J., Goyne, K.W., Margenot, A.J., Mukome, F.N., Calderón, F.J., 2013. Soil chemical insights provided through vibrational spectroscopy (No. in prep).
Piccolo, A., Zaccheo, P., Genevini, P.G., 1992. Chemical characterization of humic substances extracted from organic-waste-amended soils. Bioresource Technology 40, 275–282.
Reeves, J.B., III, 1993. Infrared spectroscopic studies on forage and by-product fibre fractions and lignin determination residues. Vibrational Spectroscopy 5, 303–310.
Reeves, J.B., III, 2012. Mid-infrared spectral interpretation of soils: Is it practical or accurate? Geoderma 189-190, 508–513. doi:10.1016/j.geoderma.2012.06.008
Rivkina, E., Gilichinsky, D., Wagener, S., Tiedje, J., McGrath, J., 1998. Biogeochemical activity of anaerobic microorganisms from buried permafrost sediments. Geomicrobiology Journal 15, 187–193.
Rivkina, E., Laurinavichius, K., McGrath, J., Tiedje, J., Shcherbakova, V., Gilichinsky, D., 2004. Microbial life in permafrost. Advances in Space Research 33, 1215–1221. doi:10.1016/j.asr.2003.06.024
Romanovsky, V.E., Smith, S.L., Christiansen, H.H., Shiklomanov, N.I., Streletskiy, D.A., Drozdov, D.S., Oberman, N.G., Kholodov, A.L., Marchenko, S.S., 2012. Permafrost, in: Jeffries, M.O., Richter-Menge, J.A., Overland, J.E. (Eds.), Arctic Report Card 2012.
Sannel, A.B.K., Kuhry, P., 2009. Holocene peat growth and decay dynamics in sub-arctic peat plateaus, west-central Canada. Boreas 38, 13–24. doi:10.1111/j.1502-3885.2008.00048.x
Sarkhot, D.V., Comerford, N.B., Jokela, E.J., Reeves, J.B., Harris, W.G., 2007. Aggregation and Aggregate Carbon in a Forested Southeastern Coastal Plain Spodosol. Soil Science Society of America Journal 71, 1779. doi:10.2136/sssaj2006.0340
Schirrmeister, L., Grosse, G., Wetterich, S., Overduin, P.P., Strauss, J., Schuur, E.A.G., Hubberten, H.-W., 2011. Fossil organic matter characteristics in permafrost deposits of the northeast Siberian Arctic. J. Geophys. Res. 116, G00M02. doi:10.1029/2011JG001647
Schmidt, M.W.I., Torn, M.S., Abiven, S., Dittmar, T., Guggenberger, G., Janssens, I.A., Kleber, M., Kögel-Knabner, I., Lehmann, J., Manning, D.A.C., Nannipieri, P., Rasse, D.P., Weiner, S., Trumbore, S.E., 2011. Persistence of soil organic matter as an ecosystem property. Nature 478, 49–56. doi:10.1038/nature10386
Schuur, E.A., Bockheim, J., Canadell, J.G., Euskirchen, E., Field, C.B., Goryachkin, S.V., Hagemann, S., Kuhry, P., Lafleur, P.M., Lee, H., 2008. Vulnerability of permafrost carbon to climate change: Implications for the global carbon cycle. BioScience 58, 701–714.

Siregar, A., Kleber, M., Mikutta, R., Jahn, R., 2005. Sodium hypochlorite oxidation reduces soil organic matter concentrations without affecting inorganic soil constituents. European Journal of Soil Science 56, 481–490. doi:10.1111/j.1365-2389.2004.00680.x

Sollins, P., Homann, P., Caldwell, B.A., 1996. Stabilization and destabilization of soil organic matter: mechanisms and controls. Geoderma 74, 65–105.

Tarnocai, C., Canadell, J.G., Schuur, E.A.G., Kuhry, P., Mazhitova, G., Zimov, S., 2009. Soil organic carbon pools in the northern circumpolar permafrost region. Global Biogeochem. Cycles 23, GB2023. doi:10.1029/2008GB003327

Tatzber, M., Stemmer, M., Splegel, H., Katziberger, C., Haberhauer, G., Mentler, A., Gerzabek, M.H., 2007. FTIR-spectroscopic characterization of humic acids and humin fractions obtained by advanced NaOH, Na4P2O7, and Na2CO3 extraction procedures. Jounal of Plant Nutrition and Soil Science 170, 522–529. doi:{10.1002/jpln.200622082}

Viscarra Rossel, R.A., Walvoort, D.J.J., McBratney, A.B., Janik, L.J., Skjemstad, J.O., 2006. Visible, near infrared, mid infrared or combined diffuse reflectance spectroscopy for simultaneous assessment of various soil properties. Geoderma 131, 59–75. doi:10.1016/j.geoderma.2005.03.007

Waldrop, M.P., Wickland, K.P., White, R.I., Berhe, A.A., Harden, J.W., Romanovsky, V.E., 2010. Molecular investigations into a globally important carbon pool: permafrost-protected carbon in Alaskan soils. Glob Change Biol 16, 2543–2554. doi:10.1111/j.1365-2486.2009.02141.x

Wallenstein, M.D., McMahon, S., Schimel, J., 2007. Bacterial and fungal community structure in Arctic tundra tussock and shrub soils. FEMS Microbiol Ecol 59, 428–435. doi:10.1111/j.1574-6941.2006.00260.x

White, D.M., Garland, D.S., Ping, C.-L., Michaelson, G., 2004. Characterizing soil organic matter quality in arctic soil by cover type and depth. Cold Regions Science and Technology 38, 63–73. doi:10.1016/j.coldregions.2003.08.001

Chapter 3: Historical community legacy and environmental filtering structure the permafrost microbial community

Introduction

The diversity and distribution of microorganisms on Earth is vast (Borden et al., 2010; Roesch et al., 2007; Torsvik, 2002; Venter, 2004), with microbial life occurring almost everywhere, even in extreme environments such as hydrothermal vents, ice caps and permafrost soils (Ernakovich, 2014; Steven et al., 2009). To sustain life in permafrost, or permanently frozen soils, microorganisms must maintain metabolic function under the stress imposed by low temperatures, frozen conditions, high salt concentrations, and gamma radiation (Bölter, 2004; Steven et al., 2009; 2006; Tarnocai, 1993). Despite these challenges, microorganisms in permafrost can sustain relatively large populations capable of functioning under *in situ* conditions (Rivkina et al., 2000; Tuorto et al., 2014) and after the stress of frozen conditions is alleviated (Gilichinsky and Wagener, 1995; Mackelprang et al., 2011; Mondav et al., 2014; Vishnivetskaya et al., 2006).

Permafrost harbors a large number of viable cells, in the same order of magnitude found in soils from temperate environments (Bölter, 2004; Hansen et al., 2007; Rivkina et al., 1998; Steven et al., 2006), and these cells are not in a state of cryoanabiosis (Gilichinsky and Wagener, 1995). Rivkina et al. (1998) detected 10^7-10^8 viable aerobes per gram of soil in permafrost soils from Northeastern Siberia sampled down to 34 meters. Lower numbers of viable aerobic cells have been detected from Canadian High Arctic permafrost soils (10^1-10^3) and Antarctic permafrost (0-10^5) (Steven et al., 2006), but considerable concentrations of viable anaerobes are also often detected (Rivkina et al., 1998). Although psychrophilic microorganisms have been

isolated from permafrost, isolates are often found to be psychrotolerant and mesophilic (Bölter, 2004; Rivkina et al., 2004; Shi et al., 1997; Steven et al., 2007a). Microbes in permafrost are capable of growth and maintenance at sub-zero conditions (Bakermans et al., 2003; Drotz et al., 2010; Gilichinsky and Wagener, 1995; Johnson et al., 2007; McMahon et al., 2009; P. B. Price and Sowers, 2004; Rivkina et al., 2000; Steven et al., 2006; 2007b; Tuorto et al., 2014). For example, Rivkina et al. (2000) detected bacterial lipid production and growth down to -20 °C. Tuorto et al. (2014) demonstrated that temperature niches exist below zero, showing that certain taxa actively grew below -6 °C and others dominated above -6 °C. In addition, Johnson et al. (2007) found evidence for *in situ* DNA repair in cells up to 600,000 years old. Products of anaerobic respiration accumulating in permafrost (Michaelson et al., 2011; Rivkina et al., 2004) and negative redox potentials (Rivkina et al., 1998), indicative of the reduction of electron acceptors higher on the redox ladder (e.g. O_2, NO_3^-), are evidence of the *in situ* activity of permafrost microorganisms.

Microorganisms survive cold conditions through a variety of physiological mechanisms, including thickening cell walls (Ponder et al., 2005; Soina et al., 1995; Suzina et al., 2004), manipulating the saturation and thus the flexibility of their lipid bilayer (Russell, 1997), and by employing cold shock proteins (Deming, 2002). In addition to cold, microorganisms in permafrost also have to survive high salt concentrations (~5 osm L^{-1}, Ponder et al., 2008), which they combat by maintaining high concentrations of compatible solutes (Thomas et al., 2001). All of these mechanisms for halotolerance also protect against ice nucleation and cell death (Ponder et al., 2005). With permafrost age, G-C content of the DNA and the proportion of gram-positive bacteria has been found to increase (Shi et al., 1997; Willerslev et al., 2004), indicating selection for a community with these particular protection mechanisms. Sporulation is also a mechanism

of survival employed by some permafrost microorganisms in some systems (Steven et al., 2007a) but not others (Shi et al., 1997). Rather than sporulation, reductions in cell size may be an important survival mechanism for other permafrost microorganisms (Bölter, 1995; Soina et al., 2004). The ability to perform DNA repair despite slow growth is possibly a more powerful survival mechanism than sporulation (Willerslev et al., 2004). Indeed, Johnson et al. (2007) determined that DNA repair results in more long-term success than dormancy or vegetative states, during which DNA slowly degrades.

Permafrost microbial communities contain similar phyla and metabolic potential to other soils (Chu et al., 2010; Tveit et al., 2012), but also contain some taxa that are thought to be endemic (Steven et al., 2009). The application of culture-independent methods for assessing microbial diversity in permafrost has broadened our understanding of the phyla present in permafrost. Acidobacteria, Actinobacteria, CFB, Firmicutes, Gemmatimonadetes, and Proteobacteria are commonly found in permafrost soils from the Canadian High Arctic and NW Canada, Northeastern Siberia, Spitsbergen, Norway, Alaska and the Antarctic Dry Valleys (Frank-Fahle et al., 2014; Gilichinsky et al., 2007; Hansen et al., 2007; Mackelprang et al., 2011; Steven et al., 2009; 2007a; Vishnivetskaya et al., 2006). Archaea, such as Euryarchaeota and Crenarchaeota, are also common to permafrost (Steven et al., 2007a) and are likely increasingly dominant with soil depth (Tveit et al., 2012). Anaerobes, including methanogens and sulfur reducers, have also been detected (Frank-Fahle et al., 2014; Rivkina et al., 2007; Zhou et al., 1997). Recent metagenomics sequencing efforts have revealed novel methanogens with correspondingly unique strategies (Mackelprang et al., 2011; Mondav et al., 2014). Mondav et al. (2014) found that thawed sites were dominated by the novel methanogen ‘Candidatus Methanoflorens stordalenmirensis’, and Mackelprang (2011) discovered a novel nitrogen fixing

methanogen from the Methanomicrobia family that was correlated with CH_4 trapped in frozen soils, which may be important in CH_4 production under frozen conditions. Active communities of methanotrophs have also been found in permafrost (Mackelprang et al., 2011; Tveit et al., 2012), and likely play an important role in methane cycling in Arctic soils (Mackelprang et al., 2011).

Permafrost microbial diversity and function have been called the "unknown" in the climate change equation (Graham et al., 2011). However, it is increasingly clear that permafrost microbes are not merely ancient relics, but a diverse and viable community that can respond quickly to thaw (Coolen et al., 2011; Mackelprang et al., 2011) and contribute to modern biogeochemical cycles (Rivkina et al., 2004; Steven et al., 2009). Northern hemisphere permafrost soils occupy 16% of the global land mass (Kuhry et al., 2009) and contain large and deep carbon (C) stocks (Hugelius et al., 2013; Tarnocai et al., 2009). The activity of permafrost microorganisms in response to a changing global temperature regime and thaw-related changes C availability will determine C loss or stabilization from permafrost systems. Thus, from both a perspective of potential function and a natural history perspective, studying the diversity of microbial communities and the factors that structure them is important.

Community composition observed through 16S rRNA gene sequencing is a snapshot of complex processes of community assembly occurring in tandem over space and time. Nemergut et al. (2013) recently adapted a framework from macro-ecology (Vellend, 2010) to describe the assembly of microbial communities. This framework concurrently considers evolution, dispersal, environmental selection for fitness—also known as environmental filtering, and random changes in the abundance of members of a community; they give these the terms diversification, dispersal, selection and drift, respectively. History also seems to play a strong role in structuring

microbial communities (Nemergut et al., 2013). Bölter (2004) posited that microbial communities from cold environments can be structured either by top-down or bottom-up forces, when, respectively, newly dispersed species undergo spontaneous mutation (dispersal) or existing species regulate their genome to fit their environment (diversification). Due to the growing lack of evidence of true psychrophiles found in permafrost, Shi et al. (1997) proposed that the low water and nutrient content in permafrost hamper growth so drastically that evolution (diversification) is limited, and that communities are survivors of, rather than evolving to fit, their environment (drift). However, selection by the habitat for fitness is likely an important mechanism of community assembly in permafrost due to the survival of community members under harsh conditions (Hansen et al., 2007).

The objective of this study was to assess how microbial diversity in the permafrost differs from active layer soils by assessing whether the permafrost microbial community diversity has the same relationship with depth and C as the active layer. I hypothesized that the frozen conditions in permafrost have placed a selection pressure on the microbial community, resulting in a community specialized for these conditions. Thus, I predicted that the species diversity would be lower in the permafrost than the active layer. I predicted that selection for these specialized traits would result in a community with a high degree of phylogenetic clustering relative to the active layer. As a null hypothesis, I assumed the active layer provides the potential species pool for the permafrost (Gilichinsky and Wagener, 1995; Gilichinsky et al., 2007). Thus, I predicted that selection for survival in the permafrost would result in the permafrost community being a phylogenetically clustered subset of the active layer community.

Methods

Description of the study site, soil sampling and processing

Organic active layer, mineral active layer, and permafrost soils were collected from Sagwon Hills, Alaska (N 69° 25' 32.190" W 148° 41' 38.731", 288 m above sea level). The soils were collected from under moist acidic tundra vegetation and are classified as Ruptic Histic Aquiturbels (Borden et al., 2010). Cores were collected from 15 plots representative of the site and covering 150 m^2. The depth of the seasonally thawed active layer was 26.8 $\pm$ 1.3 cm in August of 2009, and consisted of an organic and mineral horizon with evidence of cryoturbation (Ernakovich, 2014). The organic horizon, dominated by mildly decomposed plant material (peat) with many fine roots, was between 5 and 14 cm in depth. The remainder of the active layer was visibly gleyed mineral soil with no additional horizonation. At each plot, the active layer was removed and placed on a tarp as a monolith (average thaw depth, 26.8 $\pm$ 1.3 cm). Organic and mineral active layer soils were sampled from the monolith from the center of their respective depths (organic: 2 $\pm$ 0 cm, 99.4 $\pm$ 57.1 g; mineral: 9.4 $\pm$ 1 cm, 187.4 $\pm$ 77.9 g). In two plots, a buried organic horizon was visible. In these cases, samples were taken from the mineral soil not in the buried organic horizon. Permafrost soils were obtained as 8.0 cm diameter cores using a Tanaka auger fitted with a SIPRE-style (Snow, Ice, and Permafrost Research Establishment, (Tarnocai, 1993)) soil corer with carbide bits (Jon's Machine Shop, Fairbanks, Alaska). Permafrost cores were collected to 31.4 $\pm$ 7.3 cm, where glacial till restricted deeper sampling.

The samples were stored on dry ice in the field, at -20 °C during our eight day collection period at Toolik Biological Field Station, and then brought back to the Colorado State University EcoCore laboratory on dry ice where they were stored at -10 °C during processing and storage. Permafrost cores were scraped to remove any contamination from active layer

microbes or carbon from the field and separated into 5-cm increments, however if there was a natural fracture point at an ice lens within 2 cm of the 5cm fracture point, that point was chosen. Permafrost and organic and mineral active layer soils were homogenized while still frozen in a walk-in -10°C freezer by crushing the soils with a hammer to resemble 2 mm sieve homogenization while double wrapped in sterile plastic bags inside canvas bags. The samples were stored for 17 months at -10 °C until analysis. -10 °C is below the field temperature (average = -1 °C at the time of sampling), and because the soils remained frozen from sampling to analysis, they should represent field microbial community composition relatively well. For this analysis, I chose a subset of nine of the cores collected, including permafrost samples from 0-5 cm (n=9), 11-15 cm (n=9), 16-20 cm (n=1) and 21-25 cm (n=8), 26-30cm (n=2), 31-35 cm (n=1), 36-40 cm (n=1), 41-45 cm (n=1) below the maximum active layer thaw depth. I also included organic active layer (n=8) and mineral active layer (n=6) samples, which were also homogenized under frozen conditions with a hammer. The number of permafrost replicates deviated from nine due to the inability to collect deep cores at some sites; for the active layer replicates were reduced due to errors during field collection.

Soil Carbon and Nitrogen analysis

Subsamples were oven dried at 55°C for 36 hours, ground with a mortar and pestle, and stored in 20mL glass scintillation vials. The dried and ground soils were analyzed for total C and N content using a LECO Tru-SPEC elemental analyzer (Leco Corp., St. Joseph, MI). Between 0.10 and 0.21g (depending on C content) was analyzed. Due to the high SOM content of the organic active layer soils, a C and N standard of mixed grass was used. For mineral soils with relatively less organic matter, an agricultural soil standard from Sidney, Nebraska was used.

Microbial community analysis

Genomic DNA was extracted from the soils using the Power Soil DNA Isolation Kit (MoBio, Carlsbad, CA) following the manufacturer's instructions. Bacterial community structure was analyzed using the protocol defined by Fierer et al. (2008). Briefly, the 515-806 portion of the 16S rRNA gene was amplified. The forward primer contained the 515F primer (5'-GCCTTGCCAGCCCGCTCAGTCAGAGTTTGATCCTGGCTCAG-3'), a 'TC' linker sequence and the Roche 454 Life Sciences primer A. The reverse primer contained the 806R primer (5'-GCCTCCCTCGCGCCATCAGNNNNNNNNNNNNCATGCTGCCTCCCGTAGGAGT-3'), the Roche 454 Life Sciences primer B, a 'CA' linker and a 12 base-pair unique error-correcting barcode (NNNNNNNNNNNN in the primer sequence above) for sample identification (Hamady et al., 2008). PCR reactions contained 0.5 μL (10 μM) of forward and 0.5 μL (10 μM) reverse primer, 3 μL template DNA, and 22.5 μL Platinum PCR SuperMix (Invitrogen, Carlsbad, CA). The samples were amplified in triplicate, cleaned using a PCR Cleanup kit (MoBio Laboratories, Carlsbad, CA) and pooled. Amplicons were sequenced at the Environmental Genomics Core Facility at the University of South Carolina on a Roche FLX 454 pyrosequencing machine. 46 samples were extracted and intended for sequencing, however 3 did not successfully amplify, and thus I pooled 43 for the sequencing.

The Quantitative Insights into Microbial Ecology (Qiime) (Caporaso et al., 2010b) pipeline was used to analyze the pyrosequencing data as previously described (Evans and Wallenstein, 2011; Fierer et al., 2008). The sequences were filtered for quality and sequences shorter than 200 base-pair and with a quality score lower than 25 were removed. OTUs were clustered by 97% similarity using UCLUST and the most abundant OTU was chosen as the representative OTU (Edgar, 2010). Taxonomy was assigned using the RDP classifier (Wang et

al., 2007) trained against GreenGenes (McDonald et al., 2011; Werner et al., 2011), the sequences were aligned with PyNAST (Caporaso et al., 2010a), and a phylogenetic tree was made using FastTree (M. N. Price et al., 2010). An OTU table was produced by sequences rarified to 1740 (which resulted in a reduction of 6 samples, so 37 went into the analysis). Archaea were then removed from the OTU table and then the taxonomy was re-assigned and the sequences were re-aligned (as above). SATe (Simultaneous Alignment and Tree Estimator) was used to make the phylogenetic tree using default settings Tree Center 5 decomposition model (including FastTree as the tree estimator) (Liu et al., 2009), which continuously reiterates the tree until a certain confidence score is gained. In this case, it reiterated the tree three times.

The Qiime pipeline was used to calculate alpha diversity, specifically the number of observed species and Faith's index of phylogenetic diversity (PD whole tree) (Faith, 1992), and beta diversity, using the UniFrac measure of beta diversity (Lozupone and Knight, 2005). Weighted and unweighted UniFrac distances were analyzed using Principle Coordinates Analysis with EMPeror (Vázquez-Baeza et al., 2013) and then plotted in Sigmaplot 12.0 (Systat Software Inc, USA). The relative abundance by taxonomic level was also summarized to determine changes in the relative abundance of bacterial phyla through the depth profile. Net relatedness index (NRI) and nearest taxon index (NTI) were calculated using Phylocom 4.2 (Webb et al., 2008). The tree was annotated according to the major phyla, and visualized using the interactive tree of life (iTOL) web program (Letunic and Bork, 2011). Outer rings indicate presence and absence of OTUs in the well-replicated depths (organic and mineral active layer and permafrost from 0-5, 11-15, and 21-25 cm below the maximum active layer thaw depth). An OTU was called 'present' if it was present in at least 50% of the replicates from a particular depth.

Statistical Analysis

Relationships with alpha diversity ('observed species' and 'PD whole tree') and depth or C content for the active layer and the permafrost were analyzed using a random coefficients model (PROC MIXED, SAS 9.3, Cary, NC), with the intercept and depth as random effects. Initially, the core the sample was taken from was also considered a random effect, however it was unimportant in the model, so it was removed.

Boxplots were created using BoxPlotR (http://boxplot.tyerslab.com; (R Core Development Team, 2013; RStudio and Inc, 2013). Pairwise comparisons using a Tukey Honestly Significant Difference (HSD) multiple testing adjustment explained differences between NRI and NTI (alpha<0.05).

Results

Relationships between permafrost and active layer diversity, depth and soil carbon

Alpha diversity and depth or soil parameters

Permafrost and active layer alpha diversity had different relationships with depth (Fig. 1). For 'observed species', the active layer diversity decreased with depth (slope= -18.01 p=0.011) while the permafrost alpha diversity did not change with depth (p=0.3) (Table 3.1). The alpha diversity of the permafrost and active layer communities were insensitive to changes in C content (all slopes were non-significant from each other or zero; Table 3.1). The intercepts of the models were significantly different and showed that the active layer had 1.6 to 1.9 times greater diversity than the permafrost for the 'PD whole tree' and 'observed species' metrics, respectively (p=0.0063 and 0.0993).

Beta diversity

Community composition differed between the active layer and the permafrost, with the PCoA of the weighted and unweighted pairwise UniFrac distances separating the two layers along coordinate 1 (Fig. 2), which explained 41 and 21% of the variance, respectively. Both the weighted and unweighted UniFrac distances showed that the mineral active layer samples were more closely related to the organic active layer samples than they were to the permafrost. In addition, the permafrost samples were less closely related to each other than the two active layer depths were to each other. The first two components explained 62% and 30% of the dissimilarity in the weighted and unweighted UniFrac distances, respectively.

Phylogenetic make-up of the communities

To assess whether the microbes in the permafrost were a subset of the active layer communities or whether they were a distinct community, I compared the presence of various OTUs in the organic active layer, mineral active layer, and three permafrost depths (0-5, 11-15 and 21-25 cm below the maximum active layer thaw depth) (Fig. 3a). Only 16 of the OTUs that were present in all the permafrost layers were also present in the organic or mineral active layer. Generally, OTUs were present in either the active layer or the permafrost (Fig. 3b). The number of OTUs unique to a specific permafrost layer increased with depth from 57, 63 and 73% (0-5 cm, 11-15 cm, and 21-25 cm within the permafrost) when compared to the organic and mineral active layers.

The relative abundance of the most common taxa also changed with depth (Fig. 4). In the organic active layer, Proteobacteria was the most abundant phylum, but its relative abundance declined in the permafrost, where Actinobacteria became the most abundant phylum.

Acidobacteria and Verrucomicrobia had an intermediate level of relative abundance in the active layer, but declined by a factor of 4.5 in the permafrost. Bacteroidetes, on the other hand, was three times higher in the permafrost than the active layer. Chloroflexi also increased from the active layer to the permafrost by a small factor (1.4). Caldiserica and Firmicutes followed a different trend than the other phyla; they were very close to zero in the active layer, but then increased with depth in the permafrost from a relative abundance of 0.01 in the top of the permafrost to roughly 0.12 in the permafrost sampled 21-15cm below the maximum active layer thaw depth. AD3 and Gemma had a unique pattern; they increased from the organic to mineral active layer soils and then declined again in the permafrost.

NRI and NTI

The NRI trended towards increasing with depth, but only the deepest permafrost (21-25 cm below the maximum active layer thaw depth) was statistically different than the active layer samples (Tukey adjusted $p<0.05$) (Fig. 5 a). The NTI was 1.3 times higher for the organic active layer than the permafrost, but the mineral active layer was statistically the same as both the organic active layer and the permafrost (Fig. 5 b; Tukey adjusted $p>0.05$).

Discussion

The differences between the permafrost and the active layer with respect to their relationships of microbial diversity and depth or soil C suggest that environmental filtering, or selection, plays a role in reducing the diversity of the permafrost community relative to the active layer. Phylogenetic clustering of the permafrost microbial community further supports my hypothesis that the microbial community was selected for survival in this particular abiotic

regime. However, the permafrost microbial community was not selected from the active layer community members, and relationships derived from the similarity of UniFrac distances, depth and C indicated that the permafrost community structure was strongly affected by the site history, suggesting that the current community was selected for current conditions from a historical species pool (Fig. 6).

Evidence for environmental filtering in permafrost

Species diversity in soils typically declines with depth (Eilers et al., 2012; Federle et al., 1986; Fierer et al., 2003), and there is growing evidence that the active layer hosts a diverse community (Chu et al., 2010; Frank-Fahle et al., 2014; Tveit et al., 2012; Zhou et al., 1997) while the permafrost community is less diverse (Steven et al., 2007a; Vishnivetskaya et al., 2006). None of these previous studies explicitly investigated the differences in the relationship between microbial community structure and richness with depth or C in permafrost and active layer soils. My study reveals differences in these relationships and indicates that an environmental filter exists between the active layer and the permafrost. The active layer species richness declines with depth (Fig. 1), although the index 'PD whole tree' was not robust to the variation between the different cores and thus, the slopes were not significantly different. Similarly, Frank-Fahle et al. (2014) also observed a decline in species diversity in the active layer in Canadian Arctic polygonal tundra. In contrast, in the permafrost alpha diversity was unaffected by depth (Fig. 1), which has also been observed previously (Gilichinsky and Wagener, 1995; Steven et al., 2008).

Differences in edaphic factors, such as C chemistry and pH, have been shown to strongly control microbial community richness and structure (Chu et al., 2010; Fierer et al., 2003; Fierer

and Jackson, 2006; Lauber et al., 2009), however this seems not to be the case for the soils in this study. Soil C is four times greater in the organic active layer than the mineral active layer and permafrost (Ernakovich, 2014), and pH is the lowest for the organic active layer and similar for the mineral active layer and permafrost soils. Mineral active layer and permafrost soils have similar C content and chemistry (Ernakovich, 2014; White et al., 2004) as well as pH (Borden et al., 2010; Ernakovich, 2014). Microbial diversity did not vary predictably with soil C for either the permafrost or the active layer (Fig. 1 and Table 3.1). The active layer had a greater alpha diversity than the permafrost even at similar C contents, which can be observed in comparing the mineral active layer and permafrost soils (Fig. 1). Species composition (beta diversity) also had no relationship with C content and pH. In the active layer, mineral and organic soils have relatively similar beta diversity, but vastly different C content and chemistry. Despite the similar soil characteristics, the community composition of the mineral active layer and the permafrost was very different (Fig. 2). This difference in diversity and composition at the same values of soil C provides further support that the conditions in the permafrost impose an environmental filter that reduces diversity.

The most obvious candidate environmental filter is the persistently frozen condition on a millennial timescale in the permafrost in contrast to the seasonal transitions between above- and below-freezing temperatures in the active layer. Thus, the harsh conditions in permafrost may be responsible for the reduction in species richness (Steven et al., 2007a). Frozen conditions also result in stress to the microbes from high salt concentrations, low redox potentials, oligotrophic conditions and high radiation (Steven et al., 2007a), and could also suppress species diversity in permafrost by hampering dispersal of new species and reducing niche space caused by the relatively static nature of the temperature regime. However, introduction of species from the

active layer to the permafrost in warmer years is thought to be an important mechanism for dispersal of species into permafrost (Gilichinsky and Wagener, 1995; Gilichinsky et al., 2007), and temperature niches have been observed in the permafrost (Tuorto et al., 2014), making these mechanisms likely less likely than a reduction due to the frozen conditions.

The harsh environment in permafrost could result in (1) random chance of death for individuals resulting in a non-ordered community, or (2) selection for a community specialized for these conditions. The permafrost microbial community did not show evidence that it is a subset of the active layer community under either scenario. First, if random death played a role in structuring the permafrost microbial community, the alpha diversity would be equal between the active layer and the permafrost, which it was not (Fig. 1). However, it must be noted that if dispersal rates from the active layer to the permafrost are lower than into the active layer from elsewhere, this could result in lower alpha diversity in the permafrost. Beta diversity indicates that the active layer and permafrost communities are distinct and that the permafrost is not a subset of the active layer. The beta diversity separates along PCoA 1 between the active layer and permafrost (Fig. 2), especially for the unweighted UniFrac metric, which is particularly powerful when analyzing differences in communities due to selection pressures imposed by temperature regimes (Lozupone et al., 2007). If the permafrost community members were selected from the active layer for success in permafrost, all the species present in the permafrost would be present in the active layer. However, only 0.2% of the OTUs observed were present in all the depths sampled, and the majority of the OTUs found in the permafrost were not observed in the active layer (Fig. 3 a and b). This indicates that the permafrost microbial community did not originate through dispersal from the active layer community. However, it is possible that the permafrost OTUs are present in the active layer, but that they are rare and were not picked up by

the depth of my sequence analysis or that they were removed because they were not present in 50% of the replicates.

Actinobacteria increased with depth (Fig. 4), which is not uncommon from surface to subsurface soils (Fierer et al., 2003) or from the active layer to the permafrost (Wilhelm et al., 2011). Actinobacteria have a high G-C content, which is a known adaptation of survival in the cold (Shi et al., 1997; Willerslev et al., 2004), which might contribute to their importance in this study. Willhelm et al. (2011) found that Acidobacteria were present in the active layer but not the permafrost. My study corroborates that Acidobacteria are most prevalent in active layer soils. Acidobacteria dominate in acidic soils (Chu et al., 2010), such as the organic active layer (Wallenstein et al., 2007), but in this study, their relative abundance remained high in the less acidic mineral active layer soils, suggesting that dispersal from the organic to mineral active layer soils is important. Tuorto et al. (2014) found that relatives of known psychrophiles from the phyla Acidobacteria, Actinobacteria, Chloroflexi, Gemmatimonadetes and Proteobacteria were all active below freezing between 0 and -20 °C. All of these phyla were also the most common in the permafrost in this study (Fig. 4), supporting that selection results in a bacterial community capable of functioning in permafrost.

Previous studies have shown that the permafrost community is capable of metabolic processes under the abiotic conditions imposed by the permafrost (Rivkina et al., 2000; Santrucková et al., 2003; Tuorto et al., 2014; Waldrop et al., 2010), indicating that the community is selected at least for survival in the permafrost environment. Both the active layer and the permafrost communities are phylogenetically clustered relative to random chance (NRI and NTI>0, Fig. 5), indicating that habitat filtering likely plays a role in structuring both communities (Horner-Devine and Bohannan, 2006). The increasing trend of NRI with depth

suggests that the permafrost communities are selected for their environment, because traits are generally phylogenetically conserved (A. C. Martiny et al., 2013; Webb, 2000). However, the NTI is lower for the permafrost than the active layer, indicating that the permafrost microbes are relatively more dispersed at the tips of the tree than the active layer. Harsh environments generally increase phylogenetic clustering (Horner-Devine and Bohannan, 2006), but this decline in NTI and concurrent increase in NRI likely indicates that the ability to succeed under permafrost conditions is dictated at the phyla level rather than finer taxonomic scales. In contrast, phylogenetic relatedness in the active layer increases towards the tips of the tree.

The elevated relatedness at the phyla level of the bacteria in permafrost suggests that selection for the conditions in permafrost occurs at a relatively deep phylogenetic level and is an additional support for an environmental filter in the microbial community. The observation that the community does not originate from the active layer points to possible effects of history in structuring the microbial community. The permafrost at this site is at least 10,000 years old (Borden et al., 2010). Thus, the current permafrost community is likely shaped by both the stress imposed by the frozen conditions and the historical conditions before the formation of the permafrost (Fig. 6).

Evidence of historical influences on microbial species diversity

Discerning whether microbial diversity is controlled by the same factors as plant and animal diversity (such as MAT, PET) is a central debate in microbial ecology both from the perspective of understanding patterns of species distribution and in order to predict potential changes to community composition and function with climate change (Fierer and Jackson, 2006; Green and Bohannan, 2006; Green et al., 2008; Horner-Devine and Bohannan, 2006; J. B. H.

Martiny et al., 2006). In a global survey of microbial diversity, Fierer and Jackson (2006) found that edaphic soil properties, specifically pH, soil moisture and carbon content, were highly correlated to microbial diversity, but that site level properties, such as MAT, PET and latitude were not correlated. They interpreted this to mean that microbial systems are not structured by similar factors as macro-scale communities. Further, Chu et al. (2010) demonstrated that the relatedness of microbial members in a community from global samples was not differentiated by biome type or geographic distance, but rather pH. Together, these results indicate that edaphic soil properties are the dominant control on microbial diversity. In contrast, in the current study the similarity in C content and pH between the mineral active layer and permafrost soils concurrent with differences in alpha and beta diversity indicate controls other than edaphic properties on microbial diversity.

Both the current environmental conditions and historical conditions can play a role in structuring a microbial community (J. B. H. Martiny et al., 2006). Employing the Martiny et al. (2006) biogeography framework for its explicit inclusion of current and historic conditions, I suggest that these communities fall into the category "multiple habitats (current conditions) and multiple provinces (historical conditions)," exemplifying the importance of historical conditions in structuring a microbial community (Evans and Wallenstein, 2014). Several studies have found evidence of a historical influence on the microbial community composition at a particular site (Kennedy et al., 1994; Kieft et al., 1998; Pagaling et al., 2013; Steven et al., 2007a). An extreme and physically isolated environment, such as permafrost, allows the detection of this mechanism. Once the historical filter has selected the potential pool of species, then edaphic properties (Fierer and Jackson, 2006) can resume their role in structuring the community.

My findings that microbial community structure is affected by both the historical species pool and environmental filters is supported in other extreme environments (Fiser et al., 2012) or extreme conditions (Evans and Wallenstein, 2014). However, it is possible that permafrost can preserve DNA from dead microorganisms (Steven et al., 2007a), which would be included in the analysis of the 16S rRNA gene and my interpretation of community assembly. But, in a stable isotope probing experiment, Tuorto et al. (2014) found that 80% of the bacterial population was capable of genome replication, indicating the preservation of dead DNA does not lead to amplification of DNA from species that are no longer part of the community. On another note, my comparison of community assembly between the active layer and the permafrost only included the active layer community sampled in the summer, and it is possible that I would have seen more overlap between the active layer and permafrost community compositions if I had analyzed the winter active layer community. But, the major phyla in the active layer are consistent throughout the year (Wallenstein et al., 2007), so overlap in the communities should have been detectable if the winter community had merely decreased its relative abundance. Additionally, any potential dispersal from the active layer to the permafrost would occur when the active layer was thawed, so the summer community is an accurate reference for determining community assembly in the permafrost.

In summary, the richness and membership of the permafrost microbial community appears to be filtered by the frozen conditions, such that the community is selected for the member's ability to survive (Bölter, 1995; Soina et al., 2004) and replicate at frozen temperatures (Santrucková et al., 2003; Tuorto et al., 2014; Waldrop et al., 2010). But, this potential community is first a reflection of the historical species pool (Fig. 6). The alpha diversity is greater in the active layer than the permafrost, even at similar pH and levels of

carbon, which contradicts findings that edaphic properties are the strongest controls on microbial species diversity (Fierer and Jackson, 2006). Community structure is also different between the permafrost and active layer. The finding that the mineral active layer and permafrost soils have different community structure despite their similar pH contradicts the finding by Chu et al. (2010) that soil pH is more important in determining community structure than site level characteristics, such as temperature. Further, the clustering (indicated by the higher NRI) of the permafrost samples supports that these microbes were selected for their habitat. This indicates that the historical filter dictated the initial community composition, and that environmental filtering further selected for the microbial community currently present.

Tables

Table 3.1. Random coefficients model results for various alpha diversity indices regressed against sample depth and soil C. Estimates for the intercept and slope for the active layer and permafrost and their associated significance (difference from intercept or slope =0) are included. Whole model fit (-2 log likelihood) and p-values for layer (active layer vs. permafrost), independent variable and the interaction, as well as the associated numerator and denominator degrees of freedom (num df and den df, respectively) and F value.

	Observed Species								PD Whole Tree							
	AL est.	p	Perm est.	p	num df	den df	F	p	Fit	AL est.	p	Perm est.	p	num df	den df	F	p	Fit
Depth																		
model									395.3									300.0
layer (intercept)	733.41	***	427.39	***	1	27.6	14.7700	***		53.75	·	40.20	***	1	12.3	3.5000	·	
depth					1	27.6	13.4300	***						1	33.0	0.2200	ns	
layer*depth (slope)	-18.01	*	-2.68	ns	1	27.6	7.3700	*		-0.77	ns	-0.25	ns	1	33.0	0.0600	ns	
Carbon																		
model									400.5									238.1
layer (intercept)	530.92	·	279.91	*	1	9.4	3.3400	·		44.21	**	27.08	***	1	28.2	8.7200	**	
C					1	3.2	0.4700	ns						1	30.0	0.6100	ns	
layer*C (slope)	4.17	ns	3.78	ns	1	3.2	0.0000	ns		0.21	ns	0.19	ns	1	30.0	0.0000	ns	

*** p<0.001
**p<0.01
*p<0.05
·p<0.10

Figures

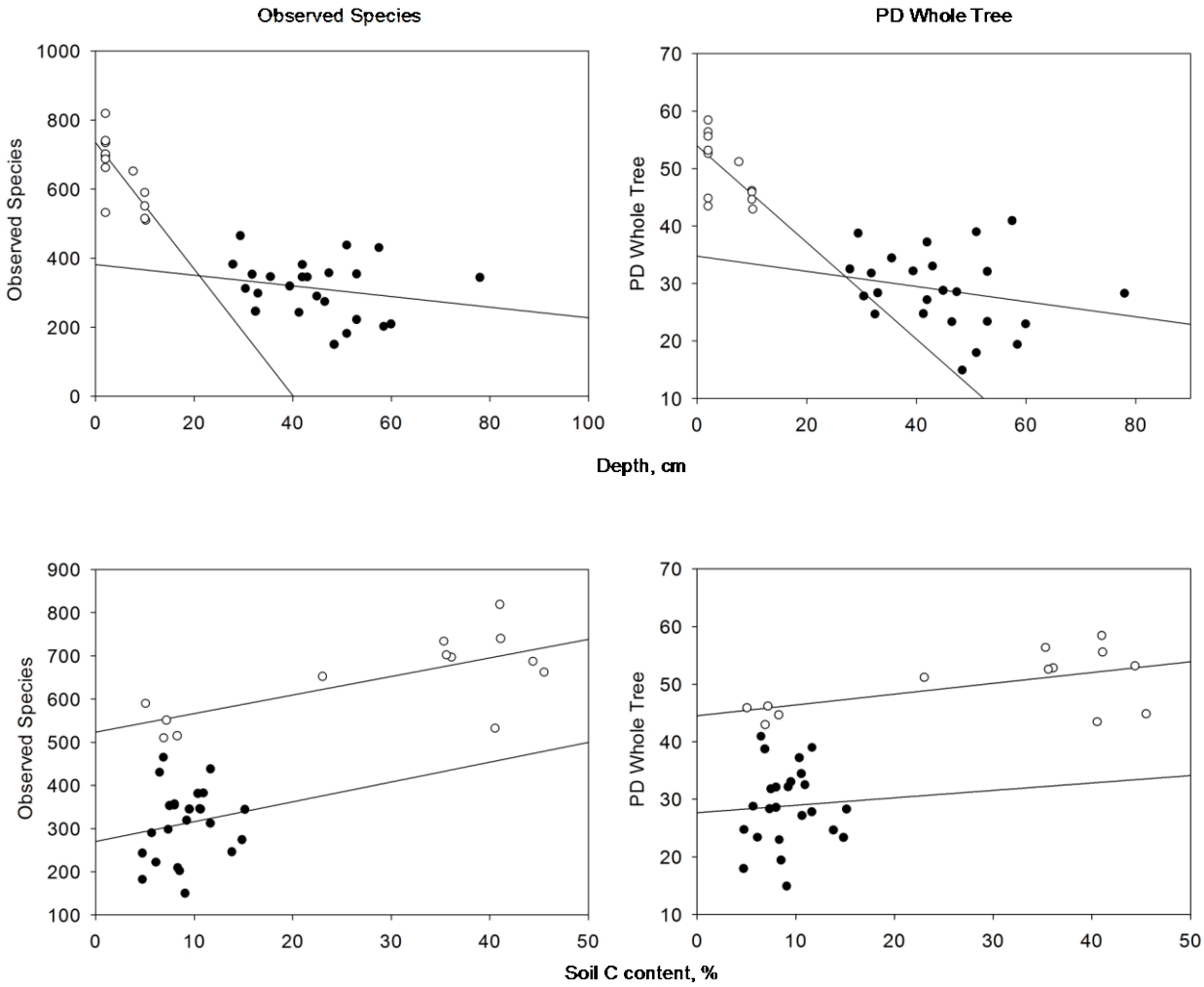

Figure 3.1. Alpha diversity metrics regressed against depth and % C. Closed circles are permafrost and open circles are active layer samples.

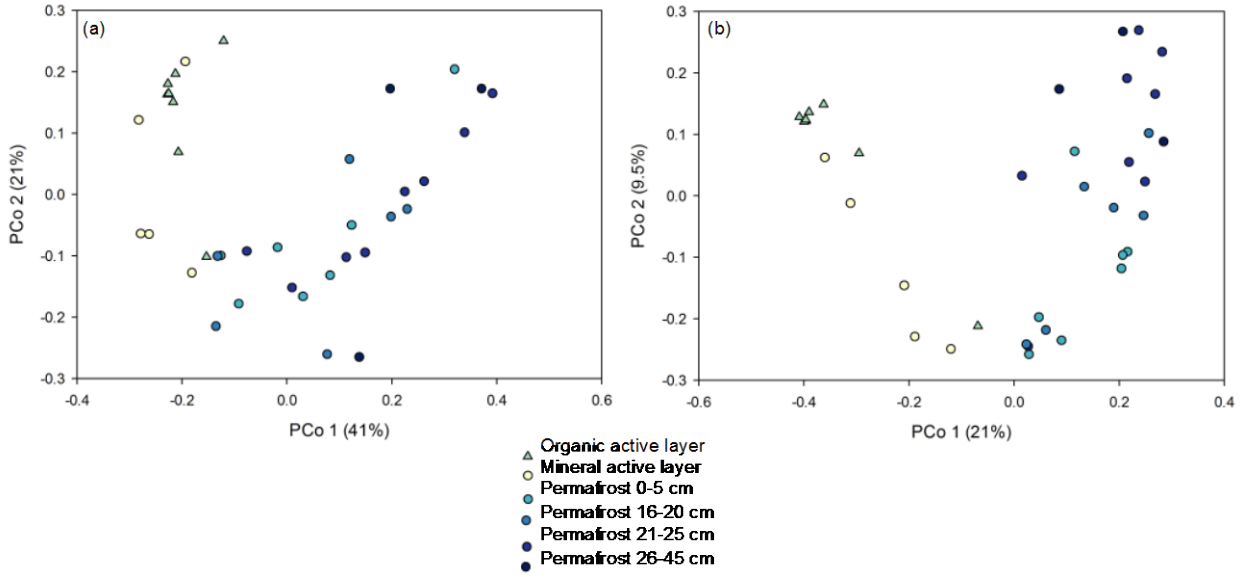

Figure 3.2. Comparison of different soil depths based on principle coordinates analysis of pairwise (a) weighted and (b) unweighted UniFrac distances.

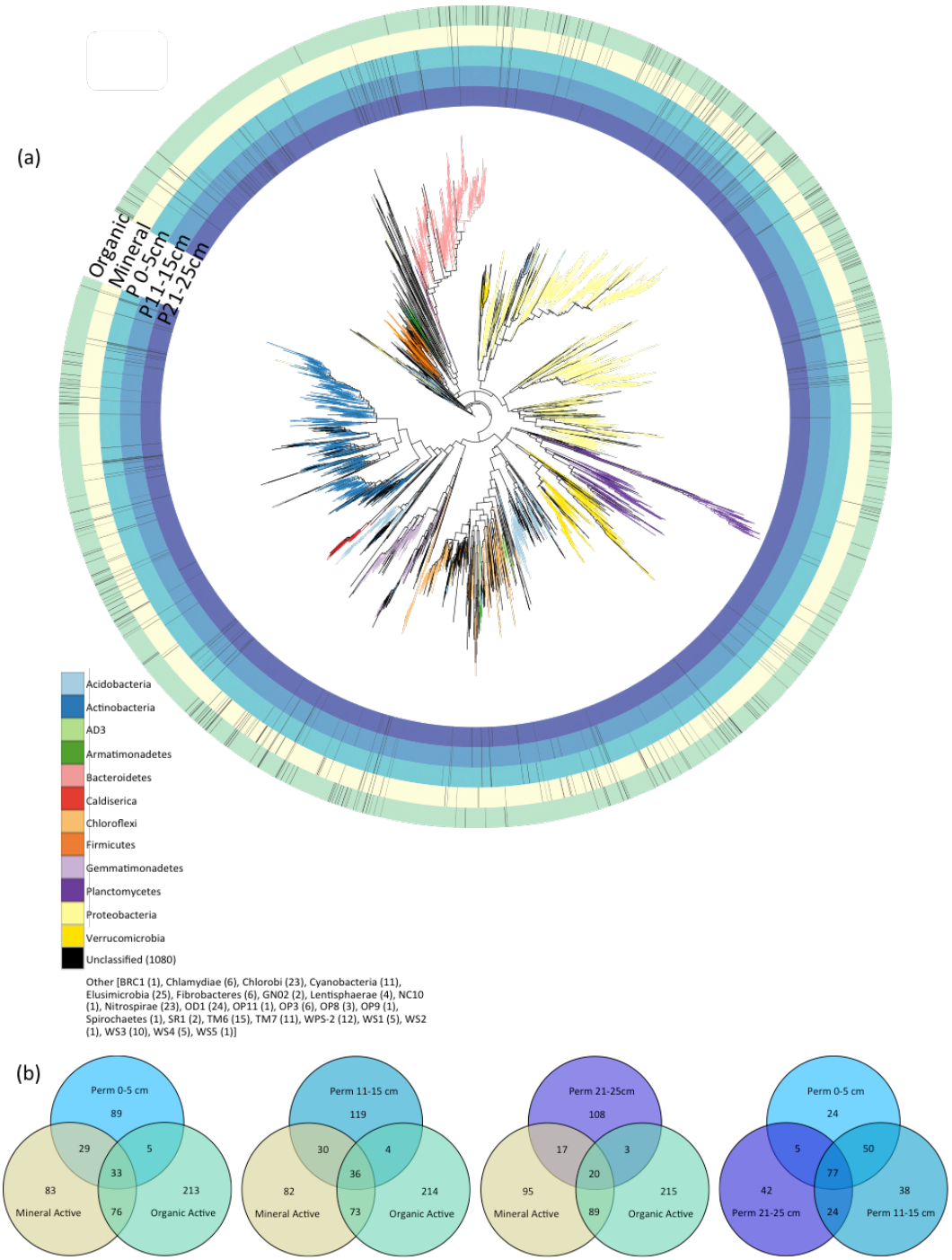

Figure 3.3. (a) ITOL figures indicating the presence of bacterial OTUs in different depths along the soil profiles. (b) Venn diagrams indicating the number of unique OTUs for different soil depths.

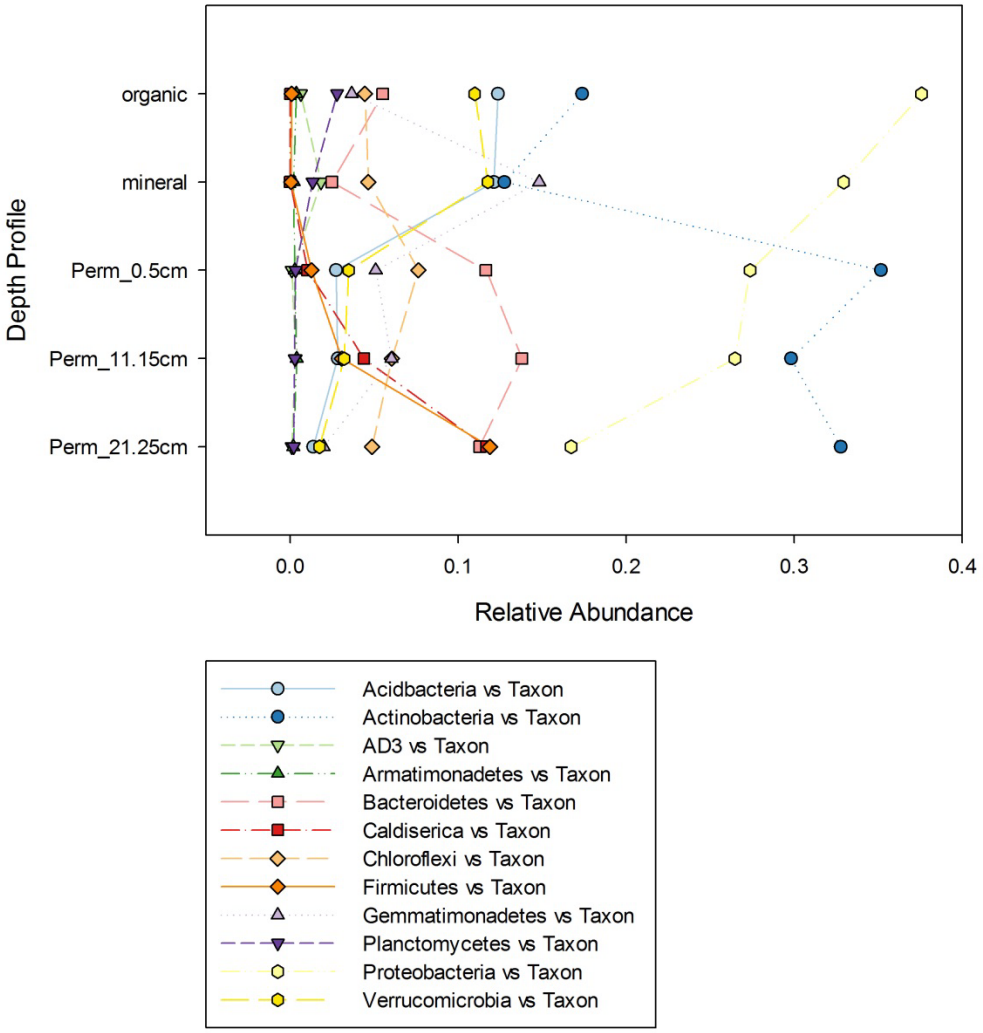

Figure 3.4. The relative abundance of bacterial taxa with depth.

(a)

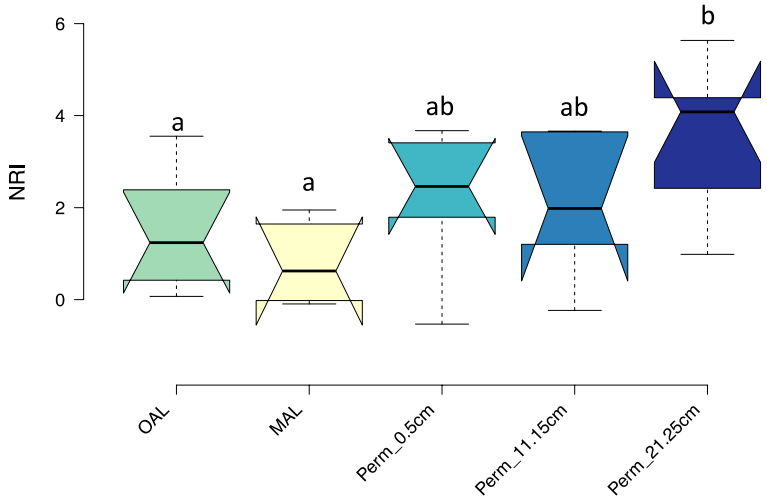

(b)

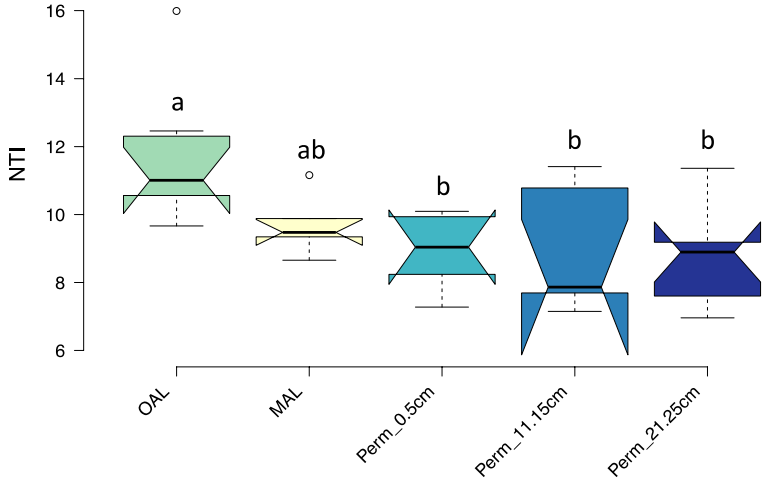

Figure 3.5. Boxplots of (a) NRI and (b) NTI. The center lines show the medians, and box limits indicate the 25th and 75th percentiles as determined by R software. The whiskers extend 1.5 times the interquartile range from the 25th and 75th percentiles, and outliers are represented by dots. n = 8, 5, 6, 6, and 8 sample points. Different letters represent statistical differences between the means after a Tukey multiple comparison adjustment.

References

Bakermans, C., Tsapin, A.I., Souza Egipsy, V., Gilichinsky, D.A., Nealson, K.H., 2003. Reproduction and metabolism at− 10 C of bacteria isolated from Siberian permafrost. Environmental Microbiology 5, 321–326.

Borden, P.W., Ping, C.-L., McCarthy, P.J., Naidu, S., 2010. Clay Mineralogy in Arctic Tundra Gelisols, Northern Alaska. Soil Science Society of America Journal 74, 580. doi:10.2136/sssaj2009.0187

Bölter, M., 1995. Distribution of bacterial numbers and biomass in soils and on plants from King George Island (Arctowski Station, Maritime Antarctica). Polar Biol 15, 115–124.

Bölter, M., 2004. Ecophysiology of psychrophilic and psychrotolerant microorganisms. Cell. Mol. Biol. (Noisy-le-grand) 50, 563–573.

Caporaso, J.G., Bittinger, K., Bushman, F.D., DeSantis, T.Z., Andersen, G.L., Knight, R., 2010a. PyNAST: a flexible tool for aligning sequences to a template alignment. Bioinformatics 26, 266–267. doi:10.1093/bioinformatics/btp636

Caporaso, J.G., Kuczynski, J., Stombaugh, J., Bittinger, K., Bushman, F.D., Costello, E.K., Fierer, N., Peña, A.G., Goodrich, J.K., Gordon, J.I., Huttley, G.A., Kelley, S.T., Knights, D., Koenig, J.E., Ley, R.E., Lozupone, C.A., McDonald, D., Muegge, B.D., Pirrung, M., Reeder, J., Sevinsky, J.R., Turnbaugh, P.J., Walters, W.A., Widmann, J., Yatsunenko, T., Zaneveld, J., Knight, R., 2010b. QIIME allows analysis of high-throughput community sequencing data. Nature Publishing Group 7, 335–336. doi:10.1038/nmeth.f.303

Chu, H., Fierer, N., Lauber, C.L., Caporaso, J.G., Knight, R., Grogan, P., 2010. Soil bacterial diversity in the Arctic is not fundamentally different from that found in other biomes. Environmental Microbiology 12, 2998–3006. doi:10.1111/j.1462-2920.2010.02277.x

Coolen, M.J.L., van de Giessen, J., Zhu, E.Y., Wuchter, C., 2011. Bioavailability of soil organic matter and microbial community dynamics upon permafrost thaw. Environmental Microbiology 13, 2299–2314. doi:10.1111/j.1462-2920.2011.02489.x

Deming, J.W., 2002. Psychrophiles and polar regions. Current Opinion in Microbiology 5, 301–309.

Drotz, S.H., Sparrman, T., Nilsson, M.B., Schleucher, J., Oquist, M.G., 2010. Both catabolic and anabolic heterotrophic microbial activity proceed in frozen soils. Proc. Natl. Acad. Sci. U.S.A. 107, 21046–21051. doi:10.1073/pnas.1008885107

Edgar, R.C., 2010. Search and clustering orders of magnitude faster than BLAST. Bioinformatics 26, 2460–2461. doi:10.1093/bioinformatics/btq461

Eilers, K.G., Debenport, S., Anderson, S., Fierer, N., 2012. Soil Biology & Biochemistry. Soil Biology and Biochemistry 50, 58–65. doi:10.1016/j.soilbio.2012.03.011

Ernakovich, J.G., 2014. The Chemical Properties of Alaskan Permafrost and Seasonally Thawed Soils, in: Wallenstein, M.D., Reardon, K.F. (Eds.), Vulnerability of Permafrost Carbon to Decomposition. Colorado State University.

Evans, S.E., Wallenstein, M.D., 2011. Soil microbial community response to drying and rewetting stress: does historical precipitation regime matter? Biogeochemistry 109, 101–116. doi:10.1007/s10533-011-9638-3

Evans, S.E., Wallenstein, M.D., 2014. Climate change alters ecological strategies of soil bacteria. Ecology Letters 17, 155–164. doi:10.1111/ele.12206

Faith, D.P., 1992. Conservation evaluation and phylogenetic diversity. Biological Conservation 61, 1–10.
Federle, T.W., Dobbins, D.C., Thornton Manning, J.R., Jones, D.D., 1986. Microbial biomass, activity, and community structure in subsurface soils. Ground Water 24, 365–374.
Fierer, N., Hamady, M., Lauber, C.L., Knight, R., 2008. The influence of sex, handedness, and washing on the diversity of hand surface bacteria. Proc. Natl. Acad. Sci. U.S.A. 105, 17994–17999. doi:10.1073/pnas.0807920105
Fierer, N., Jackson, R.B., 2006. The diversity and biogeography of soil bacterial communities. Proceedings of the National Academy of Sciences 103, 626–631. doi:10.1073/pnas.0507535103
Fierer, N., Schimel, J.P., Holden, P.A., 2003. Variations in microbial community composition through two soil depth profiles. Soil Biology and Biochemistry 35, 167–176.
Fiser, C., Blejec, A., Trontelj, P., 2012. Niche-based mechanisms operating within extreme habitats: a case study of subterranean amphipod communities. Biology Letters 8, 578–581. doi:10.1111/j.1461-0248.2007.01041.x
Frank-Fahle, B.A., Yergeau, E., Greer, C.W., Lantuit, H., Wagner, D., 2014. Microbial Functional Potential and Community Composition in Permafrost-Affected Soils of the NW Canadian Arctic. PLoS ONE 9, e84761. doi:10.1371/journal.pone.0084761.t003
Gilichinsky, D., Wagener, S., 1995. Microbial life in permafrost: a historical review. Permafrost Periglac. Process. 6, 243–250.
Gilichinsky, D.A., Wilson, G.S., Friedmann, E.I., McKay, C.P., Sletten, R.S., Rivkina, E.M., Vishnivetskaya, T.A., Erokhina, L.G., Ivanushkina, N.E., Kochkina, G.A., Shcherbakova, V.A., Soina, V.S., Spirina, E.V., Vorobyova, E.A., Fyodorov-Davydov, D.G., Hallet, B., Ozerskaya, S.M., Sorokovikov, V.A., Laurinavichyus, K.S., Shatilovich, A.V., Chanton, J.P., Ostroumov, V.E., Tiedje, J.M., 2007. Microbial Populations in Antarctic Permafrost: Biodiversity, State, Age, and Implication for Astrobiology. Astrobiology 7, 275–311. doi:10.1089/ast.2006.0012
Graham, D.E., Wallenstein, M.D., Vishnivetskaya, T.A., Waldrop, M.P., Phelps, T.J., Pfiffner, S.M., Onstott, T.C., Whyte, L.G., Rivkina, E.M., Gilichinsky, D.A., Elias, D.A., Mackelprang, R., VerBerkmoes, N.C., Hettich, R.L., Wagner, D., Wullschleger, S.D., Jansson, J.K., 2011. Microbes in thawing permafrost: the unknown variable in the climate change equation 6, 709–712. doi:10.1038/ismej.2011.163
Green, J., Bohannan, B.J.M., 2006. Spatial scaling of microbial biodiversity. Trends in Ecology & Evolution 21, 501–507. doi:10.1016/j.tree.2006.06.012
Green, J.L., Bohannan, B.J.M., Whitaker, R.J., 2008. Microbial biogeography: from taxonomy to traits. Science 320, 1039–1043. doi:10.1126/science.1153475
Hamady, M., Walker, J.J., Harris, J.K., Gold, N.J., Knight, R., 2008. Error-correcting barcoded primers for pyrosequencing hundreds of samples in multiplex. Nature Publishing Group 5, 235–237. doi:10.1038/nmeth.1184
Hansen, A.A., Herbert, R.A., Mikkelsen, K., Jensen, L.L., Kristoffersen, T., Tiedje, J.M., Lomstein, B.A., Finster, K.W., 2007. Viability, diversity and composition of the bacterial community in a high Arctic permafrost soil from Spitsbergen, Northern Norway. Environmental Microbiology 9, 2870–2884. doi:10.1111/j.1462-2920.2007.01403.x
Horner-Devine, M.C., Bohannan, B.J.M., 2006. Phylogenetic clustering and overdispersion in bacterial communities. Ecology 87, S100–8.

Hugelius, G., Tarnocai, C., Broll, G., Canadell, J.G., Kuhry, P., Swanson, D.K., 2013. The Northern Circumpolar Soil Carbon Database: spatially distributed datasets of soil coverage and soil carbon storage in the northern permafrost regions. Earth System Science Data 5, 3–13. doi:10.5879/ecds/00000001

Johnson, S.S., Hebsgaard, M.B., Christensen, T.R., Mastepanov, M., Nielsen, R., Munch, K., Brand, T., Gilbert, M.T.P., Zuber, M.T., Bunce, M., Rønn, R., Gilichinsky, D., Froese, D., Willerslev, E., 2007. Ancient bacteria show evidence of DNA repair. Proceedings of the National Academy of Sciences 104, 14401–14405. doi:10.1073/pnas.0706787104

Kennedy, M.J., Reader, S.L., Swierczynski, L.M., 1994. Preservation records of micro-organisms: evidence of the tenacity of life. Microbiology (Reading, Engl.) 140 (Pt 10), 2513–2529.

Kieft, T., Murphy, E., Haldeman, D., Amy, P., Bjornstad, B., McDonald, E., Ringelberg, D., White, D., Stair, J., Griffiths, R., Gsell, T., Holben, W., Boone, D., 1998. Microbial Transport, Survival, and Succession in a Sequence of Buried Sediments. Microb Ecol 36, 336–348.

Kuhry, P., Ping, C.-L., Schuur, E.A.G., Tarnocai, C., Zimov, S., 2009. Report from the International Permafrost Association: carbon pools in permafrost regions. Permafrost Periglac. Process. 20, 229–234. doi:10.1002/ppp.648

Lauber, C.L., Hamady, M., Knight, R., Fierer, N., 2009. Pyrosequencing-based assessment of soil pH as a predictor of soil bacterial community structure at the continental scale. Applied and Environmental Microbiology 75, 5111–5120. doi:10.1128/AEM.00335-09

Letunic, I., Bork, P., 2011. Interactive Tree Of Life v2: online annotation and display of phylogenetic trees made easy. Nucleic Acids Research 39, W475–W478. doi:10.1093/nar/gkr201

Liu, K., Raghavan, S., Nelesen, S., Linder, C.R., Warnow, T., 2009. Rapid and Accurate Large-Scale Coestimation of Sequence Alignments and Phylogenetic Trees. Science 324, 1561–1564. doi:10.1126/science.1171243

Lozupone, C., Knight, R., 2005. UniFrac: a New Phylogenetic Method for Comparing Microbial Communities. Applied and Environmental Microbiology 71, 8228–8235. doi:10.1128/AEM.71.12.8228-8235.2005

Lozupone, C.A., Hamady, M., Kelley, S.T., Knight, R., 2007. Quantitative and Qualitative Diversity Measures Lead to Different Insights into Factors That Structure Microbial Communities. Applied and Environmental Microbiology 73, 1576–1585. doi:10.1128/AEM.01996-06

Mackelprang, R., Waldrop, M.P., DeAngelis, K.M., David, M.M., Chavarria, K.L., Blazewicz, S.J., Rubin, E.M., Jansson, J.K., 2011. Metagenomic analysis of a permafrost microbial community reveals a rapid response to thaw. Nature 480, 368–371. doi:10.1038/nature10576

Martiny, A.C., Treseder, K., Pusch, G., 2013. Phylogenetic conservatism of functional traits in microorganisms. ISME J 7, 830–838. doi:10.1038/ismej.2012.160

Martiny, J.B.H., Bohannan, B.J.M., Brown, J.H., Colwell, R.K., Fuhrman, J.A., Green, J.L., Horner-Devine, M.C., Kane, M., Krumins, J.A., Kuske, C.R., Morin, P.J., Naeem, S., Øvreås, L., Reysenbach, A.-L., Smith, V.H., Staley, J.T., 2006. Microbial biogeography: putting microorganisms on the map. Nat Rev Micro 4, 102–112. doi:10.1038/nrmicro1341

McDonald, D., Price, M.N., Goodrich, J., Nawrocki, E.P., DeSantis, T.Z., Probst, A., Andersen, G.L., Knight, R., Hugenholtz, P., 2011. An improved Greengenes taxonomy with explicit ranks for ecological and evolutionary analyses of bacteria and archaea. ISME J 6, 610–618. doi:10.1038/ismej.2011.139

McMahon, S.K., Wallenstein, M.D., Schimel, J.P., 2009. Microbial growth in Arctic tundra soil at −2°C. Environmental Microbiology Reports 1, 162–166. doi:10.1111/j.1758-2229.2009.00025.x

Michaelson, G.J., Ping, C.L., Jorgenson, M.T., 2011. Methane and carbon dioxide content in eroding permafrost soils along the Beaufort Sea coast, Alaska. J. Geophys. Res. 116, G01022. doi:10.1029/2010JG001387

Mondav, R., Ben J Woodcroft, Kim, E.-H., McCalley, C.K., Hodgkins, S.B., Crill, P.M., Chanton, J., Hurst, G.B., VerBerkmoes, N.C., Saleska, S.R., Hugenholtz, P., Rich, V.I., Tyson, G.W., 2014. Discovery of a novel methanogen prevalent in thawing permafrost. Nature Communications 5, 1–7. doi:10.1038/ncomms4212

Nemergut, D.R., Schmidt, S.K., Fukami, T., O'Neill, S.P., Bilinski, T.M., Stanish, L.F., Knelman, J.E., Darcy, J.L., Lynch, R.C., Wickey, P., Ferrenberg, S., 2013. Patterns and Processes of Microbial Community Assembly. Microbiology and Molecular Biology Reviews 77, 342–356. doi:10.1128/MMBR.00051-12

Pagaling, E., Strathdee, F., Spears, B.M., Cates, M.E., Allen, R.J., Free, A., 2013. Community history affects the predictability of microbial ecosystem development 8, 19–30. doi:10.1038/ismej.2013.150

Ponder, M.A., Gilmour, S.J., Bergholz, P.W., Mindock, C.A., Hollingsworth, R., Thomashow, M.F., Tiedje, J.M., 2005. Characterization of potential stress responses in ancient Siberian permafrost psychroactive bacteria. FEMS Microbiol Ecol 53, 103–115. doi:10.1016/j.femsec.2004.12.003

Ponder, M.A., Thomashow, M.F., Tiedje, J.M., 2008. Metabolic activity of Siberian permafrost isolates, Psychrobacter arcticus and Exiguobacterium sibiricum, at low water activities. Extremophiles 12, 481–490. doi:10.1007/s00792-008-0151-0

Price, M.N., Dehal, P.S., Arkin, A.P., 2010. FastTree 2–approximately maximum-likelihood trees for large alignments. PLoS ONE 5, e9490.

Price, P.B., Sowers, T., 2004. Temperature dependence of metabolic rates for microbial growth, maintenance, and survival. Proceedings of the National Academy of Sciences 101, 4631–4636. doi:10.1073/pnas.0400522101

R Core Development Team, 2013. *R: A Language and Environment for Statistical Computing.*

Rivkina, E., Gilichinsky, D., Wagener, S., Tiedje, J., McGrath, J., 1998. Biogeochemical activity of anaerobic microorganisms from buried permafrost sediments. Geomicrobiology Journal 15, 187–193.

Rivkina, E., Laurinavichius, K., McGrath, J., Tiedje, J., Shcherbakova, V., Gilichinsky, D., 2004. Microbial life in permafrost. Advances in Space Research 33, 1215–1221. doi:10.1016/j.asr.2003.06.024

Rivkina, E., Shcherbakova, V., Laurinavichius, K., Petrovskaya, L., Krivushin, K., Kraev, G., Pecheritsina, S., Gilichinsky, D., 2007. Biogeochemistry of methane and methanogenic archaea in permafrost. FEMS Microbiol Ecol 61, 1–15. doi:10.1111/j.1574-6941.2007.00315.x

Rivkina, E.M., Friedmann, E.I., McKay, C.P., Gilichinsky, D.A., 2000. Metabolic activity of permafrost bacteria below the freezing point. Applied and Environmental Microbiology 66, 3230–3233. doi:10.1128/AEM.66.8.3230-3233.2000

Roesch, L.F.W., Fulthorpe, R.R., Riva, A., Casella, G., Hadwin, A.K.M., Kent, A.D., Daroub, S.H., Camargo, F.A.O., Farmerie, W.G., Triplett, E.W., 2007. Pyrosequencing enumerates and contrasts soil microbial diversity. ISME J. doi:10.1038/ismej.2007.53

RStudio and Inc, 2013. *shiny: Web Application Framework for R.*

Russell, N.J., 1997. Psychrophilic bacteria--molecular adaptations of membrane lipids. Comp. Biochem. Physiol. A Physiol. 118, 489–493.

Santrucková, H., Bird, M.I., Kalaschnikov, Y.N., Grund, M., Elhottova, D., Šimek, M., Grigoryev, S., Gleixner, G., Arneth, A., Schulze, E.-D., Lloyd, J., 2003. Microbial characteristics of soils on a latitudinal transect in Siberia. Glob Change Biol 9, 1106–1117.

Shi, T., Reeves, R.H., Gilichinsky, D.A., Friedmann, E.I., 1997. Characterization of viable bacteria from Siberian permafrost by 16S rDNA sequencing. Microb Ecol 33, 169–179.

Soina, V.S., Mulyukin, A.L., Demkina, E.V., Vorobyova, E.A., El-Registan, G.I., 2004. The structure of resting bacterial populations in soil and subsoil permafrost. Astrobiology 4, 345–358.

Soina, V.S., Vorobiova, E.A., Zvyagintsev, D.G., Gilichinsky, D.A., 1995. Preservation of cell structures in permafrost: a model for exobiology. Adv Space Res 15, 237–242.

Steven, B., Briggs, G., McKay, C.P., Pollard, W.H., Greer, C.W., Whyte, L.G., 2007a. Characterization of the microbial diversity in a permafrost sample from the Canadian high Arctic using culture-dependent and culture-independent methods. FEMS Microbiol Ecol 59, 513–523. doi:10.1111/j.1574-6941.2006.00247.x

Steven, B., Léveillé, R., Pollard, W.H., Whyte, L.G., 2006. Microbial ecology and biodiversity in permafrost. Extremophiles 10, 259–267. doi:10.1007/s00792-006-0506-3

Steven, B., Niederberger, T.D., Bottos, E.M., Dyen, M.R., Whyte, L.G., 2007b. Development of a sensitive radiorespiration method for detecting microbial activity at subzero temperatures. Journal of Microbiological Methods 71, 275–280. doi:10.1016/j.mimet.2007.09.009

Steven, B., Niederberger, T.D., Whyte, L.G., 2009. Bacterial and Archaeal Diversity in Permafrost, in: Margesin, R. (Ed.), Permafrost Soils. Springer Berlin Heidelberg, Berlin, Heidelberg, pp. 59–72. doi:10.1007/978-3-540-69371-0

Steven, B., Pollard, W.H., Greer, C.W., Whyte, L.G., 2008. Microbial diversity and activity through a permafrost/ground ice core profile from the Canadian high Arctic. Environmental Microbiology 10, 3388–3403. doi:10.1111/j.1462-2920.2008.01746.x

Suzina, N.E., Muliukin, A.L., Kozlova, A.N., Shorokhova, A.P., Dmitriev, V.V., Barinova, E.S., Mokhova, O.N., El'-Registan, G.I., Duda, V.I., 2004. [Ultrastructure of resting cells of some non-spore-forming bacteria]. Mikrobiologiia 73, 516–529.

Tarnocai, C., 1993. Sampling frozen soils, in: Carter, M.R. (Ed.), Soil Sampling and Methods of Analysis. Lewis Publishers, Boca Raton, pp. 755–765.

Tarnocai, C., Canadell, J.G., Schuur, E.A.G., Kuhry, P., Mazhitova, G., Zimov, S., 2009. Soil organic carbon pools in the northern circumpolar permafrost region. Global Biogeochem. Cycles 23, GB2023. doi:10.1029/2008GB003327

Thomas, T., Kumar, N., Cavicchioli, R., 2001. Effects of Ribosomes and Intracellular Solutes on Activities and Stabilities of Elongation Factor 2 Proteins from Psychrotolerant and Thermophilic Methanogens. Journal of Bacteriology 183, 1974–1982. doi:10.1128/JB.183.6.1974-1982.2001

Torsvik, V., 2002. Prokaryotic Diversity--Magnitude, Dynamics, and Controlling Factors. Science 296, 1064–1066. doi:10.1126/science.1071698
Tuorto, S.J., Darias, P., McGuinness, L.R., Panikov, N., Zhang, T., HÃggblom, M.M., Kerkhof, L.J., 2014. Bacterial genome replication at subzero temperatures in permafrost 8, 139–149. doi:10.1038/ismej.2013.140
Tveit, A., Schwacke, R., Svenning, M.M., Urich, T., 2012. Organic carbon transformations in high-Arctic peat soils: key functions and microorganisms 7, 299–311. doi:10.1038/ismej.2012.99
Vázquez-Baeza, Y., Pirrung, M., Gonzalez, A., Knight, R., 2013. EMPeror: a tool for visualizing high-throughput microbial community data. Gigascience 2, 16. doi:10.1186/2047-217X-2-16
Vellend, M., 2010. Conceptual Synthesis in Community Ecology. Q REV BIOL 85, 183–206. doi:10.1086/652373
Venter, J.C., 2004. Environmental Genome Shotgun Sequencing of the Sargasso Sea. Science 304, 66–74. doi:10.1126/science.1093857
Vishnivetskaya, T.A., Petrova, M.A., Urbance, J., Ponder, M., Moyer, C.L., Gilichinsky, D.A., Tiedje, J.M., 2006. Bacterial community in ancient Siberian permafrost as characterized by culture and culture-independent methods. Astrobiology 6, 400–414. doi:10.1089/ast.2006.6.400
Waldrop, M.P., Wickland, K.P., White, R.I., Berhe, A.A., Harden, J.W., Romanovsky, V.E., 2010. Molecular investigations into a globally important carbon pool: permafrost-protected carbon in Alaskan soils. Glob Change Biol 16, 2543–2554. doi:10.1111/j.1365-2486.2009.02141.x
Wallenstein, M.D., McMahon, S., Schimel, J., 2007. Bacterial and fungal community structure in Arctic tundra tussock and shrub soils. FEMS Microbiol Ecol 59, 428–435. doi:10.1111/j.1574-6941.2006.00260.x
Wang, Q., Garrity, G.M., Tiedje, J.M., Cole, J.R., 2007. Naive Bayesian Classifier for Rapid Assignment of rRNA Sequences into the New Bacterial Taxonomy. Applied and Environmental Microbiology 73, 5261–5267. doi:10.1128/AEM.00062-07
Webb, C.O., 2000. Exploring the Phylogenetic Structure of Ecological Communities: An Example for Rain Forest Trees. Am Nat 156, 145–155. doi:10.1086/303378
Webb, C.O., Ackerly, D.D., Kembel, S.W., 2008. Phylocom: software for the analysis of phylogenetic community structure and trait evolution. Bioinformatics 24, 2098–2100. doi:10.1093/bioinformatics/btn358
Werner, J.J., Knights, D., Garcia, M.L., Scalfone, N.B., Smith, S., Yarasheski, K., Cummings, T.A., Beers, A.R., Knight, R., Angenent, L.T., 2011. Bacterial community structures are unique and resilient in full-scale bioenergy systems. Proc. Natl. Acad. Sci. U.S.A. 108, 4158–4163. doi:10.1073/pnas.1015676108
White, D.M., Garland, D.S., Ping, C.-L., Michaelson, G., 2004. Characterizing soil organic matter quality in arctic soil by cover type and depth. Cold Regions Science and Technology 38, 63–73. doi:10.1016/j.coldregions.2003.08.001
Wilhelm, R.C., Niederberger, T.D., Greer, C., Whyte, L.G., 2011. Microbial diversity of active layer and permafrost in an acidic wetland from the Canadian High Arctic. Can. J. Microbiol. 57, 303–315. doi:10.1139/w11-004
Willerslev, E., Hansen, A.J., Rønn, R., Brand, T.B., Barnes, I., Wiuf, C., Gilichinsky, D., Mitchell, D., Cooper, A., 2004. Long-term persistence of bacterial DNA. Curr. Biol. 14, R9–10.

Zhou, J., Davey, M.E., Figueras, J.B., Rivkina, E., Gilichinsky, D., Tiedje, J.M., 1997. Phylogenetic diversity of a bacterial community determined from Siberian tundra soil DNA. Microbiology 143, 3913–3919.

Chapter 4: Permafrost microbial communities exhibit low functional diversity at *in situ* thaw temperatures

Introduction

Previously-frozen stores of organic carbon (C) are subject to increased decomposition due to warming Arctic climates and thawing permafrost (Harden et al., 2012; Hinzman et al., 2005; Osterkamp, 2007; Schuur et al., 2008). Climate models forecast continued warming at the poles and increasing rates of permafrost thaw (Koven et al., 2011; Schaefer et al., 2011). Decomposition of the organic matter in freshly thawed permafrost is dependent on interactions between C quality, abiotic conditions, geomorphology and decomposer activity (Schädel et al., 2014; Schmidt et al., 2007; Tang and Riley, 2013). But, decomposer activity is dependent on the functional traits of the microbial community in relation to these abiotic drivers, and these traits are likely to differ among microbial communities that differ in composition and structure. The functional potential of the permafrost microbial community is likely to have a large effect on the decomposition of permafrost and C flux to the atmosphere under *in situ* conditions, but this effect is difficult to predict with current knowledge (Graham et al., 2011).

Characterizing and employing microbial functional traits have been useful in explaining many ecosystem processes (Allison, 2012; Tang and Riley, 2013). However, efforts to describe broad scale ecological patterns based on traits of individual microbial species have been hampered by limited knowledge of the functions of specific taxa (Green et al., 2008). Rather, the aggregated traits of an entire microbial community may enhance our ability to predict the rates of ecosystem-level processes (Wallenstein and Hall, 2011). For example, Allison (2012) used the traits of enzymes and the physiology of microorganisms to model litter decomposition and found

the level of enzyme production for the entire community was an important predictor of decomposition rates. Follows et al (2007) developed a trait-based model using phytoplankton growth requirements to model ocean productivity, allowing phytoplankton community composition and biogeography to emerge from the traits. Evans and Wallenstein (2013) discovered that ecological strategies employed by microbial communities were related to historical environmental conditions (in this case, precipitation regime), and proposed that these strategies could be aggregated into community level traits that explained differences in functional responses to changing environmental conditions (Evans and Wallenstein, 2012). Other community functional traits, such as catabolic evenness (Degens et al., 2000), C mineralization rate (Santrucková et al., 2003), and microbial growth rate (Zak et al., 1994) have also been instrumental in linking community traits to ecosystem function. Understanding the functional traits of the permafrost microbial community may improve our predictions of their activity and potential greenhouse gas flux from permafrost after thaw.

Microbial community traits are primarily shaped by substrate availability, at least in temperate ecosystems. Degens et al. (2000) found that catabolic evenness, a component of functional diversity, was related to both total organic C and potentially mineralizable C. In this study, the soils in the organic active layer have the highest C content, followed by the top 0-15 cm of the permafrost, then the mineral active layer, and lastly the permafrost 21-25 cm below the active layer thaw depth (Table 4.1; Ernakovich, 2014a), and the functional diversity could reflect this pattern. In addition, the native temperature regime of a microbial community appears to play a role in microbial functional potential. For example, Balser and Wixon (2009) found that the temperature optimum for each of three soils from a broad range of native conditions was related to the mean annual temperature of three sites. This might be especially true for permafrost

microbial communities, which are likely structured by environmental filtering based on their ability to withstand frozen conditions, rather than substrate availability (Ernakovich, 2014b). Permafrost microorganisms are not all merely lying dormant, in wait of less metabolically restrictive conditions. Permafrost microorganisms are actively performing cellular repair (Brinton et al., 2002; Johnson et al., 2007), metabolizing substrates, and growing *in situ* (Bakermans et al., 2003; Drotz et al., 2010; McMahon et al., 2011; Price and Sowers, 2004; Rivkina et al., 2000; Santrucková et al., 2003; Tuorto et al., 2014). Thus, permafrost microbial communities may exhibit high functional potential at temperatures close to *in situ* temperatures.

I characterized the functional diversity of permafrost and active layer microbial communities by assessing 'substrate-use richness' (previously termed 'substrate richness' by Zak et al., 1994), 'substrate preference' and 'growth rate' (Zak et al., 1994) at three incubation temperatures (1, 10, 20 °C). Using an approach developed by Lindstrom et al (1998), I fit a logistic growth model to substrate utilization data from Ecolog™ plates, which allowed me to incorporate the concept of 'substrate-specific growth rate,' or the rate of growth on different substrates, into a quantitative index of functional diversity. I hypothesized environmental filtering for success at cold temperatures would structure the functional diversity of the permafrost community. I predicted that the four components of functional diversity would be greater for the permafrost than the active layer microbial communities at the lowest incubation temperature (1 °C). I also predicted that the functional diversity would be greater for the 1 °C than at 20 °C incubation temperature for the permafrost, because the latter would be above the microbial community's optimum temperature for growth. Finally, I predicted that incubation temperature would affect the substrate preference of the microbial communities.

Methods

Description of the study site, soil sampling and processing

Organic active layer, mineral active layer, and permafrost soils were collected from Sagwon Hills, Alaska (N 69° 25' 32.190" W 148° 41' 38.731", 288 m above sea level). The soils were collected from under moist acidic tundra vegetation and are classified as Ruptic Histic Aquiturbels (Borden et al., 2010). Cores were collected from 15 plots representative of the site and covering 150 m^2. The depth of the seasonally thawed active layer was 26.8 $\pm$ 1.3 cm in August of 2009, and consisted of an organic and mineral horizon with evidence of cryoturbation (Ernakovich, 2014a). The organic horizon, dominated by mildly decomposed plant material (peat) with many fine roots, was between 5 and 14 cm in depth. The remainder of the active layer was visibly gleyed mineral soil with no additional horizonation. At each plot, the active layer was removed and placed on a tarp as a monolith (average thaw depth, 26.8 $\pm$ 1.3 cm). Organic and mineral active layer soils were sampled from the monolith from the center of their respective depths (organic: 2 $\pm$ 0 cm, 99.4 $\pm$ 57.1 g; mineral: 9.4 $\pm$ 1 cm, 187.4 $\pm$ 77.9 g). In two plots, a buried organic horizon was visible. In these cases, samples were taken from the mineral soil not in the buried organic horizon. Permafrost soils were obtained as 8.0 cm diameter cores using a Tanaka auger fitted with a SIPRE-style (Snow, Ice, and Permafrost Research Establishment, (Tarnocai, 1993)) soil corer with carbide bits (Jon's Machine Shop, Fairbanks, Alaska). Permafrost cores were collected to 31.4 $\pm$ 7.3 cm, where glacial till restricted deeper sampling.

The samples were stored on dry ice in the field, at -20 °C during our eight day collection period at Toolik Biological Field Station, and then brought back to the Colorado State University EcoCore laboratory on dry ice where they were stored at -10 °C during processing and storage. Permafrost cores were scraped to remove any contamination from active layer microbes or C

from the field and separated into 5-cm increments, however if there was a natural fracture point at an ice lens within 2 cm of the 5cm fracture point, that point was chosen. Permafrost and organic and mineral active layer soils were homogenized while still frozen in a walk-in -10°C freezer by crushing the soils with a hammer to resemble 2 mm sieve homogenization while double wrapped in sterile plastic bags inside canvas bags. The samples were stored for 17 months at -10 °C until analysis. -10 °C is below the field temperature (average = -1 °C at the time of sampling), and because the soils remained frozen from sampling to analysis, they should represent field microbial community composition relatively well. Cores from nine of the 15 plots were chosen at random for this assay, but only eight organic and six mineral active layer samples were used for this assay due to errors in field collection. Thus for this analysis, I included organic active layer (n=8), mineral active layer (n=6), and permafrost samples from 0-5 cm (n=9), 10-15 cm (n=9), and 20-25 cm (n=9) below the maximum active layer thaw depth. A description of the soil characteristics is in Table 4.1 and further information about the chemistry of these soils can be found in chapter 2.

EcoPlate™ experimental setup

The Biolog EcoPlate™ (Biolog Inc., Hayward, CA) assay is similar to other widely used Biolog assays (such as Biolog GN™ and GN2™), and can be used to determine physiological profiles or metabolic fingerprints of bacterial communities from natural environments (Garland and Mills, 1991; Insam, 1997). The Biolog EcoPlate™ contains 31 substrates and a water (blank) well in triplicate in a 96 well plate. In addition to a single C source (or water), each well contains tetrazolium dye, which changes color when reduced by NADH indicating the degradation of the C substrate. Fungi are unable to be assayed by the EcoPlate assay, because they cannot reduce

the tetrazolium dye included in this assay (Dobranic and Zak, 1999). The ecological relevance of the substrate use from Biolog assays has been criticized (Konopka et al., 1998), however the substrates in the EcoPlate™ assay are more ecologically relevant than previous Biolog products (Insam, 1997), as they contain analogs of microbial products and root exudates (Campbell et al., 1997). Microorganisms can directly utilize some of the compounds, such as amino acids, while others require extracellular decomposition. Glanville et al (2012) found that the use of low molecular weight compounds in a similar laboratory assay correlated with their use in the field, suggesting that EcoPlate assays are ecologically relevant.

Field-moist active layer and permafrost soils (1 g dry weight equivalent) were weighed into autoclaved 125 mL Erlenmeyer flasks and pre-incubated at their designated incubation temperatures for three days. To reduce absorbance of the organic material in the colorimetric assay and to avoid interference from mineral particles (Balser et al., 2002), 10^{-3} soil dilutions were used for the active layers and 2.8×10^{-2} for the permafrost. Permafrost soils were diluted to 2.8×10^{-2} because preliminary experiments showed that the lag phase was too long with a 10^{-3} dilution (data not shown). All flasks were autoclaved and flame sterilized, bench surfaces were cleaned with ethanol, and dilutions and dispensing was performed in a laminar flow hood. 10^{-1} dilutions were made with sterile 0.7% NaCl, shaken for 30 minutes on a reciprocal shaker, and allowed to settle for 10 minutes. 10^{-2} and 10^{-3} dilutions were then made from the 10^{-1} dilution and sterile 0.7% NaCl. The final dilution was allowed to settle for 10 minutes before pouring the supernatant into a sterile plastic reservoir, where it was also allowed to settle for five minutes, before being dispensed into three EcoPlate™ 96-well microplates using an 8-channel pipette. Plates were placed inside lidded plastic boxes containing water to maintain humidity during the assay and placed into one of three incubators (1, 10 and 20 °C).

A time-zero absorbance reading was taken immediately at 590 nm on a Tecan Infinite M200 plate reader (Tecan, Research Triangle Park, NC) programmed to shake the 96 well plates for 15 seconds and then provide an average absorbance reading from 10 measured reads. Respiration readings were taken every 12 hours until color saturation (from the exhaustion of the tetrazolium dye) was achieved for the wells that were changing. This occurred between 1 week and 3 months depending on temperature.

Obtaining kinetic parameter estimates

One early method to analyze Biolog plates was to read the plates at a single time point and utilize the absorbance data for analysis of substrate utilization profiles or community level physiological profiles (CLPP). However, community level physiological profiles (CLPP) results are sensitive to the length of the assay (Konopka et al., 1998; Lindstrom et al., 1998) and to inoculum density (Garland, 1996; Garland and Mills, 1991; Garland et al., 2001; Haack et al., 1995; Konopka et al., 1998; Lindstrom et al., 1998). Thus, alternative methods of analysis have been proposed, including comparing substrate utilization profiles at a common average well color development (AWCD) (Garland, 1996; Garland and Mills, 1991) or modeling absorbance data with a logistic growth model (Lindstrom 1998). In both cases, a time series of data is required, called a "kinetic approach." Lindstrom et al (1998) used the kinetic approach and fit the time series of absorbance values to an adapted logistic growth model, which they called the "modified logistic growth model (Eq. 1),"

$$y = OD_{595\,nm} = \frac{K}{(1+ e^{-r(t-s)})} \quad \text{(Eq. 1)}$$

where $OD_{595\ nm}$ is the absorbance at 595 nm, K is the asymptote the absorbance reaches, r is the exponential increase in the absorbance, t is the time since inoculation and s is the time at the halfway point of the exponential phase. This was the approach I took in this study to minimize bias introduced by incubation duration and differing inoculum density.

After subtracting the absorbance from the water well, I fit the data to Eq. 1 using PROC NLIN (SAS 9.3, Cary, NC) to obtain parameter estimates for K, r, and s. In addition, I calculated a pseudo-r^2 to evaluate fit of the model to the absorbance data. Parameters were accepted for statistical analysis if the model fit had a pseudo-r^2 was between 0.8 and 1, or if the number of missing data points was below 50%. I had "missing" data if the absorbance of the water well exceeded the response to the substrate, and thus "missing" data indicated that there was not response to the substrate.

Determining functional diversity: Growth rate

The parameter r from Eq. 1 represents the exponential increase of absorbance and can be used to represent the exponential growth phase (Lindstrom et al., 1998). An estimate of the mean r for each microplate was calculated from the parameters that had a good model fit and not more than 50% missing data (as described previously). Thus, the mean of r only represents the average growth rate for substrates that were used. Boxplots were created after averaging across analytical replicates and all the substrates within a substrate class using BoxPlotR (http://boxplot.tyerslab.com; (R Core Development Team, 2013; RStudio and Inc, 2013). I also made boxplots by averaging across replicates and substrates such that there were only field replicates included in the n for the boxplot. These boxplots displayed less variability, so I decided to include the substrate class level response to display a fuller range of variability in r.

A Q_{10} function was applied to the parameter r (after collapsing over analytical replicates and averaging the r for all substrates within a substrate class) to understand the temperature sensitivity of microbial growth in the microplate assay using Eq. 2.

$$Q_{10} = \left(\frac{r_2}{r_1}\right)^{\left(\frac{10}{T_2 - T_1}\right)} \quad \text{(Eq. 2)}$$

where r_2 is the kinetic model parameter for the exponential increase in absorbance averaged over analytical replicates for the higher temperature, T_2, and r_1 the same for the lower temperature, T_1. Boxplots were made using Q_{10} for the r for each substrate class as described for the analysis of r using BoxPlotR (http://boxplot.tyerslab.com; (R Core Development Team, 2013; RStudio and Inc, 2013).

Analysis of variance (ANOVA) (SAS 9.3) was used to evaluate the effect of incubation temperature and soil depth on r and Q_{10}. Post-hoc pairwise comparisons using a Tukey Honestly Significant Difference (HSD) multiple testing adjustment were used to explain differences between r and Q_{10} by depth category ($p < 0.05$).

Determining functional diversity: Substrate-specific growth rate

To determine the effect of temperature and soil depth category on substrate-specific growth, I grouped the 31 substrates into substrate classes: amines, amino acids, carbohydrates, carboxylic acids, phosphorylated chemicals and polymers (Table 4.2). I calculated average r for each of the substrate classes by averaging across analytical replicates and substrates within a class for each sample at each temperature. I reduced the dimensionality of r using distance based redundancy analysis (db-RDA) (Oksanen et al., 2013; Ramette, 2007) to evaluate the effect of

temperature and soil depth on the microbes were sampled from on the substrate-specific growth rate for the microbes. In this procedure, missing data are not allowed, and were therefore all changed to zeros. Missing data generally occurred because the model did not fit, and can therefore be reasonably interpreted as a zero growth rate or the inability to use a substrate. If a microbial community in a microplate did not use any substrates at a particular temperature, then the whole row was removed. This was rare, but occurred for a few of the samples at 1 and 10 °C. db-RDA was performed twice, first using the soil depth category and next the incubation temperature as the factor class. The component scores from the db-RDA were used in linear regressions (PROC REG, SAS 9.3, Cary, NC) for each substrate class to assess the contribution of the substrates substrate-specific growth rates (Balser and Wixon, 2009; Garland and Mills, 1991).

Determining functional diversity: Substrate-use richness

I determined substrate-use richness, or the number of substrates the community in a plate was able to degrade (Zak et al., 1994), from whether or not the use of a substrate was a good fit to the logistic growth model fit. If the model had a good fit (as described in the "logistic growth model" section), then I counted that analytical replicate as having degraded that substrate (Lindstrom et al., 1999). If the model did not fit the data, I had to determine whether that was because the substrate was not degraded or whether the model was simply a bad fit and the data should be called missing for that point. If the mean of the water well minus the absorbance values for an analytical replicate of a substrate over time was less than zero, I determined that analytical replicate did not degrade that substrate. I designated the rest of the data as missing.

Substrate-use richness was calculated by summing the number of substrates degraded by the community within a plate (Zak et al., 1994) and dividing by 3 (the number of analytical replicates on the plate). ANOVA (SAS 9.3) was used to evaluate the effect of incubation temperature and soil depth on the community level substrate-use richness. Pairwise comparisons using a Tukey Honestly Significant Difference (HSD) multiple testing adjustment were used to compare differences between the substrate-use richness by depth ($p < 0.05$).

Determining functional diversity: Temperature dependence of substrate preference

To determine substrate preference, I grouped the substrates into classes as described previously and analyzed substrate-use richness data. db-RDA was performed for each soil depth with temperature as the factor class. In addition, I calculated the percentage of the samples that used the substrates within a class at a given temperature. The percent was calculated by dividing the sum of the number of substrates used by the number of soils in the depth category (averaged across the analytical replicates) by the product of the number of substrates included in the substrate class and the number of samples at the soil depth times 100.

Results

Growth rate and substrate-specific growth rate of microbial communities

At 1 °C, the average growth rate was equivalent for all soil depths, from the organic active layer to the deepest permafrost (20-25 cm below the maximum active layer thaw depth). At both 10 and 20 °C, the organic active layer soils had significantly higher growth rates than the mineral active layer or any of the three permafrost depths (0-5, 10-15, and 20-25 cm below the

maximum active layer thaw depth) (Fig. 4.1a). The growth rates for all soil depths increased with temperature, indicating that the temperature optima for these microbes were above 20 °C.

The Q_{10} of microbial growth was not different between the soil depths between 1 and 10 °C ($p=0.7376$) or 10 and 20 °C ($p=0.1233$) (Fig. 4.1b). The Q_{10} value roughly halved between the low and high incubation temperatures for the organic active layer, mineral active layer and the shallowest permafrost ($p<0.001$, $p=0.0476$, 0.0374 respectively). Greater variation in the Q_{10} values for the two deeper permafrost depths prevented a significant difference ($p=0.31$ and 0.16, respectively), but the means for the Q_{10} at 1 and 10 °C were higher than those at 10 and 20 °C.

The db-RDA models with the soil depth category as the factor class were significant for all three incubation temperatures ($p<0.001$) (Fig. 4.2). At all three temperatures, the first axis was highly significant but the second axis was not. At 1 °C, the organic and mineral active layer substrate growth rates were similar to each other, but different from the three permafrost depths. For 10 and 20 °C, the substrate utilization of the organic active layer separated it from the other soils, but the mineral active layer and permafrost soils behaved the same. At 1 °C, five of the six substrate classes (amines, amino acids, carboxylic acids, polymers and phosphorylated chemicals) resulted in the separation along component 1 (Table 4.3), which separated the organic active layer microbial response from the mineral active layer and the permafrost (Fig. 4.2). The utilization of carbohydrates at the coldest incubation temperature was the same for all soil depths (Table 4.3). Separations along CAP 2 were not significant, but amino acids and carboxylic acids appeared to influence the different responses of the organic and mineral active layers from one another (Table 4.3).

The db-RDA models of r using temperature as a factor class were significant for each soil depth category ($p<0.001$) (Fig. 4.3). For all five soil depths, substrate utilization separated the 1

°C samples from 10 and 20 °C (Fig. 4.3) along CAP 1 (which was always significant). For the organic active layer soil, separation along the component 2 was also significant. For the organic active layer soils, all six substrate classes contributed to the separation of the 1 °C samples from 10 and 20 °C along CAP 1 (Table 4.4). Substrate utilization at 10 and 20 °C separated along CAP 2 due to differential utilization of carbohydrates and phosphorylated chemicals. For the mineral active layer soil, the separation of 1 °C from 10 and 20 °C occurred due to use of amines, amino acids, carbohydrates, carboxylic acids and phosphorylated chemicals. The use of polymers was the same along CAP 1. For the top of the permafrost (0-5 cm), component 1 separated not only the 1 °C samples from 10 and 20 °C, but also 10 °C from 20 °C. All of the substrate classes contributed to these differences (Table 4.4). Although not significant, the separation of 10 and 20 °C samples along CAP 2 was due to amines, amino acids, and carbohydrates. The substrate utilization for the deepest (20-25 cm) and intermediate permafrost (10-15 cm) was similar, and was affected by all the substrate classes except phosphorylated chemicals.

Substrate-use richness and preference of microbial communities

The number of substrates that the permafrost and mineral active layer microbial communities degraded at 1 °C was low compared to the organic active layer (Fig. 4.4); it increased to its maximum at 10 °C and remained the same at 20°C (Fig. 4.4). The substrate-use richness of the organic active layer community was not affected by temperature ($p=0.999$). In contrast, the difference in the number of substrates that the microbial communities from the mineral active layer and permafrost 0-5 cm, 10-15 cm, and 20-25 cm used at the different

incubation temperatures indicates a dependence of substrate-use richness on temperature ($p<0.05$, Fig. 4.4).

db-RDA models of the numbers of substrates used at different temperatures (factor class) were significant for each soil depth ($p<0.001$) (Fig. 4.5). For the organic active layer and top two permafrost depths (0-5 cm and 10-15 cm below the maximum active layer thaw depth), degradation patterns within all six substrate classes (amines, amino acids, carbohydrates, carboxylic acids, polymers and phosphorylated chemicals) explained the difference in the substrate preference between 1 °C and the higher incubation temperatures (Table 4.5). In the mineral active layer, five of the substrate classes explained the differences between the number of substrates degraded by the microbes between the 1 °C and the higher incubation temperatures, but the use of polymers did not explain the difference in the number of substrates used at different incubation temperatures (Table 4.5), likely because polymers make up a greater proportion of the total substrate use for the mineral soil at 1 °C than they do at 10 or 20 °C (calculated from % in Table 4.6). For the deepest permafrost depth (20-25 cm), phosphorylated chemicals did not explain the differences in the number of substrates degraded by temperature, likely because the microbial community in this soil depth did not degrade these substrates effectively at any temperature (Table 4.6).

For all the soil depths, the number of samples that degraded the substrates increased with temperature, but this difference was less for the organic active layer, which already utilized a large proportion of the substrates even at 1 °C (Table 4.6). The organic active layer soils utilized all of the substrate types fairly evenly regardless of temperature. In contrast, the mineral active layer and permafrost soils degraded more N-containing compounds (amines and amino acids) at 1 °C than other substrates. The microbes in the mineral active layer soils also degraded less

polymers and phosphorylated chemicals than in the organic active layer soils, except at 1 °C where the mineral active layer microbes successfully degraded polymers. The microbes from the permafrost did not successfully degrade phosphorylated chemicals, but polymers nearly as well as other substrates. At 10 and 20 °C substrate degradation was fairly uniform across the substrate classes for all soil depths.

Discussion

Based on growth rate, substrate-use richness and the temperature dependence of substrate-specific growth rate and substrate preference, microbes inhabiting permafrost and mineral active layer soils from this Arctic tundra site are less functionally diverse than those from organic active layer soils. Previous studies have also found that the functional potential of soil microbial communities declines with depth towards the permafrost table in active layer soils from Svalbard, Norway and the Northwest Canadian Arctic (Frank-Fahle et al., 2014; Tveit et al., 2012). The limited ability of these permafrost microbes to degrade the diverse suite of compounds that become available upon permafrost thaw could limit gaseous C loss from thawing permafrost.

Growth rates of permafrost microbial communities

The growth rates of permafrost microbial communities were lower than or equal to organic active layer microbial communities at every temperature (Fig. 4.1). I predicted that the growth rate of the permafrost would be greater than the active layer at the lowest incubation temperature (1 °C) because microbial communities in permafrost are selected for life at cold temperatures (Rivkina et al., 2004; 2000; Santrucková et al., 2003; Waldrop et al., 2010). Rather,

I found that the organic active layer, mineral active layer and permafrost communities had the same growth rate at 1 °C. In a laboratory incubation at 5 °C, Waldrop et al (2010) also found microbial respiration rates to be the same between the active layer and permafrost from three Alaskan sites. Across the five soil depths in this study, the mean of the kinetic parameter r was 0.3664 day^{-1} at 1 °C, which is similar to that reported by Lindstrom et al (1998) once corrected for temperature. This suggests that arctic microbial communities are not capable of faster growth at low temperatures than soils from warmer climates. Balser and Wixon (2009) also found that microbial communities from soils of varying mean annual temperatures, including tropical, temperate and taiga soils all had the same growth rate at 4 °C. The similarity of the rates at low temperatures regardless of the native temperature of the soils could be due to constraints on physiology at cold temperatures (Price and Sowers, 2004) or decreased affinity for substrates at low temperatures (Nedwell, 1999).

While I expected the growth rate of the organic active layer microbes to increase with temperature, I predicted that the highest incubation temperature would be beyond the temperature optima of the permafrost community, therefore causing a decline in the growth rate at 20 °C (Balser and Wixon, 2009). Thus, I predicted that at higher incubation temperatures, the organic active layer would have a higher growth rate than the permafrost. Although the organic active layer had a higher growth rate than the permafrost at 20 °C, it was not because the permafrost was beyond its temperature optima (Fig. 4.1). In fact, the permafrost microbial communities did not increase their growth rates between 1 and 10 °C, but increased their growth between 10 and 20 °C. This indicates that permafrost communities are not dominated by specialists with a niche dependent on cold temperatures (psychrophiles), but are, rather, psychrotolerant (Bakermans et al., 2003; Rivkina et al., 2004; 2000; Steven et al., 2006).

The Q_{10} of microbial growth was not different between the five soil depths for either the lower (1 vs. 10°C) or higher (10 vs. 20 °C) temperature ranges ($p>0.05$) (Fig. 4.1b). In contrast, many studies show evidence for higher temperature sensitivity of microbial activity in organic versus mineral arctic soils. Waldrop et al (2010) found that the temperature sensitivity of respiration for organic, active layer soils was higher than permafrost soils, although this difference was exacerbated by the low activity of the organic soils and relatively higher activity of the permafrost soils at their lower incubation temperature, which was below freezing (-5 °C). Lupascu et al (2012) found the temperature sensitivity of methanogenesis decreased with depth in an active layer soil in Stordalen, Sweden. Likewise, Wallenstein et al (2009) found that beta-glucosidase activity, an indicator of overall microbial activity, was more temperature sensitive for organic than mineral soils sampled under shrub tundra immediately following soil thaw at an arctic tundra site in Alaska. The temperature sensitivity of microbial processes in soils can be confounded by other factors, such as organo-mineral interactions, aggregation, redox (Davidson et al., 2006) and substrate supply (Davidson et al., 2011; Weedon et al., 2013). Thus, it is possible that I did not observe a difference in the temperature sensitivity between the organic and mineral active layer or the organic active layer and permafrost because, once removed from the limitations imposed by the micro-scale heterogeneity of chemical properties inherent in soils, these confounding factors were not present. Rather, I observed the intrinsic temperature sensitivity of microbial substrate degradation under non-substrate limiting conditions. Alternately, degradation of labile compounds may not be temperature sensitive. Boddy et al (2008) found that microbial degradation of simple, dissolved substrates was not temperature sensitive, and temperature sensitivity was only observed later during the degradation of microbial necromass. In EcoPlate™ assays, the observed color change occurs when organic

substrates are oxidized and the dye is reduced, so it is directly related to oxidation of the labile substrates in the plate and not due to degradation of microbial products.

Substrate-use richness of permafrost microbial communities

The substrate-use richness, or the number of substrates that a microbial community was able to degrade, was lower for the permafrost and mineral active layer than the organic active layer at every temperature (Fig. 4.4, Table 4.6). Despite the fact that growth rates were similar at 1 °C for all soil depths, there were very few substrates the permafrost and mineral soils could degrade. By 10 °C, the difference between the organic active layer and the mineral active layer and permafrost soils narrowed to no more than double, and by 20 °C the difference for soil depths was minimal. The microbial community in the organic active layer degraded nearly all 31 substrates provided at 1, 10 and 20 °C. The ability to respond to many different types of substrates equally across vastly different temperatures is likely a reflection of a diverse community poised to respond to a variety of abiotic and chemical conditions (Ernakovich et al., 2014). Indeed, taxonomic diversity in the organic active layer was found to be greater than in the permafrost (Ernakovich, 2014b). However, the mineral active layer samples have higher taxonomic diversity than permafrost samples (Ernakovich, 2014b), but similar substrate-use richness. Neither the permafrost nor the mineral active layer microbial communities reached the maximum potential substrate-use richness (31), even though the substrates are all relatively easy to utilize (Campbell et al., 1997) and many can be taken up without extracellular enzymatic breakdown. Degens et al. (2000) proposed that the variation of substrate use was affected by the soil organic C content in soils with differing management histories. They found that soils under indigenous vegetation (such as native pasture) used 80- 93% of the 25 added substrates, whereas

soils under monoculture used 66-80%. Likewise, Chaer et al (2009) observed a decline in the richness of substrate degradation with soil disturbance due to declines in soil C and hydrologic conductivity. In the current study, the proportion of the substrates degraded at 20 °C by the organic active layer was relatively high (88-100%) (Table 4.6). By comparison, the top of the permafrost was less able to fully utilize the substrates provided (39-93%), however this community was capable of degrading more substrates than mineral active layer (31-72%). This pattern mirrors the C content in the different soil depths (Table 4.1; Ernakovich, 2014a), and supports the hypotheses by Degens et al (2000) and Chaer et al (2009) that substrate-use richness is related to C content. However, another of their suppositions was that the mechanism underlying this decline in substrate-use richness was the degradation of the native landscape, but these permafrost soils exhibited the low substrate-use richness without having experienced thaw or unnatural degradation, suggesting that the correlation is to C content. Other microbial components in soils, such as microbial biomass and respiration, also increase with soil C (Fierer et al., 2009; Santrucková et al., 2003; Weintraub and Schimel, 2003). This might suggest that the correlation between C content and functional diversity could be due to a sampling effect, where more microbial biomass leads to more apparent diversity. But, higher soil C content could also indicate that there is more variation in the metabolic compounds present in soils, requiring more functional diversity for decomposition.

In the permafrost soils incubated at 1°C, there was notable variability among analytical replicates in the EcoPlate™ assay. None of the 27 soil samples degraded all three analytical replicates of the 31 substrates. In contrast, the organic active layer had a more consistent response among replicates; 51% of samples had the same response in all three replicates at 1 °C. In the permafrost soils, 28-39% at 10 °C and 52-67% at 20 °C used substrates in all three

replicates. Because the same permafrost inoculum was able to use a substrate more consistently across the analytical replicates at the warmer incubation temperatures whereas the organic active layer inoculum was able to do the same at 1 °C, this is unlikely to be due to experimental error. Rather, this effect was likely due to the functional contributions of rare microbes. There was a low probability that a microbe able to degrade a particular substrate at 1°C under oxic conditions was present in the well with that substrate. This indicates that the permafrost is comprised of more rare species that are easily diluted out of the sample. The permafrost community is likely comprised partly of strict anaerobes (Rivkina et al., 1998) and therefore functional diversity of the permafrost would have been greater if I had assayed them under anoxic conditions.

Temperature response of substrate preference

The microbial communities from the permafrost and mineral active layer soils changed their substrate preference with temperature (Fig 5). At 1 °C, these soils used more N containing compounds (amino acids and amides) than others as a proportion of total compounds used (Table 4.6). N mineralization has been observed in thawed permafrost at temperatures just above 0 °C (Keuper et al 2012). In seasonally frozen and thawed soils, N mineralization commonly coincides with soil thaw due to a turnover in the microbial biomass (Buckeridge and Grogan, 2010; Schmidt et al., 2007; Schmidt and Lipson, 2004). If permafrost responds similarly, N mineralization in permafrost after thaw (such as in Keuper et al., 2012) could be due to a turnover in microbial biomass, but our results suggest a preference for N-rich substrates by the microbial community active just above thaw temperatures.

The microbes in the organic active layer had equal ability to degrade substrates regardless of temperature. Balser and Wixon (2009) found that microbial communities from various

ecosystems had differential substrate utilization at different temperatures, and that this was dependent on the initial community composition. Different consortia of bacterial taxa utilize different substrates, thus community composition affects the type of substrates a microbial community can utilize (Goldfarb et al., 2011). The ability of the organic active layer to utilize the substrates evenly across all temperatures is likely due to its greater microbial taxonomic diversity compared to the mineral and permafrost soils (Ernakovich, 2014b). Alternatively, variance in soil microbial activity has been shown to correlate with SOM content and soil texture, the latter of which also explained the temperature response of microbial activity (Santrucková et al., 2003). Both organic matter content and texture varied between the organic active layer and the other soils in this study (Table 4.1), so the differences between the permafrost and the organic active layer functional diversity could be due to soil characteristics, or the effect of soil characteristics on species diversity (Boddy et al., 2014; Fierer et al., 2009; 2007; Lauber et al., 2009).

EcoPlate™ assays and the kinetic approach to investigate microbial functional diversity

Although Biolog™ plates can differentiate between microbial communities from closely related natural systems (Bell et al., 2009; Garland and Mills, 1991; Zak et al., 1994), it has been proposed that it has inherent biases, which affect its applicability as a tool to assess microbial community functional diversity. These include that it is a culture-based method (Konopka et al., 1998; Preston-Mafham et al., 2002) not representative of the true ecology of the microbial community, and the results are not robust to differences in initial inoculum density and assay length (Garland and Mills, 1991; Haack et al., 1995; Konopka et al., 1998; Lindstrom et al., 1998; Preston-Mafham et al., 2002). Because Biolog™ assays are carried out over multiple days,

and in our case, weeks to months, microbial growth occurs in the wells of the 96-well plate, making Biolog™, by definition, a culture-based method (Preston-Mafham et al., 2002). In fact, cell densities need to be at least 10^8 cells per mL before the exponential increase in the absorbance will be observed as a color change (Konopka et al., 1998). Many environmental samples are below this cell count, and soil samples are often further diluted before plating (Balser et al., 2002; Balser and Wixon, 2009; Bell et al., 2009; Zak et al., 1994), thus requiring growth in the Biolog™ plate before the functional diversity can be assessed. Despite this, Biolog™ results have been found to be related to other soil characteristics, such as soil chemistry (Artz et al., 2006), which implies that it is relevant to the ecology of microbial communities *in situ*.

Shifts in community structure during growth in liquid media are due to variation in initial cell densities and specific growth rates for the members of the community (Konopka et al., 1998), as well as competition (Allison, 2005) and mutualism (Lindstrom et al., 1999). Changes in community composition will occur naturally in permafrost as it thaws due to the availability of previously frozen substrates and changes of the metabolic state of microbes, many of which persist in frozen permafrost through maintenance and survival metabolism (Price and Sowers, 2004). Shifts in community composition due to thaw are inevitable (Mackelprang et al., 2011), making the assessment of their potential functional diversity with Biolog™ plates relevant to greater ecological processes. Konopka et al (1998) also warn that the physiological state of microbes in the environmental sample can affect their cultivability. For example, if microbes are sporulated in a dormant state, they will not be able to respond quickly in the assay and will be left out of the assessment of functional diversity using Biolog™ plates. I argue that this is relevant to field conditions, where the activity and abundance of members of the microbial

community is a reflection of their physiological state in response to the abiotic conditions at any given moment (Lennon and Jones, 2011). This is pertinent after permafrost thaw, where drastic shifts in microbial abundance, activity, and diversity will occur in the transition from slow growth, maintenance, and survival (Brinton et al., 2002; Price and Sowers, 2004) to more rapid metabolism and growth. A drastic turnover in the active microbial community composition of arctic active layer soils and alpine soils occurs between frozen and thawed conditions during seasonal transitions (Buckeridge et al., 2013; McMahon et al., 2011; Schmidt et al., 2007). Many possible mechanisms are likely at play in this turnover of microbial biomass, including temperature niche selection (Jefferies et al., 2010). Similar shifts in permafrost community composition after thaw should be expected. In this study, I have captured the effect of temperature on the functional diversity of the microbial communities that emerge after the shift in community composition, thus justifying the use of a tool that allows the community to shift.

Many solutions have been proposed to make the Biolog^{TM} assay more robust to differences in initial inoculum density and the length of the assay. These include equal initial inoculum densities (Garland, 1996; Garland and Mills, 1991), reading the plates at multiple time points during the assay and comparing substrate use at similar average plate absorbance, commonly called average well color development (AWCD) (Balser and Wixon, 2009; Garland, 1996; Garland and Mills, 1991), or a transformation of the data to correct for initial inoculum density differences (see Preston-Mafham et al (2002) for thorough description). Rather than comparing at equal AWCD, the multiple time point data can also be fit to a non-linear growth model, such as a logistic growth curve well (see Preston-Mafham et al (2002) for thorough description). Lindstrom et al (1998) proposed the use of a modified logistic growth model that fits a parameter for the lag phase (s), the exponential increase in absorbance that can also be

interpreted as growth (r), and the asymptote the absorbance data reaches when microbial oxidation of the substrate is complete (K), either due to depletion or competition for other resources. The kinetic parameters r and K have been shown to be unaffected by inoculum density (Belete et al., 2001; Lindstrom et al., 1998), however this is not always the case in mixed communities, especially at low inoculum concentrations (e.g. 4 cells mL-1) (Campbell et al., 1997; Garland et al., 2001). I am confident that my inoculum density was not this low, allowing me to use the model parameter r to differentiate between samples. Furthermore, I used different dilution factors between the active layer and permafrost soils to equalize the inoculum densities between soils to some degree. In our study, comparisons across temperature can be made without concern for differences in inoculum density, because the soil sample was the same.

The length of the assay has been shown to affect the contribution of different substrates to utilization patterns (Garland, 1996), however this can be disregarded when using this approach, because I am comparing the model parameter r, which is insensitive to the length of the lag phase (Lindstrom et al., 1999; 1998). In addition, because substrate-use richness was determined from model fit, I can also compare this between samples without concern that it would be different had I performed the assay for longer. The use of the kinetic approach to determine functional diversity reduced methodological uncertainty in our estimates of the components of functional diversity proposed by Zak et al (1994) (e.g. growth rate, Fig. 4.1; substrate-use richness, Fig. 4.4; substrate preference, Fig. 4.5). Analysis of the kinetic parameter r also allowed me to expand the definition of functional diversity to include substrate dependent growth, or the *rate* of substrate use (Lindstrom et al., 1999), which clearly differentiated the communities from the different soil depths (Fig. 4.2 and Table 4.3).

Conclusions

The functional diversity of the permafrost microbial community appears to be low relative to the organic active layer based on the temperature dependence of growth rates and substrate-use richness. The permafrost microbial community was unable to grow as quickly as the organic active layer, possibly because it is comprised of slow growing, conservative microbes adapted for persistence under C starvation conditions (Ekschmitt et al., 2005; Morita, 1997). The mineral active layer community also behaved similarly, consistent with the concept that mineral soils with a lower native C content host oligotrophic microbes. The permafrost microbes were equally temperature sensitive as the organic active layer at both the low and high temperature range, but the permafrost microbial community was unable to degrade as many substrates as the organic active layer. This might reflect trade-offs of being specialized for life at cold temperatures (Wallenstein and Hall, 2011).

When permafrost temperatures increase, previously frozen organic C is subject to decomposition. However, the limited capacity of the permafrost microbial community to degrade even simple substrates at low temperatures could result in slower decomposition rates than might otherwise be expected from inferences about organic active layer microbial communities and simple Q_{10} functions based on growth. There may be a delay of at least a few growing seasons after permafrost thaw to allow for the microbial community composition to shift and increase its ability to degrade organic matter at post-thaw soil temperatures. As temperatures rise, the permafrost community will become more active and able to degrade a larger diversity of substrates. Because the functional diversity and growth rates of organic active layer are much greater than in permafrost soil, decomposition rates in warming active layer soils will likely rapidly increase.

Tables

Table 4.1. Characteristics of the soils used in this study. GWC= gravimetric water content; dws= dry weight soil; C= carbon; N= nitrogen; OM= organic matter.

Soil Depth	GWC, g water/g dws	SE	C, mgC/g dws	SE	N, mg N/g dws	SE	C:N	SE	OM, mg/ g dws	SE	Depth, cm	SE
Organic AL	3.33	0.58	399.45	13.91	15.31	0.82	26.67	1.86	8.23	0.21	2.00	0.00
Mineral AL	1.13	0.73	94.77	27.42	5.45	1.16	16.46	0.90	1.28	0.14	9.45	0.41
Perm 0-5 cm	1.47	0.11	101.68	9.59	5.55	0.44	18.18	0.45	1.90	0.35	31.74	0.75
Perm 11-15cm	1.76	0.16	108.00	9.89	5.78	0.44	18.86	0.63	1.98	0.29	41.18	1.04
Perm 21-25cm	1.68	0.25	71.02	7.78	4.26	0.44	17.03	0.58	1.35	0.06	50.40	1.26

Table 4.2. Substrates in Ecoplate™ (Biolog, Inc.) categorized by substrate classes (Zak et al., 1994). Note: I am calling the substrate groups 'classes' rather than 'guilds' (Balser and Wixon, 2009). ᵀ indicates substances present in root exudates (Campbell et al., 1997)**.**

Substrate Class	Substrate Name
amines	
	Phenylethylamine
	Putrescine
amino acid	
	Glycyl-L-Glutamic Acid
	L-Arginine ᵀ
	L-Asparagine ᵀ
	L-Phenylalanine ᵀ
	L-Serine ᵀ
	L-Threonine ᵀ
carbohydrate	
	D-Cellobiose
	D-Mannitol
	D-Xylose ᵀ
	i-Erythritol
	N-Acetyl-D-Glucosamine
	α-D-Lactose
	β-Methyl-D-Glucoside
carboxylic acid	
	2-Hydroxy benzoic acid ᵀ
	4-Hydroxy benzoic acid
	D-Galactonic acid γ-lactone
	D-Galacturonic Acid
	D-Glucosaminic acid
	D-Malic acid ᵀ
	Itaconic Acid
	Pyruvic acid methyl ester
	α-Ketobutyric Acid
	γ-Hydroxybutyric Acid
Phosphorylated chemicals	
	D,L-α-Glycerol Phosphate
	Glucose-1-phosphate
Polymers	
	Glycogen
	Tween 40
	Tween 80
	α-Cyclodextrin

Table 4.3. R^2 and p-values for linear regressions between growth on substrate classes and CAP 1 and 2 from db-RDA in Fig. 4.2, where r was the response variable and soil depth was the factor class.

	1 °C		10 °C		20 °C	
Effect	CAP 1	CAP 2	CAP 1	CAP 2	CAP 1	CAP 2
amines/amides	0.56***	ns	0.69***	ns	0.66***	0.09
amino acids	0.18**	0.33**	0.85***	ns	0.71***	ns
carbohydrates	ns	ns	0.71***	ns	0.62***	ns
carboxylic acids	0.36***	0.25**	0.76***	ns	0.75***	ns
miscellaneous	0.37***	ns	0.54***	ns	0.66***	ns
polymers	0.46***	ns	0.26**	ns	0.34***	0.10*

p<0.1

*p<0.05

**p<0.01

***p<0.0001

ns, not significant

Table 4.4. R^2 and p-values for linear regressions between growth on substrate classes and CAP 1 and 2 from db-RDA in Fig. 4.3, where r was the response variable and incubation temperature was the factor class.

	Organic		Mineral		Permafrost 0-5 cm		Permafrost 11-15 cm		Permafrost 21-25 cm	
Effect	CAP 1	CAP 2	CAP 1	CAP 2	CAP 1	CAP 2	CAP 1	CAP 2	CAP 1	CAP 2
amines/amides	0.83***	ns	0.67***	0.24*	0.49***	0.21*	0.55***	0.19*	0.54***	ns
amino acids	0.87***	ns	0.64**	0.27*	0.60***	0.19*	0.45**	0.25**	0.27**	0.45**
carbohydrates	0.70***	0.18*	0.67***	ns	0.41**	0.30**	0.52***	ns	0.39**	0.22*
carboxylic acids	0.77***	ns	0.72***	ns	0.77***	ns	0.50***	ns	0.61***	ns
miscellaneous	0.56***	0.30**	0.41**	ns	0.25**	ns	ns	0.25**	ns	ns
polymer	0.48**	ns	ns	0.26*	0.56***	ns	0.60***	ns	0.36**	ns

*p<0.05

**p<0.01

***p<0.0001

ns, not significant

Table 4.5. R^2 and p-values for linear regressions between growth on substrate classes and CAP 1 and 2 from db-RDA shown in Fig. 4.5, where substrate-use richness was the response variable and incubation temperature was the factor class.

	Organic		Mineral		Permafrost 0-5 cm		Permafrost 11-15 cm		Permafrost 21-25 cm	
Effect	CAP 1	CAP 2	CAP 1	CAP 2	CAP 1	CAP 2	CAP 1	CAP 2	CAP 1	CAP 2
amines/amides	0.63***	ns	0.40**	0.40**	0.87***	ns	0.80***	ns	0.86***	0.15
amino acids	0.84***	ns	0.67***	0.37**	0.91***	ns	0.90***	ns	0.83***	0.20
carbohydrates	0.74***	ns	0.73***	0.19	0.85***	ns	0.94***	ns	0.87***	0.19*
carboxylic acids	0.84***	0.36**	0.77***	0.21	0.74***	0.13	0.80***	ns	0.70***	0.37**
miscellaneous	0.54**	0.30**	0.32*	ns	0.28**	0.16*	0.21*	0.1231	ns	ns
polymer	0.59***	ns	ns	0.64**	0.65***	0.11	0.79***	ns	0.54***	0.40**

p<0.1

*p<0.05

**p<0.01

***p<0.0001

ns, not significant

Table 4.6. The percentage of samples within a soil depth category that degrade the substrates within a class at each temperature. The number of substrates in each class is noted in the parentheses next to the substrate class names and the number of samples included in each soil depth is noted in the parentheses next to the soil depth.

		Substrate Class					
	Soil Depth/Type	amides (2)	amino acids (6)	carbohydrates (7)	carboxylic acids (10)	polymers (4)	Phosphorylated chemicals (2)
1 °C	Organic (8)	63	69	76	66	73	52
	Mineral (6)	19	6	6	3	17	6
	Permafrost 0-5 cm (9)	6	2	4	4	2	2
	Permafrost 10-15 cm (9)	4	11	8	5	5	4
	Permafrost 20-25 cm (9)	2	7	4	7	5	0
10 °C	Organic (8)	90	94	92	81	92	65
	Mineral (6)	36	51	42	34	19	17
	Permafrost 0-5 cm (9)	78	77	72	44	47	15
	Permafrost 10-15 cm (9)	69	77	71	54	47	17
	Permafrost 20-25 cm (9)	63	56	54	36	28	0
20 °C	Organic (8)	98	100	96	92	96	88
	Mineral (6)	67	72	52	55	36	31
	Permafrost 0-5 cm (9)	93	89	89	68	61	39
	Permafrost 10-15 cm (9)	76	90	90	69	56	33
	Permafrost 20-25 cm (9)	81	75	76	53	56	20

Figures

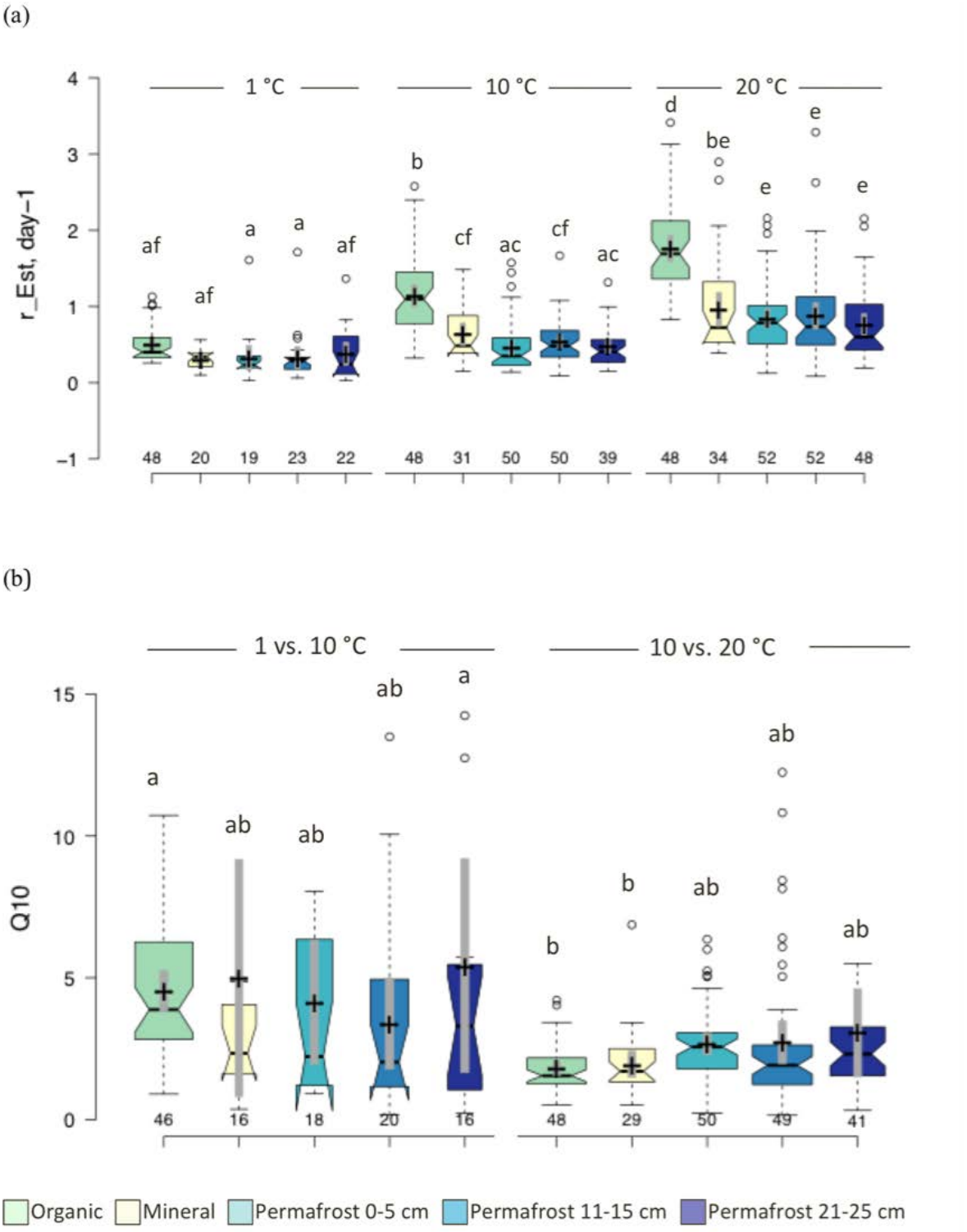
(a)
1 °C
10 °C
20 °C
r_Est, day−1
af af a a af b cf ac cf ac d be e e e
48 20 19 23 22 48 31 50 50 39 48 34 52 52 48
(b)
1 vs. 10 °C
10 vs. 20 °C
Q10
a ab ab ab a b b ab ab ab
46 16 18 20 16 48 29 50 49 41
Organic
Mineral
Permafrost 0-5 cm
Permafrost 11-15 cm
Permafrost 21-25 cm

Figure 4.1. (a) Boxplots of estimated growth rate, r, (for the substrates that could be modeled with the logistic growth model) of microbial communities from different soil depths at different incubation temperatures. Analytical replicates and substrates within a substrate group were averaged to provide one estimated growth rate per field replicate per substrate class, which are then represented by 'n' under the boxplot. (b) The temperature sensitivity, calculated with a Q_{10} function on the average of the analytical replicates of growth rate, r, for microbes from a soil on a substrate. 'n' represents the number of substrate classes and field replicates. For (a) and (b), center lines show the medians, and box limits indicate the 25th and 75th percentiles as determined by R software. Whiskers extend 1.5 times the interquartile range from the 25th and 75th percentiles, and outliers are represented by dots. Crosses represent sample means and grey bars indicate 95% confidence intervals of the means. The width of the boxes is proportional to the square root of the sample size. n is also listed at the bottom of the figure and was described above.

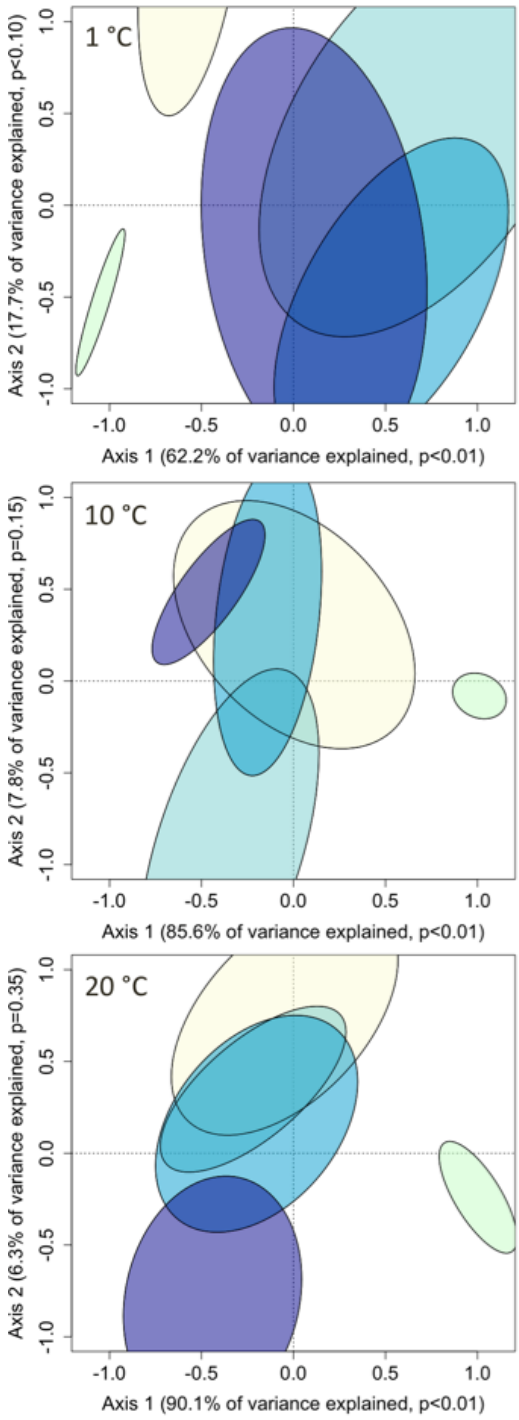

Organic
Mineral
Permafrost 0-5 cm
Permafrost 11-15 cm
Permafrost 21-25 cm

Figure 4.2. The db-RDA of r on substrate classes at each temperature reveals differences in substrate-specific growth rates for the different soil depths at each temperature. Ellipses are the 95% confidence intervals of the microbial growth rates for each soil depth (factor class). The axes indicate the percent variance explained.

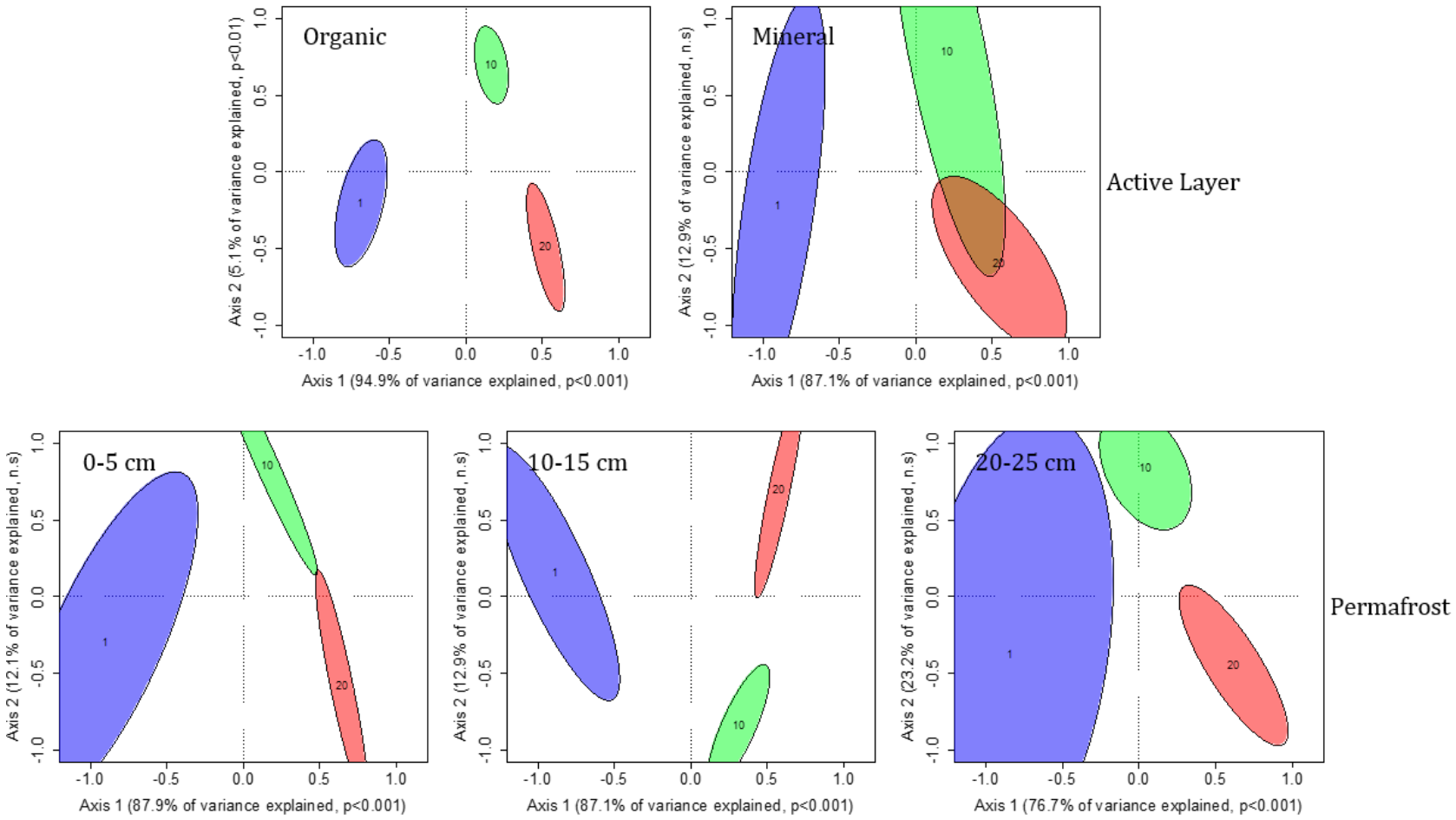

Figure 4.3. The db-RDA of r on substrate classes reveals the differences in substrate-specific growth rates by temperature for each of the different soil depths. Ellipses are the 95% confidence interval of the growth rates at each temperature. The axes indicate the percent variance explained.

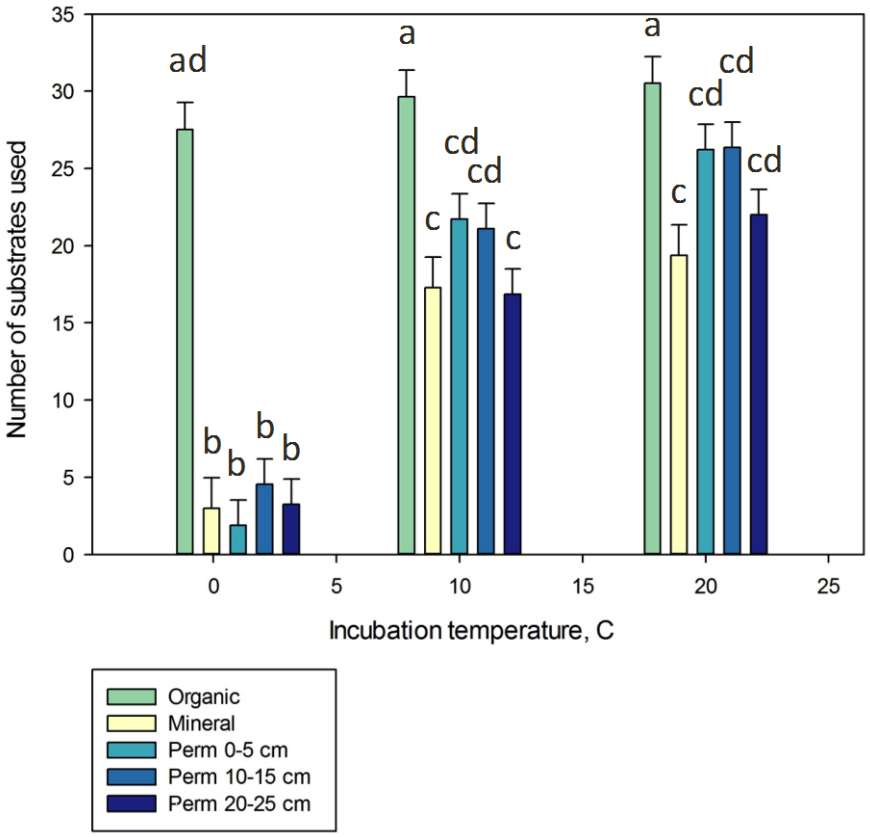

Figure 4.4. Substrate-use richness, as defined by the number of substrates a microbial community is able to use (Zak et al., 1994). The maximum number of substrates possible is 31.

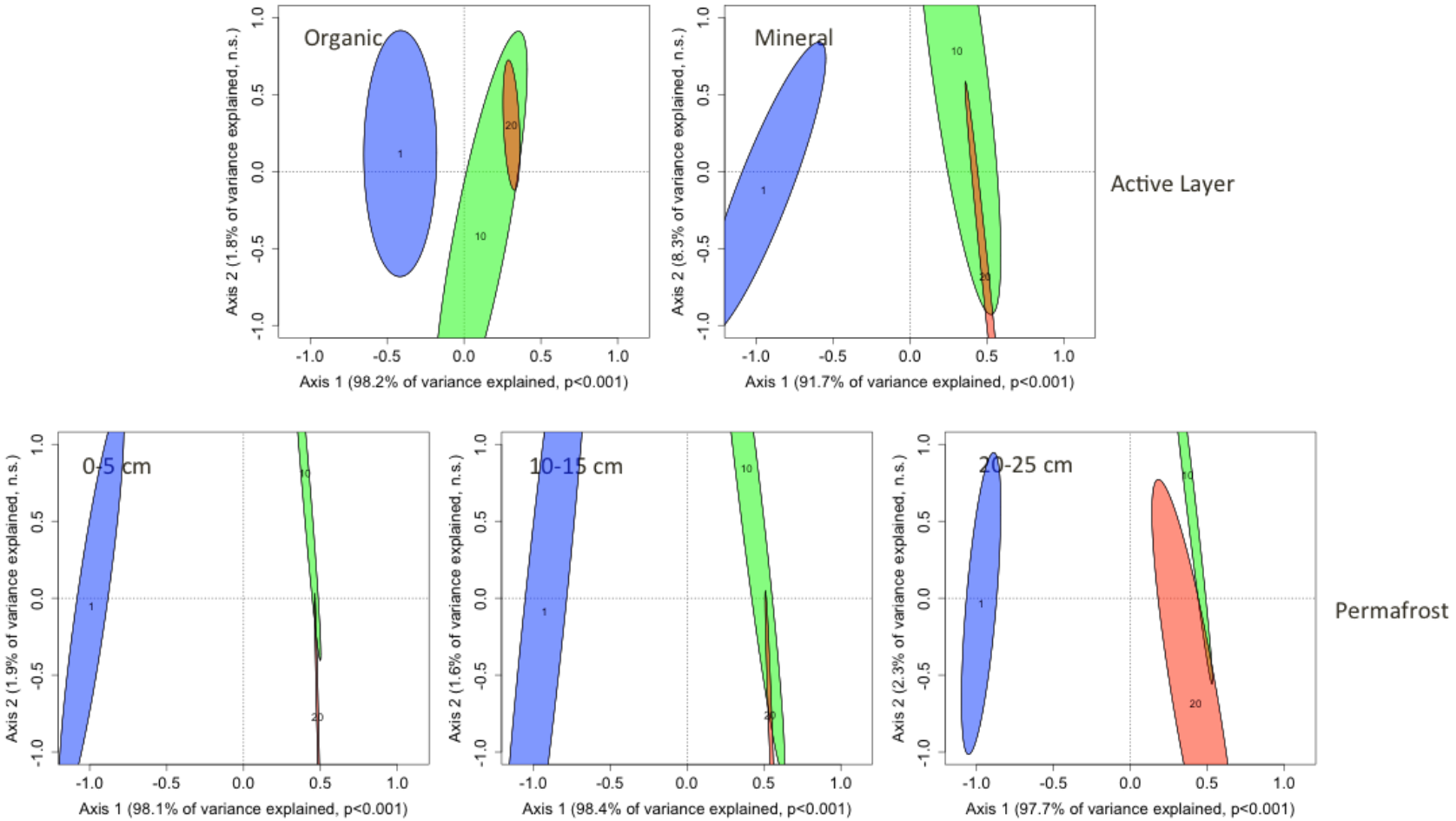

Figure 4.5. The db-RDA of the temperature dependence of substrate preference for each soil depth. Ellipses are the 95% confidence intervals of the number of substrates used at each temperature. The axes indicate the percent variance explained.

References

Allison, S.D., 2005. Cheaters, diffusion and nutrients constrain decomposition by microbial enzymes in spatially structured environments. Ecology Letters 8, 626–635.

Allison, S.D., 2012. A trait-based approach for modelling microbial litter decomposition. Ecology Letters 15, 1058–1070.

Artz, R.R.E., Chapman, S.J., Campbell, C.D., 2006. Substrate utilisation profiles of microbial communities in peat are depth dependent and correlate with whole soil FTIR profiles. Soil Biology and Biochemistry 38, 2958–2962.

Bakermans, C., Tsapin, A.I., Souza Egipsy, V., Gilichinsky, D.A., Nealson, K.H., 2003. Reproduction and metabolism at− 10 C of bacteria isolated from Siberian permafrost. Environmental Microbiology 5, 321–326.

Balser, T.C., Kirchner, J.W., Firestone, M.K., 2002. Methodological variability in microbial community level physiological profiles. Soil Science Society of America Journal 66, 519–523.

Balser, T.C., Wixon, D.L., 2009. Investigating biological control over soil carbon temperature sensitivity. Glob Change Biol 15, 2935–2949.

Belete, L., Egger, W., Neunhäuserer, C., Caballero, B., Insam, H., 2001. Can community level physiological profiles be used for compost maturity testing? Compost science & utilization 9, 6–18.

Bell, C.W., Acosta-Martinez, V., McIntyre, N.E., Cox, S., Tissue, D.T., Zak, J.C., 2009. Linking microbial community structure and function to seasonal differences in soil moisture and temperature in a Chihuahuan Desert grassland. Microb Ecol 58, 827–842.

Boddy, E., Roberts, P., Hill, P.W., Farrar, J., Jones, D.L., 2014. Changes of the soil ecosystem along a receding glacier: Testing the correlation between environmental factors and bacterial community structure. Soil Biology and Biochemistry 40, 1557–1566.

Borden, P.W., Ping, C.-L., McCarthy, P.J., Naidu, S., 2010. Clay Mineralogy in Arctic Tundra Gelisols, Northern Alaska. Soil Science Society of America Journal 74, 580.

Brinton, K.L.F., Tsapin, A.I., Gilichinsky, D., McDonald, G.D., 2002. Aspartic acid racemization and age-depth relationships for organic carbon in Siberian permafrost. Astrobiology 2, 77–82.

Buckeridge, K.M., Banerjee, S., Siciliano, S.D., Grogan, P., 2013. The seasonal pattern of soil microbial community structure in mesic low arctic tundra. Soil Biology and Biochemistry 65, 338–347.

Buckeridge, K.M., Grogan, P., 2010. Deepened snow increases late thaw biogeochemical pulses in mesic low arctic tundra. Biogeochemistry 101, 105–121.

Campbell, C.D., Grayston, S.J., Hirst, D.J., 1997. Use of rhizosphere carbon sources in sole carbon source tests to discriminate soil microbial communities. Journal of Microbiological Methods 30, 33–41.

Davidson, E.A., Janssens, I.A., Luo, Y., 2006. On the variability of respiration in terrestrial ecosystems: moving beyond Q10. Glob Change Biol 12, 154–164.

Davidson, E.A., Samanta, S., Caramori, S.S., Savage, K., 2011. The Dual Arrhenius and Michaelis-Menten kinetics model for decomposition of soil organic matter at hourly to seasonal time scales. Glob Change Biol 18, 371–384.

Degens, B.P., Schipper, L.A., Sparling, G.P., Vojvodic-Vukovic, M., 2000. Decreases in organic C reserves in soils can reduce the catabolic diversity of soil microbial communities. Soil Biology and Biochemistry 32, 189–196.
Dobranic, J.K., Zak, J.C., 1999. Microtiter plate procedure for evaluating fungal functional diversity. Mycologia.
Drotz, S.H., Sparrman, T., Nilsson, M.B., Schleucher, J., Oquist, M.G., 2010. Both catabolic and anabolic heterotrophic microbial activity proceed in frozen soils. Proc. Natl. Acad. Sci. U.S.A. 107, 21046–21051.
Ekschmitt, K., Liu, M., Vetter, S., Fox, O., Wolters, V., 2005. Strategies used by soil biota to overcome soil organic matter stability — why is dead organic matter left over in the soil? Geoderma 128, 167–176.
Ernakovich, J.G., 2014a. The Chemical Properties of Alaskan Permafrost and Seasonally Thawed Soils, in: Wallenstein, M.D., Reardon, K.F. (Eds.), Vulnerability of Permafrost Carbon to Decomposition. Colorado State University.
Ernakovich, J.G., 2014b. Phylogenetic diversity of Arctic soils, in: Wallenstein, M.D. (Ed.), Vulnerability of Permafrost Carbon to Decomposition. Colorado State University, Fort Collins.
Ernakovich, J.G., Hopping, K.A., Berdanier, A.B., Simpson, R.T., Kachergis, E.J., Steltzer, H., Wallenstein, M.D., 2014. Predicted responses of arctic and alpine ecosystems to altered seasonality under climate change. Glob Change Biol n/a–n/a.
Fierer, N., Bradford, M.A., Jackson, R.B., 2007. Toward an ecological classification of soil bacteria. Ecology 88, 1354–1364.
Fierer, N., Strickland, M.S., Liptzin, D., Bradford, M.A., Cleveland, C.C., 2009. Global patterns in belowground communities. Ecology Letters 12, 1238–1249.
Follows, M.J., Dutkiewicz, S., Grant, S., Chisholm, S.W., 2007. Emergent Biogeography of Microbial Communities in a Model Ocean. Science 315, 1843–1846.
Frank-Fahle, B.A., Yergeau, E., Greer, C.W., Lantuit, H., Wagner, D., 2014. Microbial Functional Potential and Community Composition in Permafrost-Affected Soils of the NW Canadian Arctic. PLoS ONE 9, e84761.
Garland, J.L., 1996. Analytical approaches to the characterization of samples of microbial communities using patterns of potential C source utilization. Soil Biology and Biochemistry 28, 213–221.
Garland, J.L., Mills, A.L., 1991. Classification and characterization of heterotrophic microbial communities on the basis of patterns of community-level sole-carbon-source utilization. Applied and Environmental Microbiology 57, 2351–2359.
Garland, J.L., Mills, A.L., Young, J.S., 2001. Relative effectiveness of kinetic analysis vs single point readings for classifying environmental samples based on community-level physiological profiles (CLPP). Soil Biology and Biochemistry 33, 1059–1066.
Glanville, H., Rousk, J., Golyshin, P., Jones, D.L., 2012. Mineralization of low molecular weight carbon substrates in soil solution under laboratory and field conditions. Soil Biology and Biochemistry 48, 88–95.
Goldfarb, K.C., Karaoz, U., Hanson, C.A., Santee, C.A., Bradford, M.A., Treseder, K.K., Wallenstein, M.D., Brodie, E.L., 2011. Differential growth responses of soil bacterial taxa to carbon substrates of varying chemical recalcitrance. Front. Microbio. 2, 94.
Graham, D.E., Wallenstein, M.D., Vishnivetskaya, T.A., Waldrop, M.P., Phelps, T.J., Pfiffner, S.M., Onstott, T.C., Whyte, L.G., Rivkina, E.M., Gilichinsky, D.A., Elias, D.A.,

Mackelprang, R., VerBerkmoes, N.C., Hettich, R.L., Wagner, D., Wullschleger, S.D., Jansson, J.K., 2011. Microbes in thawing permafrost: the unknown variable in the climate change equation 6, 709–712.
Green, J.L., Bohannan, B.J.M., Whitaker, R.J., 2008. Microbial biogeography: from taxonomy to traits. Science 320, 1039–1043.
Haack, S.K., Garchow, H., Klug, M.J., Forney, L.J., 1995. Analysis of factors affecting the accuracy, reproducibility, and interpretation of microbial community carbon source utilization patterns. Applied and Environmental Microbiology 61, 1458–1468.
Harden, J.W., Koven, C.D., Ping, C.-L., Hugelius, G., David McGuire, A., Camill, P., Jorgenson, T., Kuhry, P., Michaelson, G.J., O'Donnell, J.A., 2012. Field information links permafrost carbon to physical vulnerabilities of thawing. Geophys. Res. Lett. 39.
Hinzman, L.D., Bettez, N.D., Bolton, W.R., Chapin, F.S., Dyurgerov, M.B., Fastie, C.L., Griffith, B., Hollister, R.D., Hope, A., Huntington, H.P., Jensen, A.M., Jia, G.J., Jorgenson, T., Kane, D.L., Klein, D.R., Kofinas, G., Lynch, A.H., Lloyd, A.H., McGuire, A.D., Nelson, F.E., Oechel, W.C., Osterkamp, T.E., Racine, C.H., Romanovsky, V.E., Stone, R.S., Stow, D.A., Sturm, M., Tweedie, C.E., Vourlitis, G.L., Walker, M.D., Walker, D.A., Webber, P.J., Welker, J.M., Winker, K.S., Yoshikawa, K., 2005. Evidence and Implications of Recent Climate Change in Northern Alaska and Other Arctic Regions. Climatic Change 72, 251–298.
Insam, H., 1997. A new set of substrated proposed for community characterization in environmental samples, in: Insam, H., Rangger, A. (Eds.), Microbial Communities: Functional Versus Structural Approaches. Springer, New York, pp. 259–260.
Jefferies, R.L., Walker, N.A., Edwards, K.A., Dainty, J., 2010. Is the decline of soil microbial biomass in late winter coupled to changes in the physical state of cold soils? Soil Biology and Biochemistry 42, 129–135.
Johnson, S.S., Hebsgaard, M.B., Christensen, T.R., Mastepanov, M., Nielsen, R., Munch, K., Brand, T., Gilbert, M.T.P., Zuber, M.T., Bunce, M., Rønn, R., Gilichinsky, D., Froese, D., Willerslev, E., 2007. Ancient bacteria show evidence of DNA repair. Proceedings of the National Academy of Sciences 104, 14401–14405.
Keuper, F., Bodegom, P.M., Dorrepaal, E., Weedon, J.T., Hal, J., Logtestijn, R.S., Aerts, R., 2012. A frozen feast: thawing permafrost increases plant-available nitrogen in subarctic peatlands. Glob Change Biol 18, 1998–2007.
Konopka, A., Oliver, L., Turco, R., 1998. The use of carbon substrate utilization patterns in environmental and ecological microbiology. Microb Ecol 35, 103–115.
Koven, C.D., Ringeval, B., Friedlingstein, P., Ciais, P., Cadule, P., Khvorostyanov, D., Krinner, G., Tarnocai, C., 2011. Permafrost carbon-climate feedbacks accelerate global warming. Proc. Natl. Acad. Sci. U.S.A. 108, 14769–14774.
Lauber, C.L., Hamady, M., Knight, R., Fierer, N., 2009. Pyrosequencing-based assessment of soil pH as a predictor of soil bacterial community structure at the continental scale. Applied and Environmental Microbiology 75, 5111–5120.
Lennon, J.T., Jones, S.E., 2011. Microbial seed banks: the ecological and evolutionary implications of dormancy. Nat Rev Micro 9, 119–130.
Lindstrom, J.E., Barry, R.P., Braddock, J.F., 1998. Microbial community analysis: a kinetic approach to constructing potential C source utilization patterns. Soil Biology and Biochemistry 30, 231–239.

Lindstrom, J.E., Barry, R.P., Braddock, J.F., 1999. Long-term effects on microbial communities after a subarctic oil spill. Soil Biology and Biochemistry 31, 1677–1689.
Lupascu, M., Wadham, J.L., Hornibrook, E.R.C., Pancost, R.D., 2012. Temperature sensitivity of methane production in the permafrost active layer at Stordalen, Sweden: a comparison with non-permafrost northern wetlands. Arctic, Antarctic, and Alpine Research 44, 469–482.
Mackelprang, R., Waldrop, M.P., DeAngelis, K.M., David, M.M., Chavarria, K.L., Blazewicz, S.J., Rubin, E.M., Jansson, J.K., 2011. Metagenomic analysis of a permafrost microbial community reveals a rapid response to thaw. Nature 480, 368–371.
McMahon, S.K., Wallenstein, M.D., Schimel, J.P., 2011. A cross-seasonal comparison of active and total bacterial community composition in Arctic tundra soil using bromodeoxyuridine labeling. Soil Biology and Biochemistry 43, 287–295.
Morita, R.Y., 1997. Bacteria in oligotrophic environments starvation-survival lifestyle. Chapman and Hall, New York.
Oksanen, A., Blanchet, F.G., Kindt, R., Pierre Legen- dre, P.R.M., OHara, R.B., Simpson, G.L., Peter Solymos, M.H.H.S., Wagner, H.L., 2013. vegan: Community Ecology Package.
Osterkamp, T.E., 2007. Characteristics of the recent warming of permafrost in Alaska. J. Geophys. Res. 112, F02S02.
Preston-Mafham, J., Boddy, L., Randerson, P.F., 2002. Analysis of microbial community functional diversity using sole-carbon-source utilisation profiles - a critique. FEMS Microbiol Ecol 42, 1–14.
Price, P.B., Sowers, T., 2004. Temperature dependence of metabolic rates for microbial growth, maintenance, and survival. Proceedings of the National Academy of Sciences 101, 4631–4636.
R Core Development Team, 2013. *R: A Language and Environment for Statistical Computing.*
Ramette, A., 2007. Multivariate analyses in microbial ecology. FEMS Microbiol Ecol 62, 142–160.
Rivkina, E., Gilichinsky, D., Wagener, S., Tiedje, J., McGrath, J., 1998. Biogeochemical activity of anaerobic microorganisms from buried permafrost sediments. Geomicrobiology Journal 15, 187–193.
Rivkina, E., Laurinavichius, K., McGrath, J., Tiedje, J., Shcherbakova, V., Gilichinsky, D., 2004. Microbial life in permafrost. Advances in Space Research 33, 1215–1221.
Rivkina, E.M., Friedmann, E.I., McKay, C.P., Gilichinsky, D.A., 2000. Metabolic activity of permafrost bacteria below the freezing point. Applied and Environmental Microbiology 66, 3230–3233.
RStudio and Inc, 2013. *shiny: Web Application Framework for R.*
Santrucková, H., Bird, M.I., Kalaschnikov, Y.N., Grund, M., Elhottova, D., Šimek, M., Grigoryev, S., Gleixner, G., Arneth, A., Schulze, E.-D., Lloyd, J., 2003. Microbial characteristics of soils on a latitudinal transect in Siberia. Glob Change Biol 9, 1106–1117.
Schaefer, K., Zhang, T., Bruhwiler, L., Barrett, A.P., 2011. Amount and timing of permafrost carbon release in response to climate warming. Tellus B 63, 165–180.
Schädel, C., Schuur, E.A.G., Bracho, R., Elberling, B., Knoblauch, C., Lee, H., Luo, Y., Shaver, G.R., Turetsky, M.R., 2014. Circumpolar assessment of permafrost C quality and its vulnerability over time using long-term incubation data. Glob Change Biol 20, 641–652.
Schmidt, S.K., Costello, E.K., Nemergut, D.R., Cleveland, C.C., Reed, S.C., Weintraub, M.N., Meyer, A.F., Martin, A.M., 2007. Biogeochemical consequences of rapid microbial turnover and seasonal succession in soil. Ecology 88, 1379–1385.

Schmidt, S.K., Lipson, D.A., 2004. Microbial growth under the snow: implications for nutrient and allelochemical availability in temperate soils. Plant Soil 259, 1–7.
Schuur, E.A., Bockheim, J., Canadell, J.G., Euskirchen, E., Field, C.B., Goryachkin, S.V., Hagemann, S., Kuhry, P., Lafleur, P.M., Lee, H., 2008. Vulnerability of permafrost carbon to climate change: Implications for the global carbon cycle. BioScience 58, 701–714.
Steven, B., Léveillé, R., Pollard, W.H., Whyte, L.G., 2006. Microbial ecology and biodiversity in permafrost. Extremophiles 10, 259–267.
Tang, J.Y., Riley, W.J., 2013. A total quasi-steady-state formulation of substrate uptake kinetics in complex networks and an example application to microbial litter decomposition. Biogeosciences Discuss. 10, 10615–10683.
Tarnocai, C., 1993. Sampling frozen soils, in: Carter, M.R. (Ed.), Soil Sampling and Methods of Analysis. Lewis Publishers, Boca Raton, pp. 755–765.
Tuorto, S.J., Darias, P., McGuinness, L.R., Panikov, N., Zhang, T., HÃggblom, M.M., Kerkhof, L.J., 2014. Bacterial genome replication at subzero temperatures in permafrost 8, 139–149.
Tveit, A., Schwacke, R., Svenning, M.M., Urich, T., 2012. Organic carbon transformations in high-Arctic peat soils: key functions and microorganisms 7, 299–311.
Waldrop, M.P., Wickland, K.P., White, R.I., Berhe, A.A., Harden, J.W., Romanovsky, V.E., 2010. Molecular investigations into a globally important carbon pool: permafrost-protected carbon in Alaskan soils. Glob Change Biol 16, 2543–2554.
Wallenstein, M.D., Hall, E.K., 2011. A trait-based framework for predicting when and where microbial adaptation to climate change will affect ecosystem functioning. Biogeochemistry 109, 35–47.
Wallenstein, M.D., McMahon, S.K., Schimel, J.P., 2009. Seasonal variation in enzyme activities and temperature sensitivities in Arctic tundra soils. Glob Change Biol 15, 1631–1639.
Weedon, J.T., Aerts, R., Kowalchuk, G.A., van Logtestijn, R., Andringa, D., van Bogedom, P.M., 2013. Temperature sensitivity of peatland C and N cycling: Does substrate supply play a role? Soil Biology and Biochemistry 61, 109–120.
Weintraub, M.N., Schimel, J.P., 2003. Interactions between carbon and nitrogen mineralization and soil organic matter chemistry in arctic tundra soils. Ecosystems 6, 129–143.
Zak, J.C., Willig, M.R., Moorhead, D.L., Wildman, H.G., 1994. Functional diversity of microbial communities: a quantitative approach. Soil Biology and Biochemistry 26, 1101–1108.

Chapter 5: Unraveling the complex drivers of CO_2 and CH_4 flux in permafrost soils

Introduction

Permafrost contains vast stores of organic carbon (C) that are vulnerable to decomposition following thaw (Harden et al., 2012; Hugelius et al., 2013; Schädel et al., 2014; Tarnocai et al., 2009), and rapid climate change at northern latitudes is leading to widespread permafrost thaw (Vaughan et al., 2013). Permafrost thaw could increase greenhouse gas (GHG) emissions leading to a potential C-climate feedback (Anisimov, 2007; Koven et al., 2011; D. M. Lawrence et al., 2008; Schaefer et al., 2011). However the complexity and interactions of the mechanisms controlling the rate of GHG emissions and the partitioning between CO_2 and CH_4 make it difficult to predict GHG emissions from thawing permafrost (Lee et al., 2012). The concentration of soil oxygen and other electron acceptors is a major controlling factor determining whether aerobic or anaerobic decomposition will occur following permafrost thaw, and these vary with geomorphology at the landscape scale (Lipson et al., 2012; Treat et al., 2014). Freely drained upland soils produce CO_2 as a result of aerobic respiration, whereas saturated soils quickly become anoxic, favoring anaerobic processes such as denitrification, fermentation, iron or sulfate reduction and methanogenesis. The amount of GHG produced from thawed permafrost is also dependent on the activity and size of the decomposer biomass pool (Santrucková et al., 2003), as well as the chemical structure and physical accessibility of the organic matter (Schädel et al., 2014; Schmidt et al., 2011).

In many ecosystems dominated by aerobic conditions, soil C flux can generally be predicted from abiotic factors such as temperature, moisture, and C content (Jenkinson and Rayner, 1977; Parton et al., 1987) and some mechanistic models have gained additional

resolution by including the size and activity of the microbial biomass pool (Moorhead and Sinsabaugh, 2006; Schimel and Weintraub, 2003; Wieder et al., 2013). However, these relationships may not apply to anaerobic metabolism under cold conditions. Q_{10} values (the activity multiplier for a 10 °C increase in temperature) for methane production have been observed to vary widely, from 2 (Lupascu et al., 2012) to over100 (Dunfield et al., 1993; Treat et al., 2014), which likely reflects not only the complexity of the processes, but also variability among field and laboratory replicates (Knoblauch et al., 2013; Wachinger et al., 2000). Aerobic respiration, on the other hand, typically has a Q_{10} around 2 in temperate ecosystems (Bowles and Aber, 1994) and a Q_{10} between 6 and 9 in soils from cold ecosystems (Kirschbaum, 1995; Mikan et al., 2002; Waldrop et al., 2010).

The amount of C available for decomposition is an important controller on CO_2 flux, and models that include multiple soil C pools accurately predict CO_2 production from thawed permafrost under both aerobic and anaerobic conditions (Dutta et al., 2006; Knoblauch et al., 2013; Lee et al., 2012; Schädel et al., 2014; Weintraub and Schimel, 2003). However, CH_4 flux does not appear to be strongly correlated to total soil C pools (Treat et al., 2014), likely because CH_4 production is sensitive to the lability of the organic matter. Soils with more labile litter have more CH_4 production than sites that have more chemically recalcitrant compounds, such as *Sphagnum* moss litter (Lupascu et al., 2012) or partially-decomposed peat (Hodgkins et al., 2014). In addition to chemical lability, little is known about other organic matter protection mechanisms in permafrost. Studies investigating the bioavailability of organic matter preserved in frozen permafrost are not consistent as to whether the organic matter is protected by the mineral matrix. Some studies show evidence of passive organic matter (Schädel et al., 2014); some show evidence of moderate amounts of mineral-associated organic matter (Dutta et al.,

2006; Kawahigashi et al., 2006); and others show that the organic matter in permafrost is as labile as non-mineral soils (Lee et al., 2012; Waldrop et al., 2010). Thus, the relationships developed between soil C and CO_2 flux for temperate systems may not be applicable to the prediction of GHG flux from Arctic soils generally, and permafrost soils specifically.

Microorganisms have narrow stoichiometric flexibility in their demand for nutrients in order to build biomass (Cleveland and Liptzin, 2007; Sistla and Schimel, 2012), and microbial growth in the Arctic is thought to be nutrient-limited during the growing season (Edwards et al., 2006; Sistla et al., 2012) and C-limited when frozen (Buckeridge and Grogan, 2008; Uhlířová et al., 2007). Anoxia can result in a relief of P limitations on microbial growth (Liptzin and Silver, 2009), however anaerobic metabolism yields less energy, which can impose a different constraint on microbial growth (Roden and Jin, 2011). To my knowledge, there are no published models of CH_4 production that use microbial biomass as a parameter. It is possible that, just as is the case for CO_2 (see(Allison et al., 2010; Ernakovich, 2014; C. R. Lawrence et al., 2009; Wieder et al., 2013), a variable microbial biomass pool could improve CH_4 predictions. Alternatively, the contrast in energy and nutrient limitations on microbial growth under anoxic versus oxic conditions could result in different relationships between microbial biomass and gas flux.

The objective of this study was to determine the mechanisms controlling GHG flux from permafrost soil, comparing methanogenesis to CO_2 production. I hypothesized that oxygen availability may impose limitations on decomposition due directly to energy and indirectly to nutrient limitations, such that it would be energy-limited under anaerobic conditions and nutrient-limited under oxic conditions. Because GHG production is the result of microorganisms acting on organic matter, I wanted to explore the microbial biomass and dissolved organic matter (DOM) pools and their impact on GHG flux explicitly. Firstly, I predicted that microbial biomass

would be energy limited under anoxic conditions and nutrient limited under oxic conditions. Secondly, I predicted that these differences between energy and nutrient limitations would cause the chemistry of the DOM pool to differ under oxic and anoxic conditions, because quicker decomposition rates under oxic conditions would result in a reduction of labile to recalcitrant compounds relative to anoxic conditions in this pool of bioavailable C. This same trend would occur for higher temperatures than lower temperatures, however I predicted that redox state would be more influential in determining DOM chemistry than temperature. Further, I anticipated that fermentation end products, such as organic acids, would accumulate in the DOM under anoxic conditions. My final objective was to use these findings about microbial biomass and C availability to inform empirical relationships on the controls of CH_4 and aerobic and anaerobic CO_2 production in permafrost. I predicted that my model refined with nutrient and energy limitations on biomass growth, rather that a parameter representing microbial biomass, and C bioavailability, rather than C content, would explain more of the variance in GHG flux rates.

Methods

Description of the study site and soil sampling and processing

Organic active layer, mineral active layer, and permafrost soils were collected from Sagwon Hills, Alaska (N 69° 25’ 32.190” W 148° 41’ 38.731”, 288 m above sea level). The soils were collected from under moist acidic tundra vegetation and are classified as Ruptic Histic Aquiturbels (Borden et al., 2010). Cores were collected from 15 plots representative of the site and covering 150 m^2. The depth of the seasonally thawed active layer was 26.8 $\pm$ 1.3 cm in August of 2009, and consisted of an organic and mineral horizon with evidence of cryoturbation

(Ernakovich, 2014). The organic horizon, dominated by mildly decomposed plant material (peat) with many fine roots, was between 5 and 14 cm in depth. The remainder of the active layer was visibly gleyed mineral soil with no additional horizonation. At each plot, the active layer was removed and placed on a tarp as a monolith (average thaw depth, 26.8 $\pm$ 1.3 cm). Organic and mineral active layer soils were sampled from the monolith from the center of their respective depths (organic: 2 $\pm$ 0 cm, 99.4 $\pm$ 57.1 g; mineral: 9.4 $\pm$ 1 cm, 187.4 $\pm$ 77.9 g). In two plots, a buried organic horizon was visible. In these cases, samples were taken from the mineral soil not from within the buried organic horizon. Permafrost soils were obtained as 8.0 cm diameter cores using a Tanaka auger fitted with a SIPRE-style (Snow, Ice, and Permafrost Research Establishment; Tarnocai, 1993) soil corer with carbide bits (Jon's Machine Shop, Fairbanks, Alaska). Permafrost cores were collected to 31.4 $\pm$ 7.3 cm, where glacial till restricted deeper sampling.

The samples were stored on dry ice in the field, at -20 °C during our eight day collection period at Toolik Biological Field Station, and then brought back to the Colorado State University EcoCore laboratory on dry ice where they were stored at -10 °C during processing and storage. Permafrost cores were scraped to remove any contamination from active layer microbes or C from the field and separated into 5-cm increments, however if there was a natural fracture point at an ice lens within 2 cm of the 5cm fracture point, that point was chosen. Permafrost and organic and mineral active layer soils were homogenized while still frozen in a walk-in -10°C freezer by crushing the soils with a hammer to resemble 2 mm sieve homogenization while double wrapped in sterile plastic bags inside canvas bags. The samples were stored for 36 months at -10 °C until incubation. -10 °C is below the field temperature (average = -1 °C at the time of sampling), and because the soils remained frozen from sampling to analysis, they should

represent field soils relatively well. For this incubation, I chose a subset of plots (n=12). In chapter 2, total C and N and mid-infrared analysis indicated that the top 15 cm of the permafrost was chemically similar, and the 16-30 cm cores were similar. So, I recombined the 0-5 cm and 6-10 cm subsamples and the 16-20 and 20-25 subsamples from each core in equal amounts for the incubation. The 11-15 cm subsamples were omitted to obtain soil cores from two depths with distinct chemistry.

Incubation design

Samples were randomly selected for either oxic or anoxic treatments, and each subsample was split for incubation at 1 °C or 15 °C and for initial soil chemical analysis. Both depths from a particular core went into the same treatment (anoxic, oxic). As they thawed, oxic samples were allowed to drain freely from 16 oz. plastic containers (Silgan Plastics Corporation, Norcross, GA) with holes drilled approximately every cm. Samples were placed in half gallon glass jars with metal lids (with rubber O-ring for gastight seal) fitted with two septa ports. Inverted specimen cups elevated the plastic containers off the bottom of the glass jar to allow the water to drain. Anoxic samples had the same set-up, except no holes were drilled in the plastic containers, so the samples were inundated with water after thaw. In addition, jars were flushed with CO_2-free air in the oxic treatment and with N_2 gas in the anoxic treatment. All samples were flushed at the same time for 20 minutes in a 4 °C walk-in refrigerator using a system of tubing and regulators to ensure that all the samples received the same airflow during the headspace flushing process. Samples in the anoxic treatment were not opened during the course of the 90-day incubation, and the oxic samples were opened once at 5 days for the 15 °C samples and 10 days for the 1 °C samples to remove drained water. Half of the incubation samples were started on one

day, and the other half two days later due to the time demands of setting up the incubation and doing the initial and final chemical analyses.

Chemical analysis

The following chemical analyses were performed at the time of the incubation set-up (initial) and after 90 days of incubation on samples from both depths and all incubation treatments: total soil C and N, pore water C and N, total and ferrous iron, pH, soil water content, and Fourier transformed mid-infrared spectroscopy (MidIR) of the pore water dissolved organic matter (DOM). Soil redox was also measured at the end of the incubation. The following analyses were performed on samples from the 0-10 depth only: microbial biomass C, N and P, salt extractable DOC and N, inorganic N (NH_4^+, NO_3^-), total free amino acids (TFAA), and a suit of soil enzymes (α-glucosidase, β-glucosidase, Cellobiohydrolase, Xylosidase, Acid phosphomonoesterase, N-acetylglucosaminidase, Leucine-aminopeptidase). All analyses were done at the EcoCore Analytical Services (Colorado State University, Fort Collins, CO) unless otherwise noted.

Soil water content was determined by weighing soils and drying them for 48 hours at 55 °C. These soils were then ground with a mortar and pestle and analyzed for total soil C and N on a LECO Tru-SPEC elemental analyzer (Leco Corp., St. Joseph, MI). Pore water DOC and N was collected using 0.45 μm nylon spin filters (Grace Discovery, Bannockburn, IL) that had been cleaned with deionized (DI) water by spinning them at 2500 rpm for 5 minutes three times. DOC and N were obtained by spinning soil samples for 30 minutes at 2500 rpm, and was then frozen for approximately one month at -20 C until analysis for C and N content on a Shimadzu Total Organic Carbon Analyzer. The initial pore water samples were run in Dr. Michael Weintraub's

Laboratory (University of Toledo, Toledo, OH), and final samples were analyzed at the EcoCore Analytical Services Laboratory. Lyophilized pore water samples (1 μg C: 1 mg KBr) were scanned undiluted (neat) in the mid-infrared region on a Digilab FTS 7000 Fourier transform spectrometer (Varian, Inc., Palo Alto, CA) with a deuterated, Peltier-cooled, triglycine sulfate detector and KBr beam splitter. The spectrometer was fitted with a Pike AutoDIFF diffuse reflectance accessory (Pike Technologies, Madison, WI) and KBr was used as background. Data was obtained as pseudo-absorbance (log [1/Reflectance]). Spectra were collected at 4 cm^{-1} resolution, with 64 co-added scans per spectrum from 4000 to 400 cm^{-1}. Duplicate scans of each sample were performed and averaged. pH was measured on a 1:5 soil:DI water solution stirred for 30 minutes and measured with a TTT85 Titrator (Radiometer, Copenhagen, Denmark). The total and ferrous iron was determined using inductively coupled plasma spectroscopy (Thermo Jarrell Ash Iris Advantage ICP Spectrometer, Thermo Electron Corp., Milford, MA) at the Soil, Water, Plant Testing Laboratory (Colorado State University, Fort Collins, CO). Soil redox was measured per the manufacturers' instructions with a VWR sympHony epoxy combination redox electrode probe and Thermo Scientific Orion 3 Star meter. A minimum of three redox values were obtained per sample by inserting the probe from the top of the sample immediately after opening the jar, but if redox values were highly variable or very different from the other samples, up to five measurements were taken. Salt extractable carbon and nitrogen were determined by shaking 30 mL 0.5 M K_2SO_4 with 5 g wet weight soil for 4 hours. Microbial biomass was determined using the chloroform-slurry technique as described in Fierer and Schimel (2003). Briefly, 0.5 mL ethanol-free chloroform was shaken with replicate soil samples to the salt extractable carbon for 4 hours, after which the chloroform was removed by bubbling with air. The extracts (both initial and final) were analyzed on a Shimadzu Total Organic Carbon

Analyzer for DOC and DN, but also for NH_4^+, NO_3^- and TFAA (Cavanaugh, 1997; Darrouzet-Nardi and Weintraub, 2014; Hurvich and Tsai, 1989) in Dr. Michael Weintraub's Laboratory (University of Toledo, Toledo, OH). Microbial biomass P was measured similarly to microbial biomass C and N, however a 1:20 soil: 0.5 M $NaHCO_3$ solution was used. Extracts were analyzed with ICP at the Soil, Water, Plant Testing Laboratory (Colorado State University, Fort Collins, CO). Enzyme potentials were analyzed using fluorescently labeled substrates as described in Bell et al. (2013).

Statistical Analysis

Statistical differences in the mean gas flux and soil characteristics at the final time point were determined using analysis of variance (ANOVA) using a mixed effect model (PROC MIXED, SAS 9.3, Cary NC) using the incubation conditions (temperature and oxic vs. anoxic) as fixed effects and the day the sample was set-up on, the core the sample was from, and the incubation treatment nested within the core it was taken from as random effects. Data were log transformed in order to satisfy the assumption of normality. For the soil characteristics, the model was the same as described above for the gas flux, except the initial values for the samples were also included in the model as fixed effects to account for differences due to initial values rather than the laboratory treatments. Due to methodological difficulties, initial values do not exist for microbial biomass phosphorus or enzyme potentials. Post hoc tests were done using a Tukey Honestly Significant Difference (HSD) multiple testing adjustment.

Principle Components Analysis (PCA) of the MidIR data was performed (PROC PRINCOMP, SAS 9.3, Cary NC) on selected peak heights, which were calculated by subtracting the baseline immediately preceding the peak from the maximum peak height for each sample.

Peaks included were: 1041, 1130, 1620, 1655, 2910, and 3377 cm^{-1}. These peaks were chosen after determining that these did not correlate, which would violate the assumptions of PCA.

Mixed effects modeling (PROC MIXED, SAS 9.3 Cary, NC) was also used to build models to explain CO_2 and CH_4 data using the same random effects as above and incubation temperature, treatment (anoxic, oxic), and soil chemicals as fixed effects. When needed, data were log transformed in order to satisfy the assumption of normality. Model fits were evaluated using the Akaike Information Criterion corrected for small sample sizes (Cavanaugh, 1997; Hurvich and Tsai, 1989), where a smaller number is a better model fit.

Results

GHG production

All of the incubation conditions produced measureable amounts of CH_4 and CO_2 (Figs. 5.1 and 5.2), however CO_2 production was at least an order of magnitude greater. For CO_2 production, there was no difference between the depths (Table 5.3[1] and Fig. 5.1). For CH_4 production, only the 0-10 cm depth anoxic 15 °C produced a different amount of gas from the other samples (Table 5.3 and Fig. 5.1). Therefore, the rest of the statistical analysis was done on only the 0-10 cm samples. The samples incubated at 15 °C under oxic conditions produced the greatest CO_2, followed by the anoxic samples incubated at 15 °C, then the oxic samples incubated at 1 °C, and lastly the anoxic samples incubated at 1 °C. Both temperature and whether the samples were incubated under anoxic or oxic conditions significantly affected the cumulative CO_2 produced (log transformed) ($p<0.01$), but their interaction did not ($p= 0.9092$). The average

[1] Raw data (including soil chemical properties, microbial parameters and greenhouse gas flux rates) are stored in the ACADIS data repository (http://nsidc.org/acadis/search/) within the Ernakovich profile.

CH_4 production under anoxic conditions was 23 times greater at 15 °C than 1 °C ($p=0.0098$), and the CH_4 production from the oxic samples at 15 °C and 1 °C was similar to that of the anoxic 1 °C ($p>0.9$). The variation in CH_4 production was greater than CO_2 production (Fig. 5.2, inset). After 90 days of incubation, both the CO_2 and CH_4 production were still continuing and had not leveled out at 15 °C. In the anoxic 15 °C treatment, the rates of methane production started low and then increased with time. In contrast, CO_2 production rates were the highest in the initial phase of the incubations.

The activity of methanogens relative to CO_2 producers under anoxic conditions was lower than thermodynamics would predict (Fig. 5.3). Iron reduction yields roughly 40 times more energy than hydrogenotrophic methanogenesis, and the dotted line indicates 40 CO_2: 1 CH_4. The relationship between CH_4 and CO_2 for the anoxic samples (Fig. 5.3) indicated that only one sample was capable of producing both high levels of CH_4 and CO_2, and that it produced more CH_4 than would be expected by the 1:40 line. Three of the 15 °C replicates and all the 1 °C replicates fell below the line because they produced more CO_2 than CH_4. Two replicates fell on the theoretical 1:40 line. The samples below the line had high redox values and the samples on and above the line had lower redox values (Table 5.4).

Energy and nutrient limitations on microbial growth

Microbial biomass C was higher for the samples in the anoxic treatment than the oxic treatment ($p= 0.0001$), and also for samples incubated at the higher temperature for each redox condition (interaction term $p=0.0113$) (Fig. 5.4). Microbial biomass N was greater for samples incubated at the higher temperature ($p=0.02$), but there was no effect of treatment (oxic vs.

anoxic). There were no significant effects of the treatments on microbial biomass P, however it appears that the anoxic samples had higher biomass-P than the oxic samples ($p>0.05$).

Both microbial biomass C and P showed a relationship with soil ferrous iron for the anoxic treatment (Fig. 5.5; MBC: $r2>0.51$ and $p<0.0202$; MBP: $r2>0.69$ and $p<0.006$), but not for the oxic treatment (MBC: $r2<0.1008$ and $p>0.3147$; MBP: $r2<0.0052$ and $p>0.8431$). The relationship between ferrous iron and MBP and MBC was not sensitive to temperature (anoxic: $p= 0.7184$ and 0.3139, log MBP and C). In the oxic treatment, microbial biomass was positively correlated with both increasing dissolved N (Fig. 5.6) ($r2=0.6074$, $p=0.0028$) and C (Fig. 5.7) ($r2=0.4570$, $p= 0.0158$) in the pore water, neither of which were related to microbial biomass C in the anoxic treatment. Temperature also does not seem to play a role in the relationship between dissolved N and C with microbial biomass C under oxic conditions (log TN $p=0.0731$ and log TOC $p= 0.2564$ for log MBC). Additionally, the microbial biomass C had a weaker relationship with ammonium and total free amino acid concentrations ($r2= 0.2387$ and 0.2388, $p=0.1070$ and 0.1069, respectively).

DOM chemistry under oxic and anoxic conditions

The C/N ratio of the pore water decreased over the incubation regardless of whether the samples were incubated under oxic or anoxic conditions (both $p<0.0023$) or at 1 °C or 15 °C (both $p<0.0001$) (Fig. 5.8). However, the constituents of the DOM pool were different depending on the incubation conditions (Fig. 5.9 a and b). DOM from all of the incubation conditions had compounds that contained OH and/or NH bonds (~3400 cm^{-1}). Between 1650 and 1530 cm^{-1}, there were subtle differences between the treatments. The oxic samples contained peaks at 1640 and 1530 cm^{-1} regardless of incubation temperature, and the average spectrum for

the anoxic samples incubated at 1 °C had some modest features in this region. 1640 cm^{-1} is indicative of either aromatic C=C and amide I bonds (Movasaghi et al., 2008), and 1530 cm^{-1} is indicative of aromatic C-H bending and amide II bonds (Haberhauer and Gerzabek, 1999; Movasaghi et al., 2008). The anoxic samples incubated at 15 °C had only one peak in this regions (1590 cm^{-1}), which was also present in the samples before incubation. 1590 cm^{-1} is indicative of phenyl C=C bonds (Movasaghi et al., 2008). The peak at 1390 cm^{-1} was present in all the samples, but it was also present in blanks. In the region between 1180 and 950 cm^{-1}, the oxic samples incubated at 15 °C had a different abundance of the functional groups representative of those peaks than the other incubation conditions. They had a peak at 1180, 1130 and 1090 cm^{-1}, and a small shoulder at 1030 cm^{-1}, indicative of lignin C-O, the vibrations of C-O in nucleic acids and proteins, and polysaccharide C-O vibrations and bending, respectively (Movasaghi et al., 2008). The oxic samples incubated at 1 °C had a small peak at 1180, the peak at 1130, and then a shoulder at 1090 leading into a peak at 1030. The 1030 cm^{-1} peak was also present in the initial DOM samples as well as the anoxic samples, however it was lower in the anoxic samples incubated at 15 °C than 1 °C. PCA of selected peak heights (1040, 1130, 1620, 1655, 2910 and 3377 cm^{-1}) (Fig. 5.9 b) revealed that samples cluster by temperature rather than by whether they were incubated under oxic or anoxic conditions. The ratio of carbohydrates to carboxylates (1040/1620) is an indicator of the degree of decomposition. The ratio decreased with incubation at 15 °C relative to 1 °C, however whether the samples were incubated under oxic or anoxic conditions did not make a difference in the ratio, which corroborates the PCA results.

There was little to no evidence of organic acids (1720 cm^{-1}) (Hodgkins et al., 2014) in the samples (Fig. 5.11 a and b). Subtle increases from the baselines existed at 1720 cm^{-1} in the initial

samples as well as the samples incubated under oxic conditions (Fig. 5.11 a), but the magnitude of these peaks was ten times less than other peaks in the spectra. When peak heights were calculated (Fig. 5.11 b), the greatest increase from the baseline occurred in the oxic samples, indicating that some fermentation occurred even in the oxic treatments and also that organic acids were depleted in the anoxic treatments.

Empirical relationships with greenhouse flux in permafrost

Analysis of mixed models with the incubation treatments (temperature and oxic vs. anoxic) revealed that the models explaining the variability in the CO_2 and CH_4 production are similar, and that the null model containing the microbial biomass C (at the harvest of the incubation) and the initial C content, as well as the incubation conditions, was generally a relatively good fit (as determined by the AICc index, Hurvich and Tsai, 1989) (Fig. 5.12). However, for the CH_4 models, neither covariate was significant, and for CO_2, only the microbial biomass C was significant ($p<0.05$). For CH_4, a model containing the final soil redox values and incubation conditions ($p=0.1138$) and a model containing the final pore water dissolved organic C content (TOC) and incubation conditions ($p=0.0008$) had lower AICc than the null model. For both CO_2 and CH_4, models containing values from the first component of the PCA (PCA 1) had lower AICc than the null model. Values of the coordinate from PCA analysis using only the soils in this study are on the left. On the right, PCA 1 values are from an analysis also including deeper soils incubated in the same experiment, but not used elsewhere in this analysis. For the CO_2 gas production, the model using the latter PCA 1 has a low AICc value and a nearly significant p-value ($p=0.0532$).

Discussion

Methane flux is small, but highly variable

The objective of this study was to elucidate the mechanisms controlling GHG flux from permafrost soil, specifically comparing methanogenesis to CO_2 production. All treatments produced considerable amounts of CO_2 (e.g. oxic conditions at 15 °C: 0.317-1.97 mg CO_2-C $gdws^{-1}$). The rate of CO_2 production under oxic conditions was as expected from previous observations (Fig. 5.2; Conant et al., 2008), with high initial rates and a rapid decline to a lower rate. CO_2 production under anoxic conditions follows the same pattern, but reaches the lower rate more quickly. CH_4 production was highly variable (e.g. anoxic conditions at 15 °C 0.44-67 μg CH_4-C $gdws^{-1}$ for samples incubated), and this variability was not explained by soil C content (2-603 μg CH_4 g soil C^{-1}), indicating that the activity of the methanogens can be highly uneven across arctic landscapes and in laboratory incubations (Fig. 5.2; Knoblauch et al., 2013; Lee et al., 2012; Lupascu et al., 2012; Wachinger et al., 2000). The variability of CH_4 production exceeded that of CO_2 production, even for anaerobic CO_2 production. There are three probable explanations that might explain this seemingly random variability: the abundance of methanogen populations, substrate supply, or the activity of other anaerobes.

The abundance of methanogens is controlled by site characteristics and the prevalence of labile organic matter. In previous studies, methanogen populations have been observed to be high in organic active layer soils and to decline with depth (Ganzert et al., 2006), but there is an active methanogen community in permafrost (Mackelprang et al., 2011; Rivkina et al., 2007; Waldrop et al., 2010). Potential methanogenesis rates seem to be highly dependent on the water table depth in the field (Lupascu et al., 2012; Mondav et al., 2014; Treat et al., 2014), presumably because these conditions support large methanogen communities (Høj et al., 2006).

However, even within a site with similar water table depth, methanogenesis can be very spatially variable (Wachinger et al., 2000). In a study using tomography, Wachinger et al (2000) found that cores with large CH_4 production had more non-decomposed organic matter than cores with lower CH_4 production. Although they concluded that sites with high labile organic matter content contained more archaeal biomass, this relationship was not true for all of their soil types, notably their wettest site. The abundance of methanogens has been found to correlate with methanogenesis rates in some sites or studies (Mackelprang et al., 2011; Mondav et al., 2014; Waldrop et al., 2010), but not in others (Frank-Fahle et al., 2014; Mondav et al., 2014). It appears that the simple presence of labile plant inputs and methanogens will not necessarily produce methane. Substrates for methanogenesis are the end products of other anaerobic metabolic pathways, such as H_2 from fermentation, CO_2 from iron reduction, and acetate from acetogenesis. Thus, Drake et al (2009) proposed that anaerobic metabolism terminating in methanogenesis should be viewed akin to a cellular network of pathways required to transform plant inputs to CH_4, which they termed "intermediary ecosystem metabolism". Methanogens, as the agents of the terminal step, can be outcompeted for energy by anaerobes higher on the redox ladder or substrate limited, both of which limit methanogenesis. In this study, we found evidence for both limitations to methanogenesis at play.

Evidence that methanogens are limited by the activity of other anaerobes

The relationship between microbial biomass (C or P) and soil nutrient concentration varied with incubation conditions, indicating that there were different controls on microbial growth under oxic and anoxic conditions (Figs. 5.5-5.7). Under anoxic conditions, both microbial biomass C and P were positively correlated to ferrous iron, but not to pore water C or

N. In contrast, under oxic conditions, both the pore water C and N were correlated with the size of the microbial biomass C pool, but not ferrous iron. These differences did not seem to be dependent on energy, because temperature did not significantly affect these relationships. For example, in the anoxic treatment, microbial biomass C was higher at 1 °C than 15 °C. Also, microbial biomass C and P were greater under anoxic conditions than oxic conditions, indicating that iron may indeed play a role in relieving the microbial community from a P limitation on growth. But, these findings were not as I predicted from theory. I expected iron to limit microbial biomass more under oxic conditions due to the occlusion of P with iron oxides (Walker and Syers, 1976). I observed that under oxic conditions, there was no relationship with iron, but rather, there was a relationship between microbial biomass C and pore water C and N, the former of which can indicate substrate depletion (Buckeridge and Grogan, 2008) and the latter of which has been shown previously to limit microbial pool sizes (Sistla et al., 2012).

The observation that ferrous iron and microbial biomass C and P had a strong relationship under anoxic conditions suggests that this may not be due to a nutrient limitation, but rather an indicator of anaerobic metabolism, specifically iron reduction active under anoxic conditions. When used to explain the heterogeneity in the CH_4 production, the model containing Fe^{2+} resulted in the lowest AICc (but the p-value for the covariate did not indicate that it was significant), and this correlation, although weak, suggests that the activity of the iron-reducing bacteria impacts methane production. In addition, soil redox potentials at the end of the experiment were also highly variable, and were a modestly good predictor of CH_4 production, supporting the idea that the microbial activity of other anaerobes affects methanogenesis. Although thermodynamics would lead one to expect the inhibition of CH_4 concurrent with the activity of other anaerobes, Bethke et al. (2011) demonstrated that mutualistic behavior results in

simultaneous methanogenesis, iron and sulfate reduction. But, I found evidence that CH_4 production was inhibited by anaerobe activity (Fig. 5.3). Only one replicate was capable of producing both high levels of CH_4 and CO_2, and half samples incubated under anoxic conditions at 15 °C had CH_4: CO_2 relationships below the expected by energy yield between hydrogenotrophic methanogenesis and iron reduction (1:40). Together, the relationships with microbial biomass C and Fe^{2+}, explanatory power of Fe^{2+} and redox potential for CH_4 production, and relationships between CH_4 and CO_2 production indicate that the activity of anaerobes higher on the redox ladder limited the production of CH_4 in this study.

Evidence that methanogenesis is affected by organic matter lability and substrate limitation

Both temperature and incubation conditions altered the chemistry of the DOM pool, with temperature driving gross changes (such as the ratio of carbohydrates to carboxylates) and incubation conditions driving the pathways used for substrates to enter the DOM pool. Under oxic conditions, the higher absorbance of the bands at 1640 and 1530 cm^{-1} indicates that products of depolymerization accumulated because these peaks represent amide I or aromatic C=C and aromatic C-H, respectively. For the oxic 15 °C samples, and to a lesser extent the oxic 1 °C samples, this was likely the result of the depolymerization of both lignin and other aromatic compounds and proteins, because in addition to the peaks at 1640 and 1530 cm^{-1}, these samples had peaks at both 1180 and 1130 cm^{-1}, which indicate lignin C-O and C-O vibrations from either nucleic acids or proteins (Movasaghi et al., 2008). The difference between the DOM chemistry produced at different temperatures under oxic conditions suggested faster rates of depolymerization at higher temperatures. The absence of the peak at 1180 cm^{-1} in the anoxic spectra suggests that the peaks at 1640, 1530 and 1590 cm^{-1} were products of the

depolymerization of proteins rather than lignin or other aromatic compounds, as expected by the known inhibition of oxidative enzymes under anoxic conditions (Freeman et al., 2001). I did not detect differences in the enzyme activity of a protein-depolymerizing enzyme (Leucine-aminopeptidase) under the different treatments (Table 5.2), suggesting that amino acid content entering the DOM pool was similar, which was also supported by our assay of total free amino acids in the soil (Table 5.2). The MidIR data suggested that although the pathways of DOM production were different between oxic and anoxic conditions, the products in the DOM pool were fairly similar regardless of incubation treatment. However, it is possible that using a tool with finer molecular resolution would have yielded different results, since MidIR aggregates compounds according into classes of functional groups.

Carbohydrates are relatively labile compounds, owing to their reactivity. Evidence of polysaccharides (1090 and 1030 cm^{-1}) was found under all incubation conditions, however the relative abundance of these peaks changed with incubation conditions. Analyzing a ratio of a compound known to deplete in incubations (i.e. carbohydrates, 1030 cm^{-1}) to a compound known to accumulate (i.e. carboxylates, 1620 cm^{-1}) can be a helpful way to investigate changes in chemistry (Artz et al., 2006; Calderón et al., 2006; Haberhauer et al., 1998). At the end of the incubation at 15 °C, the abundance of carbohydrates relative to carboxylates decreased, regardless of whether the samples were incubated under oxic or anoxic conditions. This confirms previous findings that labile C compounds, such as carbohydrates, are important for decomposition under both oxic and anoxic conditions (Hodgkins et al., 2014; Lupascu et al., 2012; Weintraub and Schimel, 2003).

Models built to explain CO_2 and CH_4 production were both improved with the inclusion of parameters to describe the DOM pool at the end of the incubation, such as pore water DOC

and N content. However, both DOC and N were also related to the size of the microbial biomass C pool under oxic conditions, so they may not represent direct relationships between GHG production and substrate chemistry. I also used PCA to examine how multivariate descriptors of substrate chemistry (from the MidIR analysis) explained GHG flux. The relationship between CO_2 flux and the first component of the PCA were nearly significant ($p=0.0532$) and this model had a much lower AICc than other models. Although this parameter also reduced the AICc for the CH_4 production model, it was not significant. The relationship between GHG flux and the ratio of carbohydrates to carboxylates, was nearly significant for CH_4 production ($p=0.1180$) but not for CO_2 production, where it actually increased the AICc. These results suggest that differences in DOM chemistry affect CO_2 flux, but that the lability of the substrate pool was particularly important to CH_4 production, which has been observed in other studies (Lupascu et al., 2012; Wachinger et al., 2000). However, the limited ability of substrate chemistry to explain GHG fluxes suggests that other factors were also important.

Organic acids did not accumulate in the anoxic treatment, however their rapid consumption likely limited their detection (Drake et al., 2009). This suggests that methanogenesis, which relies on the products of fermentation (both organic acids and H_2), was substrate limited, which has been observed previously (Ganzert et al., 2006). In addition, previous studies have shown that soils with high methanogen abundance often have low levels of the substrates required for methanogenesis (Høj et al., 2006; 2005; Tveit et al., 2012), suggesting that this process is often substrate limited.

Consequences for predicting the terminal step in organic matter degradation

Variability in methane production is a common observation (Knoblauch et al., 2013; Lee et al., 2012; Lupascu et al., 2012; Treat et al., 2014; Wachinger et al., 2000). The abundance of methanogen populations, substrate supply, and the activity of other anaerobes are interacting mechanisms controlling CH_4 production. Methanogenesis is carried out by a phylogenetically narrow group of Archaea, so it is possible that low CH_4 production observed in this study was due to limited abundance of these microbes. Although I did not perform a community analysis in this experiment, I can presume that, at the very least, methanogen communities would be regulated by the same endemic factors, since organic matter content and pH are similar across field replicates (Table 5.1; Ernakovich, 2014) and these samples have the same position in the water table. In addition, phylogenetic analysis of permafrost has revealed significant methanogen populations (Mackelprang et al., 2011; Rivkina et al., 2007; Waldrop et al., 2010), so population size is unlikely to limit methanogenesis. It appears that methanogens are present given the correct conditions, which include labile organic matter and water-logging in the field (Lupascu et al., 2012; Wachinger et al., 2000).

The supply of organic substrates has been shown to be important to methanogenesis (Hodgkins et al., 2014; Lupascu et al., 2012). Lupascu et al (2012) found that labile litter material and root exudates stimulated methanogenesis. In this study, I found that the ratio between carbohydrates and carboxylates correlated with CH_4 flux, while a soil chemistry parameter more representative of the whole DOM pool (PCA 1) was more important for predicting CO_2 flux, suggesting that the lability of substrates is more important to methanogenesis.

This relationship between lability and methanogenesis is likely indirect, because labile organic matter supports the activity of other anaerobes that produce the substrates for CH_4 production (Drake et al., 2009). These substrates, then, control methanogenesis. Christensen et al (2003) found a strong relationship between CH_4 production and organic acid concentrations. While this indicates that methanogenesis can be substrate limited (Ganzert et al., 2006), it also exemplifies the control of other anaerobes on the production of CH_4. In this study, I observed that organic acids did not accumulate in the DOM pool, indicating that methanogenesis is, indeed, substrate limited. Models explaining CH_4 production were improved by adding parameters explaining the activity of other anaerobes, such as Fe^{2+} concentration and soil redox potential.

As permafrost thaws, whether soil conditions will be aerobic or anaerobic depends on the topography of the site, but this is not the only factor important in determining GHG flux. Methanogenesis is the terminal step in the decomposition of organic matter under anoxic conditions and it is reliant on a consortium of anaerobic microorganisms to proceed (Drake et al., 2009; Morris et al., 2012; Murrell and Jetten, 2009; Tveit et al., 2012). Here, I propose that the variability in CH_4 observed can be attributed to the many processes required by the consortium to enable methanogenesis. Production of methane via anaerobic respiration is highly variable due to the many interacting controls on its production, such as the lability of the OM, the activity of other anaerobes higher on the redox ladder, and the substrate supply to methanogens. Prediction of GHG fluxes will be crucial to our understanding of the impact of permafrost C on the global C cycle (Koven et al., 2011). This study highlights the need for a more mechanistic understanding of the processes governing anaerobic GHG flux than is used to predict aerobic CO_2 and resulting C-climate feedbacks.

Tables

Table 5.1. Average and standard error of soil chemical parameters of permafrost soils measured prior to the incubation for depths 0-10 cm and 16-25 cm below the maximum active layer thaw depth.

Depth	0-10 cm	SE	16-25 cm	SE
TOC (ug-C/g dry)	98.39	10.36	109.95	22.55
TN (ug-C/g dry)	2.96	0.53	3.99	1.10
TOC/TN pore	37.50	3.15	31.09	2.31
Total Fe (mg/ g dws)	39.66	3.48	35.50	2.37
Ferrous Fe (mg/ g dws)	18.09	1.68	14.56	1.23
LECO (mg C/g dws)	129.50	20.15	87.93	8.75
LECO (mg N/g dws)	5.85	0.53	4.66	0.33
LECO C/N	21.43	1.21	18.54	0.62
pH	5.37	0.11	6.27	0.32
dws/wws	0.38	0.02	0.39	0.02
EDOC (ug-C/g dry)	412.87	41.93	n/a	
ETN (ug-C/g dry)	50.95	8.00	n/a	
EDOC/ETN	8.70	0.65	n/a	
Biomass-C (ug-C/g dry)	126.23	50.10	n/a	
Biomass-N (ug-C/g dry)	10.88	4.25	n/a	
Biomass C/N	20.57	5.23	n/a	
NH4-N (ug gdws-1)	31.40	7.16	n/a	
NO3-N (ug gdws-1)	1.45	0.29	n/a	
TFAA (nmol gdws-1)	123.19	17.68	n/a	

Table 5.2. Average and standard error of soil chemical properties measured at the end of a 90-day incubation under oxic and anoxic conditions at 1 and 15 °C in permafrost soils sample 0-10 cm and 16-25 cm below the maximum active layer thaw depth.

	0-10							
	anoxic 15C	SE	anoxic 1C	SE	oxic 15C	SE	oxic 1C	SE
TOC pore (ug-C/g dry)	60.27	14.65	58.67	12.23	31.69	8.96	68.90	17.33
TN pre (ug-C/g dry)	2.88	0.61	3.14	0.80	3.02	1.64	4.04	0.89
TOC/TN pore	20.54	1.20	19.52	0.77	15.39	2.85	16.79	0.65
LECO (mg C/g dws)	109.34	16.37	114.48	15.78	104.65	14.03	99.40	7.93
LECO (mg N/g dws)	5.98	0.72	6.27	0.63	6.10	0.64	5.80	0.40
LECO C/N	17.99	0.64	17.95	0.72	17.00	0.42	17.08	0.23
pH	6.24	0.18	6.11	0.42	5.93	0.19	6.02	0.17
Minimum redox	174.25	79.90	328.23	9.93	347.18	11.13	332.35	12.16
dws/wws	0.49	0.04	0.51	0.02	0.55	0.03	0.55	0.02
Total Fe (mg/ g dws)	22.45	0.70	22.10	1.59	20.73	1.73	20.93	2.14
Ferrous Fe (mg/ g dws)	7.66	1.19	8.62	1.10	9.65	0.88	10.54	1.03
EDOC (ug-C/g dry)	202.62	20.86	192.57	30.88	151.05	31.51	214.60	36.81
ETN (ug-C/g dry)	36.81	4.34	35.00	6.60	45.84	7.15	45.95	9.37
EDOC/ETN	5.84	0.79	5.67	0.28	3.61	0.70	4.94	0.44
Biomass-C (ug-C/g dry)	31.60	6.78	56.26	11.49	35.18	7.44	28.67	10.16
Biomass-N (ug-C/g dry)	4.48	0.84	2.20	0.94	6.39	2.79	2.25	0.78
Biomass C/N	7.74	1.25	110.50	65.14	10.08	2.89	30.53	12.80
Biomass-P (ug P/ g dws)	9.74	2.85	10.79	3.60	6.96	2.79	7.10	2.23
NH4-N (ug gdws-1)	19.94	1.58	22.22	5.19	35.03	7.51	31.86	7.99
NO3-N (ug gdws-1)	2.23	0.43	2.91	0.48	5.21	2.94	3.47	0.77
TFAA (nmol gdws-1)	96.64	27.31	90.42	26.18	105.82	21.55	106.84	22.21
BG (nmols/g dws/hr)	31.71	4.94	42.42	6.76	33.43	9.69	34.37	10.92
CB (nmols/g dws/hr)	16.77	2.06	17.21	2.02	19.07	5.04	18.24	5.19
LAP (nmols/g dws/hr)	4.92	1.47	3.94	0.68	2.91	1.25	1.69	0.62
NAG (nmols/g dws/hr)	50.24	12.39	41.12	5.30	55.00	13.90	59.30	16.10
PHOS (nmols/g dws/hr)	74.58	18.50	58.16	9.01	79.27	7.67	70.07	13.85
XYL (nmols/g dws/hr)	11.63	1.97	8.62	1.02	13.77	4.00	10.21	2.29

	16-25							
	anoxic 15C	SE	anoxic 1C	SE	oxic 15C	SE	oxic 1C	SE
TOC pore (ug-C/g dry)	45.32	9.25	53.11	11.37	58.60	19.07	72.21	18.42
TN pre (ug-C/g dry)	3.64	1.03	2.79	0.83	4.85	1.31	4.82	1.21
TOC/TN pore	15.10	2.31	23.97	6.42	12.26	1.62	14.91	0.47
LECO (mg C/g dws)	72.87	7.50	76.15	5.49	72.30	10.97	68.74	16.85
LECO (mg N/g dws)	4.27	0.35	4.52	0.31	4.38	0.69	3.87	0.94
LECO C/N	16.99	0.46	16.85	0.17	17.04	1.25	18.21	1.64
pH	7.41	0.23	7.18	0.16	7.08	0.41	6.95	0.38
Minimum redox	282.48	20.48	300.08	10.76	302.13	28.84	273.32	30.44
dws/wws	0.56	0.03	0.58	0.03	0.60	0.03	0.61	0.03

Table 5.3. Average and standard error for GHG production from permafrost samples

	0-10							
	anoxic 15C	SE	anoxic 1C	SE	oxic 15C	SE	oxic 1C	SE
CO2 (ug C/g dws)	525.45	89.30	185.71	25.61	1054.12	233.78	382.64	81.76
CO2 (ug C/g C)	5869.86	2140.32	1756.64	535.71	9289.76	1715.78	3211.32	583.28
CH4 (ug C/g dws)	17.62	10.45	0.77	0.54	0.73	0.22	0.78	0.41
CH4 (ug C/g C)	201.56	104.06	5.24	3.84	6.16	1.36	5.60	2.59
	16-25							
	anoxic 15C	SE	anoxic 1C	SE	oxic 15C	SE	oxic 1C	SE
CO2 (ug C/g dws)	492.73	216.58	323.18	110.39	995.57	159.39	243.79	29.38
CO2 (ug C/g C)	6012.69	2521.59	3761.30	1247.83	12167.60	2180.81	3215.60	793.63
CH4 (ug C/g dws)	1.85	1.07	0.71	0.43	0.41	0.10	0.22	0.05
CH4 (ug C/g C)	22.26	12.91	8.34	5.02	5.26	1.89	2.54	0.46

Table 5.4. Soil redox values at the end of the 90-day incubation under oxic and anoxic conditions at 1 and 15 °C in permafrost soils sample 0-10 cm and 16-25 cm below the maximum active layer thaw depth. Due to large differences within samples subjected to the same treatments, raw data (redox 1-5) and summary data (min=minimum, max=maximum, ave=average, std dev= standard deviation) were included. Redox values were generally measured at 3 locations in the core, but up to 5 depending on stability of results.

plot #	depth, cm	trt	inc. temp., C	redox 1	redox 2	redox 3	redox 4	redox 5	notes	min. redox	max redox	ave. redox	std. dev.
1	0-10	anoxic	1	334.7	358.3	375.9				334.7	375.9	356.3	20.7
1	0-10	anoxic	15	376.3	344.7	349.5				344.7	376.3	356.8	17.0
1	16-25	anoxic	1	301.1	256.2	250.5				250.5	301.1	269.3	27.7
1	16-25	anoxic	15	269.3	308.4	306.9				269.3	308.4	294.9	22.2
2	0-10	anoxic	1	344	346.3	329.3				329.3	346.3	339.9	9.2
2	0-10	anoxic	15	-13.3	-42	-21.5	-68.9	-56.8	soupier, oily appearance	-68.9	-13.3	-40.5	23.3
2	16-25	anoxic	1	328.4	316.2	316.9	324.1			316.2	328.4	321.4	5.9
2	16-25	anoxic	15	321.2	330.2	331.9				321.2	331.9	327.8	5.8
3	0-10	anoxic	1	352	354.2	359				352	359	355.1	3.6
3	0-10	anoxic	15	374.8	378.1	377				374.8	378.1	376.6	1.7
3	16-25	anoxic	1	326.4	317.2	319.5				317.2	326.4	321.0	4.8
3	16-25	anoxic	15	222.5	221	230.5				221	230.5	224.7	5.1
6	0-10	anoxic	1	367	354.5	354.6				354.5	367	358.7	7.2
6	0-10	anoxic	15	114.2	127.6	132.4				114.2	132.4	124.7	9.4
6	16-25	anoxic	1	313	296.4	295.3				295.3	313	301.6	9.9
6	16-25	anoxic	15	265.4	260.2	227.9				227.9	265.4	251.2	20.3
8	0-10	oxic	1	301.3	296	295.9				295.9	301.3	297.7	3.1
8	0-10	oxic	15	316.3	319.5	313.9				313.9	319.5	316.6	2.8
8	16-25	oxic	1	336	382.8	458.7			unsure of last number	336	458.7	392.5	61.9
8	16-25	oxic	15	350.3	385	396.1			not stable	350.3	396.1	377.1	23.9
9	0-10	oxic	1	317.8	344.8	347.4				317.8	347.4	336.7	16.4
9	0-10	oxic	15	350	376	386.7				350	386.7	370.9	18.9
9	16-25	oxic	1						not collected	.	.	.	.
9	16-25	oxic	15	347.8	361.8	358.9				347.8	361.8	356.2	7.4

10	0-10	oxic	1	384	370.6	370				370	384	374.9	7.9
10	0-10	oxic	15	377.3	380.1	381.1				377.3	381.1	379.5	2.0
10	16-25	oxic	1	283.3	288.7	291				283.3	291	287.7	4.0
10	16-25	oxic	15	256	265.5	277.2				256	277.2	266.2	10.6
11	0-10	anoxic	1	306.7	315	298				298	315	306.6	8.5
11	0-10	anoxic	15	303.7	253.7	85.5	-28.8	2.6	rust colored	-28.8	303.7	123.3	148.9
11	16-25	anoxic	1	324.5	322.3	321				321	324.5	322.6	1.8
11	16-25	anoxic	15	322.9	340.7	349.7				322.9	349.7	337.8	13.6
12	0-10	oxic	1	360.7	357	353.3				353.3	360.7	357.0	3.7
12	0-10	oxic	15	380.3	380.2	380.4				380.2	380.4	380.3	0.1
12	16-25	oxic	1	227	206	213				206	227	215.3	10.7
12	16-25	oxic	15	232	227.2	210.6				210.6	232	223.3	11.2
13	0-10	oxic	1	351	357	357				351	357	355.0	3.5
13	0-10	oxic	15	336.7	339.3	351				336.7	351	342.3	7.6
13	16-25	oxic	1	354.8	353.3	361.5				353.3	361.5	356.5	4.4
13	16-25	oxic	15	395.2	402.7	391.4				391.4	402.7	396.4	5.8
14	0-10	oxic	1	311.7	332.3	306.1				306.1	332.3	316.7	13.8
14	0-10	oxic	15	325	334.8	328.2				325	334.8	329.3	5.0
14	16-25	oxic	1	193	188	192				188	193	191.0	2.6
14	16-25	oxic	15	300.1	257.4	256.7				256.7	300.1	271.4	24.9
15	0-10	anoxic	1	300.9	319.2	338.8				300.9	338.8	319.6	19.0
15	0-10	anoxic	15	309.5	309.8	320.8				309.5	320.8	313.4	6.4
15	16-25	anoxic	1	308.8	304.2	300.3			not stable	300.3	308.8	304.4	4.3
15	16-25	anoxic	15	342.4	337.6	332.6				332.6	342.4	337.5	4.9

Figures

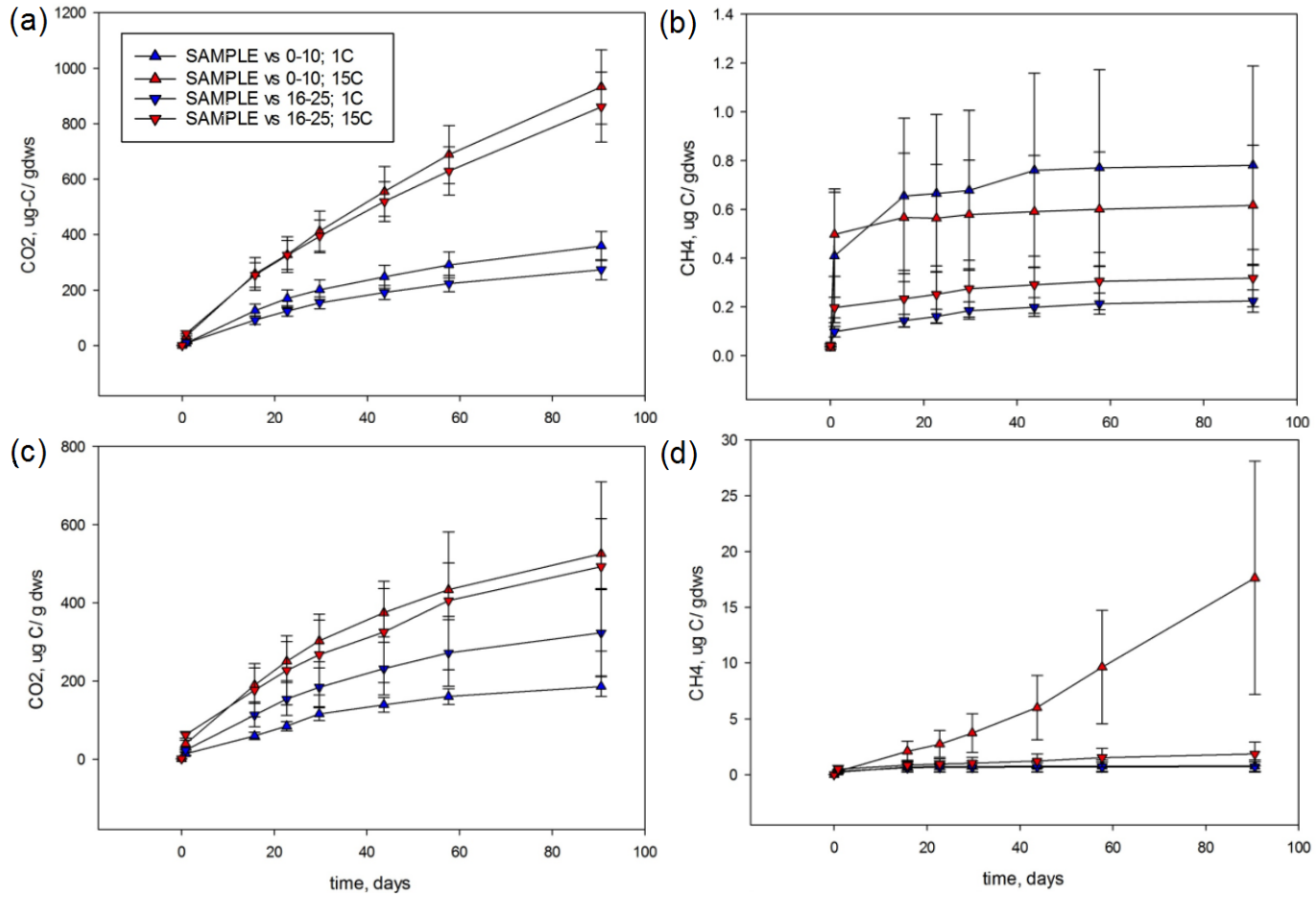

Figure 5.1. Temperature response of cumulative CO_2 (a) and CH_4 (b) production under oxic conditions and anoxic (c, d) conditions for permafrost sampled 0-10 cm and 16-25 cm below the maximum active layer thaw depth.

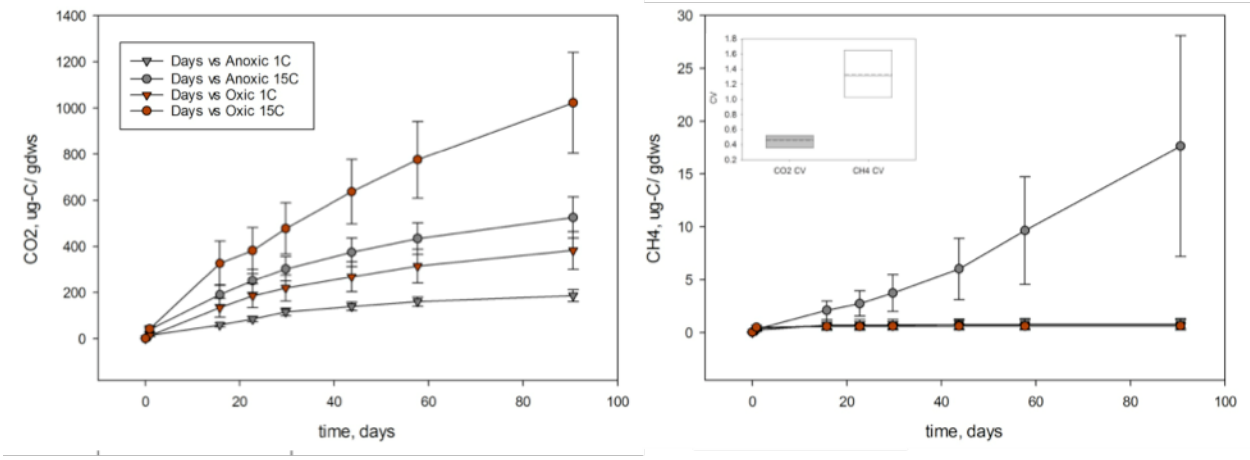

Figure 5.2. Average cumulative CO_2 (left) and CH_4 (right) production under oxic and anoxic conditions for 0-10 cm permafrost. Error bars are one standard error of the mean. The inset depicts a boxplot of the coefficient of variation in the mean gas flux at the final sampling point with CO_2 (grey) and CH_4 (white).

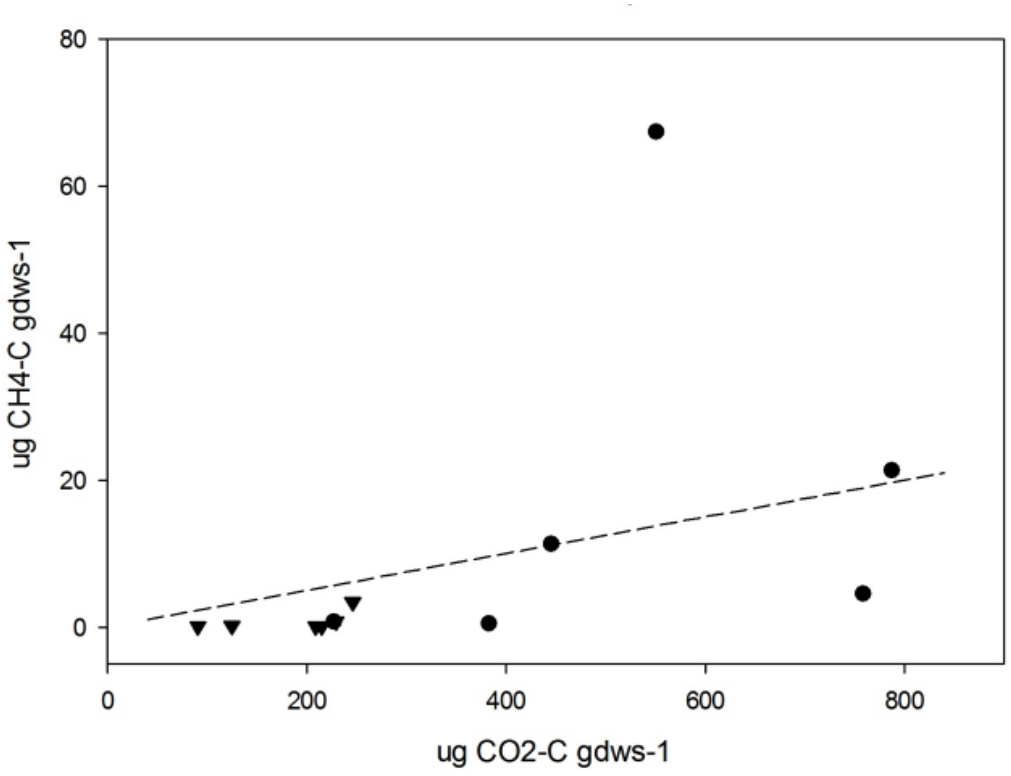

Figure 5.3. Activity of methanogens to CO_2 producers under anoxic conditions. Circles represent samples incubated at 15 °C and triangles 1 °C. Iron reduction yields roughly 40 times more energy than hydrogenotrophic methanogenesis, and the dotted line demarks the 40 CO_2: 1 CH_4 line. Points that fall on the line show equal activity (when normalized for energy gained) of methanogens and CO_2 producers. Samples above the line indicate high CH_4 production, and samples below the line have low CH_4 production.

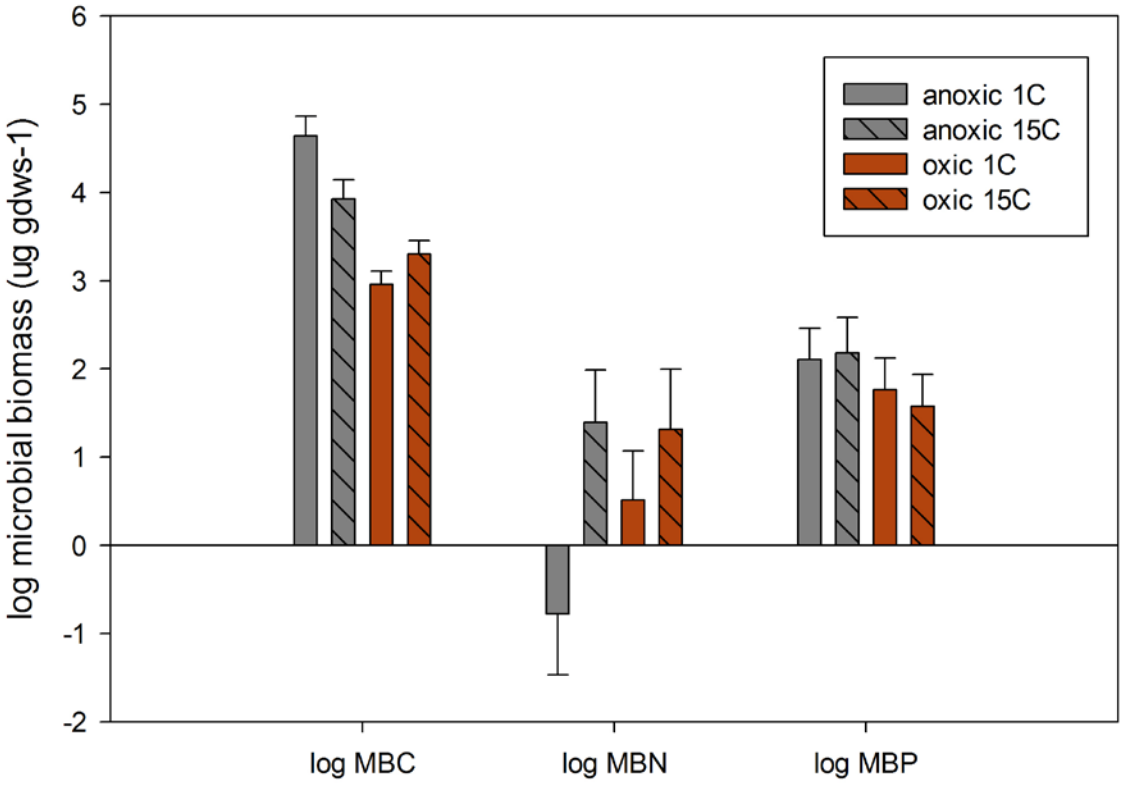

Figure 5.4. Mean of log microbial biomass (C, N, and P) under the different incubation conditions. Error bars are one standard error of the mean.

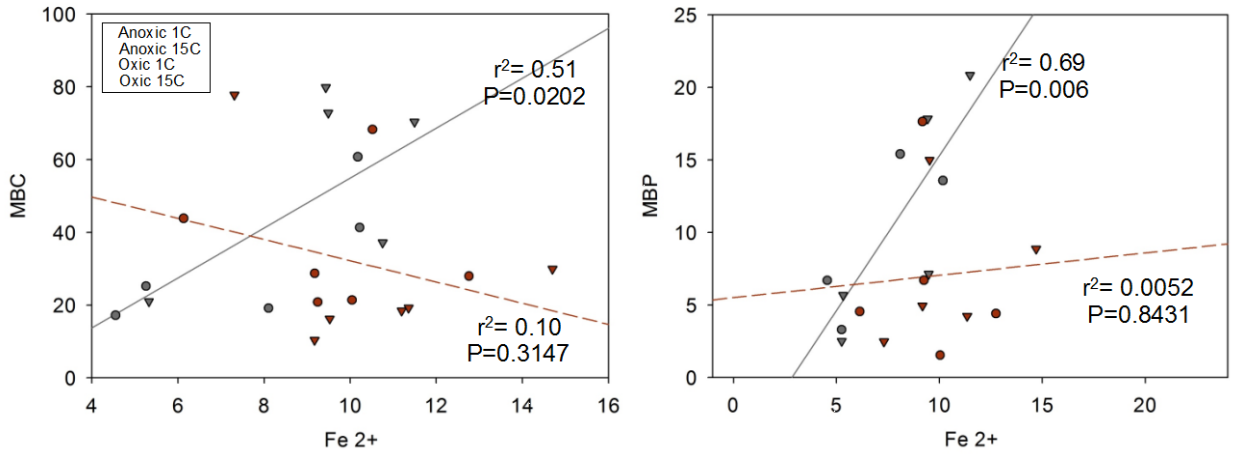

Figure 5.5. The relationship for microbial biomass C (left) and P (right) and ferrous iron. Grey indicates samples that were incubated under anoxic conditions, and rust indicates samples that were incubated under oxic conditions. Circles are samples incubated at 15 °C and triangles are samples incubated at 1 °C.

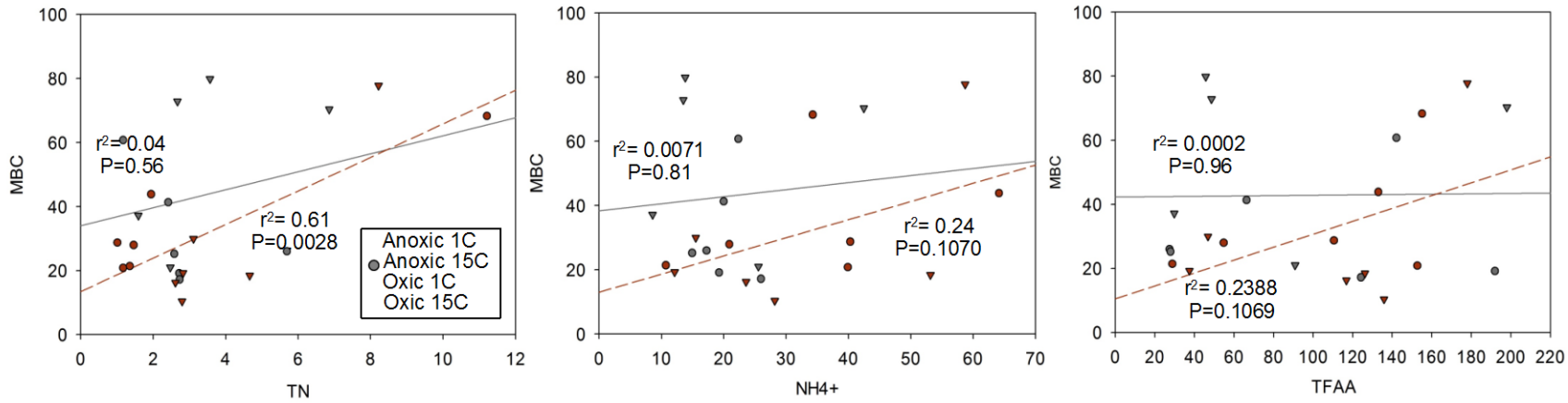

Figure 5.6. The relationship between microbial biomass C and pore water dissolved N (left), ammonium (center), and total free amino acids (right). Grey indicates samples that were incubated under anoxic conditions, and rust indicates samples that were incubated under oxic conditions. Circles are samples incubated at 15 °C and triangles are samples incubated at 1 °C.

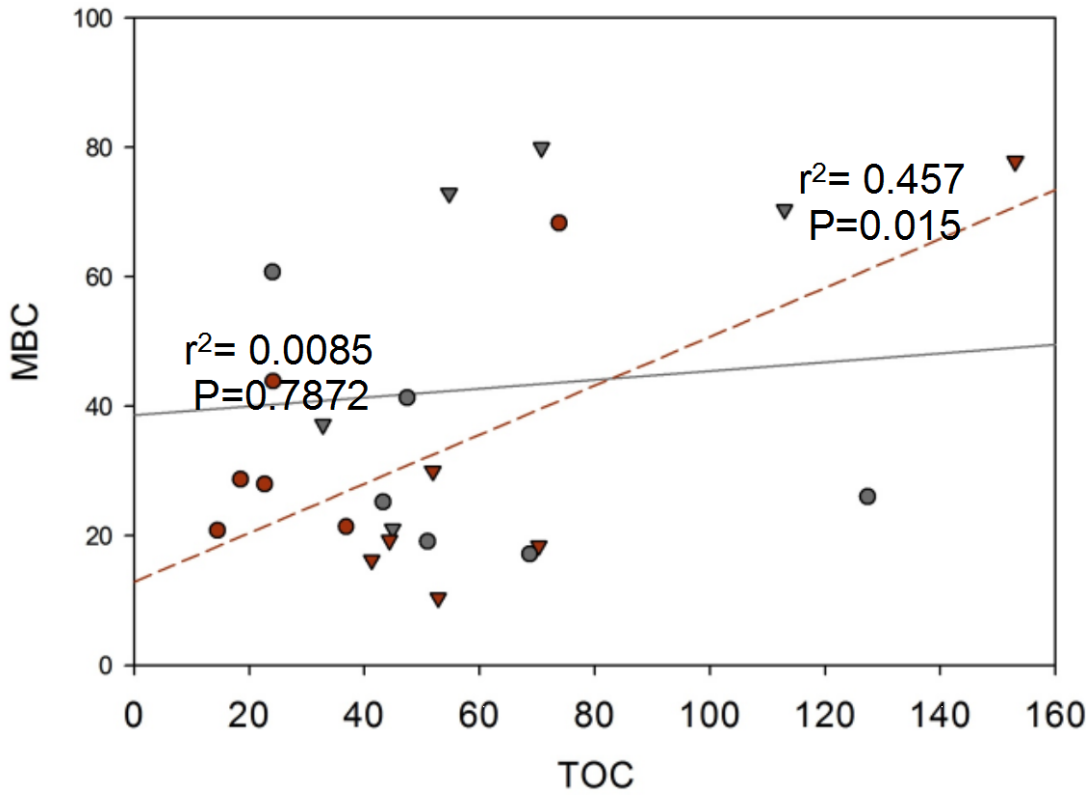

Figure 5.7. The relationship between microbial biomass C and pore water dissolved C. Grey indicates samples that were incubated under anoxic conditions, and rust indicates samples that were incubated under oxic conditions. Circles are samples incubated at 15 °C and triangles are samples incubated at 1 °C.

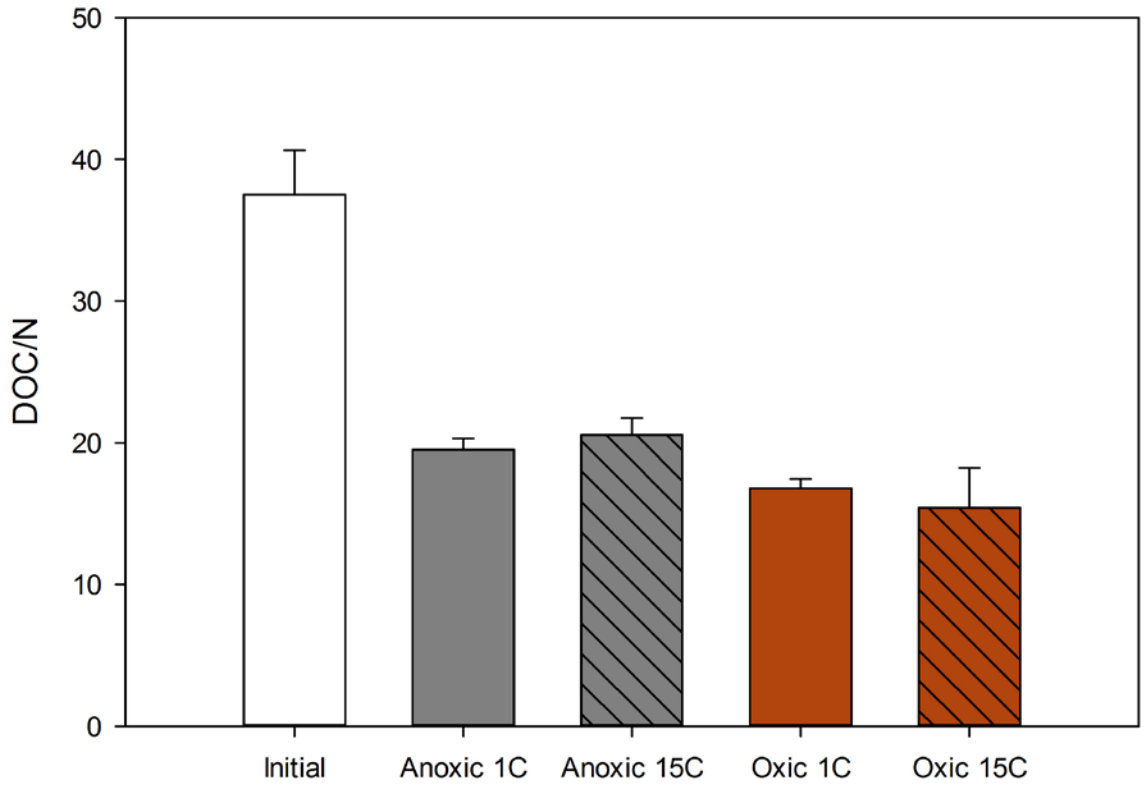

Figure 5.8. Pore water dissolved organic C to N ratio before the incubation and after 90.5 days of incubation under anoxic and oxic conditions at 1 °C and 15 °C. Error bars are one standard error of the mean.

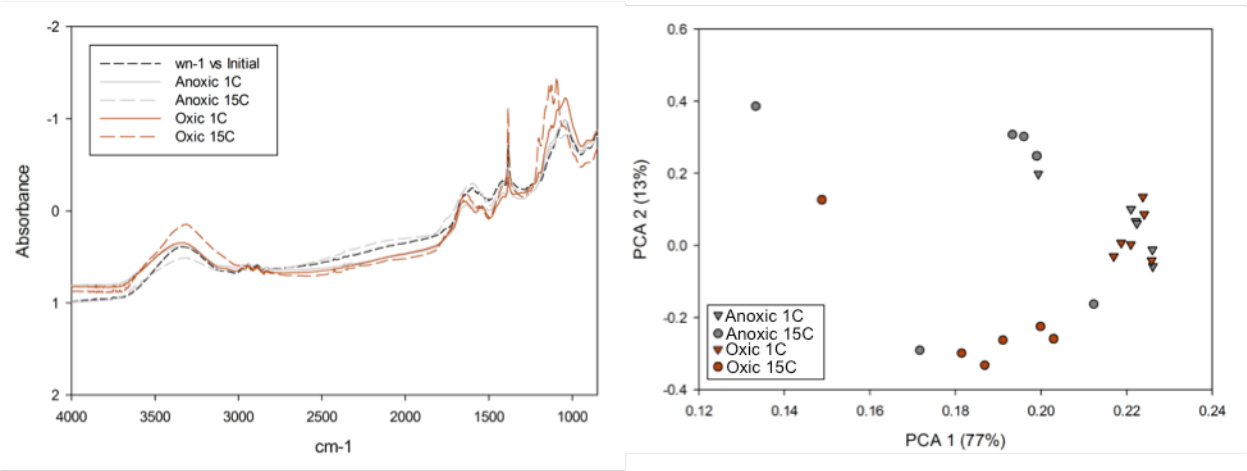

Figure 5.9. (a) Average spectra of dissolved organic matter fraction of the soils incubated under different conditions. (b) PCA of selected peak heights.

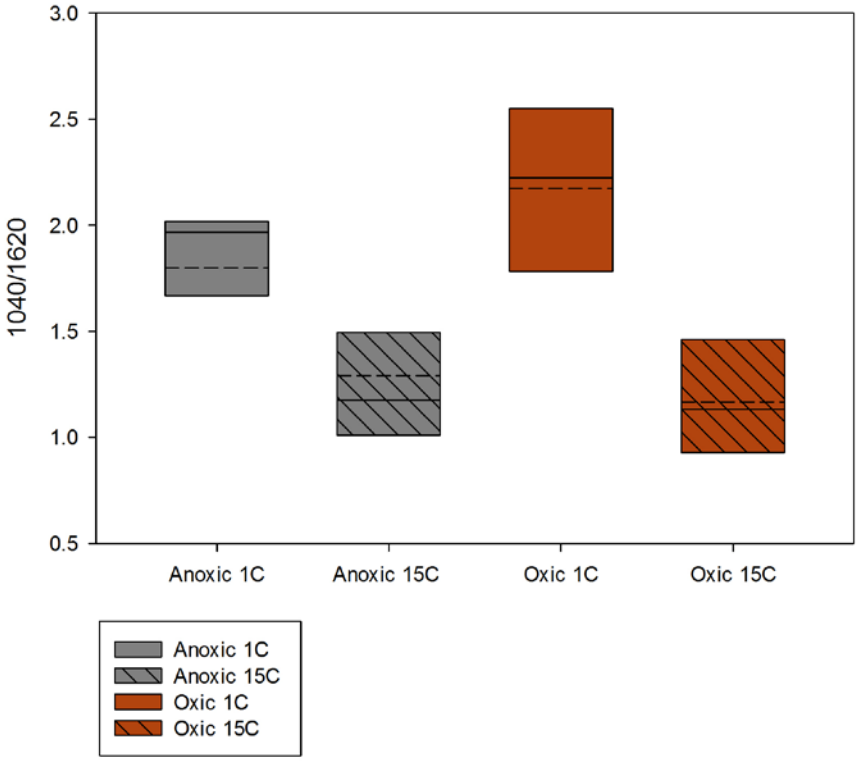

Figure 5.10. Boxplots of the MidIR ratios of 1040/1620 calculated using peak heights. The solid line is the median of the ratio, the dashed line is the mean, and the top and bottom of the boxes represent the first and third quartiles.

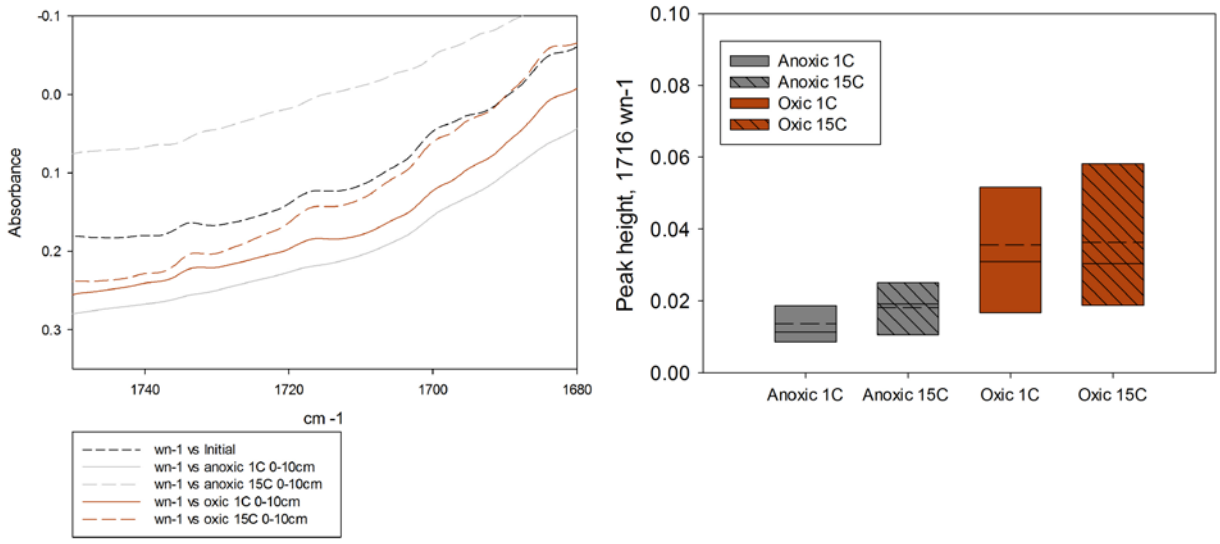

Figure 5.11. (a) Average spectra at 1720 cm^{-1}. (b) Boxplots of the peak heights at 1720 cm^{-1}.

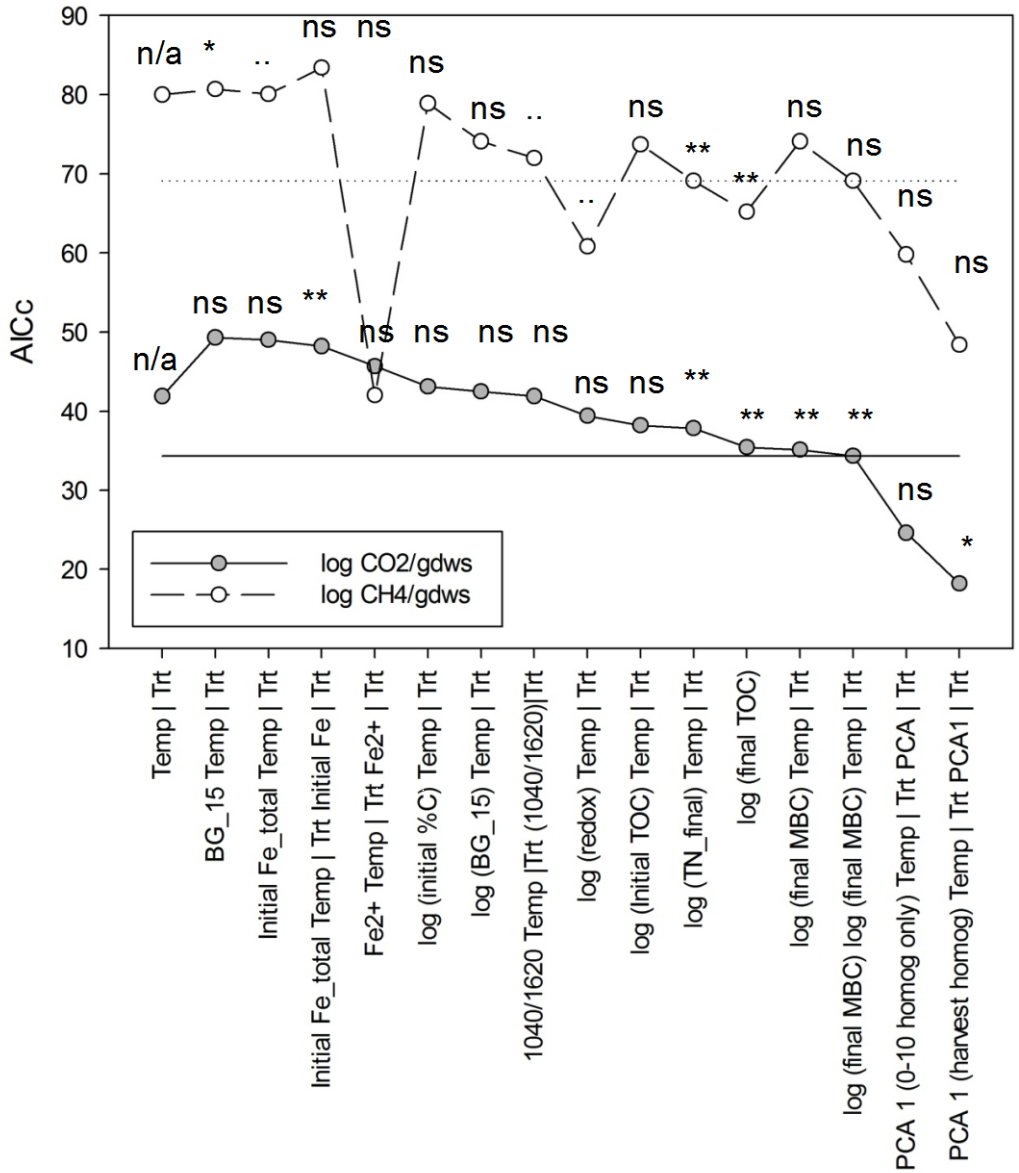

Figure 5.12. Model fits for CO_2 production (per g dws) (solid line) and CH_4 production (per g dws) (dashed line). Reference lines are to show AICc for the model with microbial biomass, %C, temperature, treatment (oxic/anoxic) and the interaction between temperature and treatment. AICc values above the reference line for each gas are a worse model fit, and values below the line are a better model fit. p-values are to indicate the significance of the additional covariate or the interaction between the covariate and "trt". ".." indicates a p-value just above 0.10, "*" indicates the p-value is significant at a 0.10 level, and "**" indicates significance at $p<0.05$.

References

Allison, S.D., Wallenstein, M.D., Bradford, M.A., 2010. Soil-carbon response to warming dependent on microbial physiology. Nature Geosci 3, 336–340. doi:10.1038/ngeo846

Anisimov, O.A., 2007. Potential feedback of thawing permafrost to the global climate system through methane emission. Environ. Res. Lett. 2, 045016. doi:10.1088/1748-9326/2/4/045016

Artz, R.R.E., Chapman, S.J., Campbell, C.D., 2006. Substrate utilisation profiles of microbial communities in peat are depth dependent and correlate with whole soil FTIR profiles. Soil Biology and Biochemistry 38, 2958–2962. doi:10.1016/j.soilbio.2006.04.017

Bell, C.W., Fricks, B.E., Rocca, J.D., Steinweg, J.M., McMahon, S.K., D, W.M., 2013. High-throughput fluorometric measurement of potential soil extracellular enzyme activities. J. Vis. Exp e50961. doi:10.3791/50961

Bethke, C.M., Sanford, R.A., Kirk, M.F., Jin, Q., Flynn, T.M., 2011. The thermodynamic ladder in geomicrobiology. American Journal of Science 311, 183–210. doi:10.2475/03.2011.01

Borden, P.W., Ping, C.-L., McCarthy, P.J., Naidu, S., 2010. Clay mineralogy in Arctic tundra Gelisols, Northern Alaska. Soil Science Society of America Journal 74, 580. doi:10.2136/sssaj2009.0187

Bowles, F.P., Aber, J.D., 1994. Responses of trace gas fluxes and N availability to experimentally elevated soil temperatures. Ecol Appl 4, 617–625.

Buckeridge, K.M., Grogan, P., 2008. Deepened snow alters soil microbial nutrient limitations in arctic birch hummock tundra. Applied Soil Ecology 39, 210–222. doi:10.1016/j.apsoil.2007.12.010

Calderón, F.J., McCarty, G.W., Reeves, J.B., III, 2006. Pyrolisis-MS and FT-IR analysis of fresh and decomposed dairy manure. Journal of Analytical and Applied Pyrolysis 76, 14–23. doi:10.1016/j.jaap.2005.06.009

Cavanaugh, J.E., 1997. Unifying the derivations for the Akaike and corrected Akaike information criteria. Statistics & Probability Letters 33, 201–208.

Christensen, T.R., Panikov, N., Mastepanov, M., Joabsson, A., Stewart, A., Oquist, M., Sommerkorn, M., Reynaud, S., Svensson, B., 2003. Biotic controls on CO2 and CH4 exchange in wetlands–a closed environment study. Biogeochemistry 64, 337–354.

Cleveland, C.C., Liptzin, D., 2007. C:N:P stoichiometry in soil: is there a “Redfield ratio” for the microbial biomass? Biogeochemistry 85, 235–252. doi:10.1007/s10533-007-9132-0

Conant, R.T., Drijber, R.A., Haddix, M.L., Parton, W.J., Paul, E.A., Plante, A.F., Six, J., Steinweg, J.M., 2008. Sensitivity of organic matter decomposition to warming varies with its quality. Glob Change Biol 14, 868–877. doi:10.1111/j.1365-2486.2008.01541.x

Darrouzet-Nardi, A., Weintraub, M.N., 2014. Evidence for spatially inaccessible labile N from a comparison of soil core extractions and soil pore water lysimetry. Soil Biology and Biochemistry 73, 22–32. doi:10.1016/j.soilbio.2014.02.010

Drake, H.L., Horn, M.A., Wüst, P.K., 2009. Intermediary ecosystem metabolism as a main driver of methanogenesis in acidic wetland soil. Environmental Microbiology Reports 1, 307–318. doi:10.1111/j.1758-2229.2009.00050.x

Dunfield, P., Dumont, R., Moore, T.R., 1993. Methane production and consumption in temperate and subarctic peat soils: response to temperature and pH. Soil Biology and Biochemistry 25, 321–326.
Dutta, K., Schuur, E.A.G., Neff, J.C., Zimov, S.A., 2006. Potential carbon release from permafrost soils of Northeastern Siberia. Glob Change Biol 12, 2336–2351. doi:10.1111/j.1365-2486.2006.01259.x
Edwards, K.A., McCulloch, J., Kershaw, P.G., Jefferies, R.L., 2006. Soil microbial and nutrient dynamics in a wet Arctic sedge meadow in late winter and early spring. Soil Biology and Biochemistry 38, 2843–2851. doi:10.1016/j.soilbio.2006.04.042
Ernakovich, J.G., 2014. The chemical properties of Alaskan permafrost and seasonally thawed soils, in: Wallenstein, M.D., Reardon, K.F. (Eds.), Vulnerability of Permafrost Carbon to Decomposition. Colorado State University.
Fierer, N., Schimel, J.P., 2003. A proposed mechanism for the pulse in carbon dioxide production commonly observed following the rapid rewetting of a dry soil. Soil Science Society of America Journal 67, 798–805.
Frank-Fahle, B.A., Yergeau, E., Greer, C.W., Lantuit, H., Wagner, D., 2014. Microbial functional potential and community composition in permafrost-affected soils of the NW Canadian Arctic. PLoS ONE 9, e84761. doi:10.1371/journal.pone.0084761.t003
Freeman, C., Ostle, N., Kang, H., 2001. An enzymic “latch” on a global carbon store. Nature 409, 149. doi:10.1038/35051650
Ganzert, L., Jurgens, G., MÃ¼nster, U., Wagner, D., 2006. Methanogenic communities in permafrost-affected soils of the Laptev Sea coast, Siberian Arctic, characterized by 16S rRNA gene fingerprints. FEMS Microbiol Ecol 59, 476–488. doi:10.1111/j.1574-6941.2006.00205.x
Haberhauer, G., Gerzabek, M.H., 1999. Drift and transmission FT-IR spectroscopy of forest soils: an approach to determine decomposition processes of forest litter. Vibrational Spectroscopy 19, 413–417.
Haberhauer, G., Rafferty, B., Strebl, F., Gerzabek, M.H., 1998. Comparison of the composition of forest soil litter derived from three different sites at various decompositional stages using FTIR spectroscopy. Geoderma 83, 331–342.
Harden, J.W., Koven, C.D., Ping, C.-L., Hugelius, G., David McGuire, A., Camill, P., Jorgenson, T., Kuhry, P., Michaelson, G.J., O'Donnell, J.A., 2012. Field information links permafrost carbon to physical vulnerabilities of thawing. Geophys. Res. Lett. 39. doi:10.1029/2012GL051958
Hodgkins, S.B., Tfaily, M.M., McCalley, C.K., Logan, T.A., Crill, P.M., Saleska, S.R., Rich, V.I., Chanton, J.P., 2014. Changes in peat chemistry associated with permafrost thaw increase greenhouse gas production. Proc. Natl. Acad. Sci. U.S.A. doi:10.1073/pnas.1314641111
Hugelius, G., Tarnocai, C., Broll, G., Canadell, J.G., Kuhry, P., Swanson, D.K., 2013. The Northern Circumpolar Soil Carbon Database: spatially distributed datasets of soil coverage and soil carbon storage in the northern permafrost regions. Earth System Science Data 5, 3–13. doi:10.5879/ecds/00000001
Hurvich, C.M., Tsai, C.-L., 1989. Regression and time series model selection in small samples. Biometrika 76, 297–307.

Høj, L., Olsen, R.A., Torsvik, V.L., 2005. Archaeal communities in High Arctic wetlands at Spitsbergen, Norway (78Â°N) as characterized by 16S rRNA gene fingerprinting. FEMS Microbiol Ecol 53, 89–101. doi:10.1016/j.femsec.2005.01.004

Høj, L., Rusten, M., Haugen, L.E., Olsen, R.A., Torsvik, V.L., 2006. Effects of water regime on archaeal community composition in Arctic soils. Environmental Microbiology 8, 984–996. doi:10.1111/j.1462-2920.2005.00982.x

Jenkinson, D.S., Rayner, J.H., 1977. The turnover of soil organic matter in some of the Rothamsted classical experiments. Soil Science 123, 298–305.

Kawahigashi, M., Kaiser, K., Rodionov, A., Guggenberger, G., 2006. Sorption of dissolved organic matter by mineral soils of the Siberian forest tundra. Glob Change Biol 12, 1868–1877. doi:10.1111/j.1365-2486.2006.01203.x

Kirschbaum, M.U., 1995. The temperature dependence of soil organic matter decomposition, and the effect of global warming on soil organic C storage. Soil Biology and Biochemistry 27, 753–760.

Knoblauch, C., Beer, C., Sosnin, A., Wagner, D., Pfeiffer, E.-M., 2013. Predicting long-term carbon mineralization and trace gas production from thawing permafrost of Northeast Siberia. Glob Change Biol 19, 1160–1172. doi:10.1111/gcb.12116

Koven, C.D., Ringeval, B., Friedlingstein, P., Ciais, P., Cadule, P., Khvorostyanov, D., Krinner, G., Tarnocai, C., 2011. Permafrost carbon-climate feedbacks accelerate global warming. Proc. Natl. Acad. Sci. U.S.A. 108, 14769–14774. doi:10.1073/pnas.1103910108

Lawrence, C.R., Neff, J.C., Schimel, J.P., 2009. Does adding microbial mechanisms of decomposition improve soil organic matter models? A comparison of four models using data from a pulsed rewetting experiment. Soil Biology and Biochemistry 41, 1923–1934. doi:10.1016/j.soilbio.2009.06.016

Lawrence, D.M., Slater, A.G., Romanovsky, V.E., Nicolsky, D.J., 2008. Sensitivity of a model projection of near-surface permafrost degradation to soil column depth and representation of soil organic matter. J. Geophys. Res. 113, F02011. doi:10.1029/2007JF000883

Lee, H., Schuur, E.A.G., Inglett, K.S., Lavoie, M., Chanton, J.P., 2012. The rate of permafrost carbon release under aerobic and anaerobic conditions and its potential effects on climate. Glob Change Biol 18, 515–527. doi:10.1111/j.1365-2486.2011.02519.x

Lipson, D.A., Zona, D., Raab, T.K., Bozzolo, F., Mauritz, M., Oechel, W.C., 2012. Water-table height and microtopography control biogeochemical cycling in an Arctic coastal tundra ecosystem. Biogeosciences 9, 577–591. doi:10.5194/bg-9-577-2012

Liptzin, D., Silver, W.L., 2009. Effects of carbon additions on iron reduction and phosphorus availability in a humid tropical forest soil. Soil Biology and Biochemistry 41, 1696–1702. doi:10.1016/j.soilbio.2009.05.013

Lupascu, M., Wadham, J.L., Hornibrook, E.R.C., Pancost, R.D., 2012. Temperature sensitivity of methane production in the permafrost active layer at Stordalen, Sweden: a comparison with non-permafrost northern wetlands. Arctic, Antarctic, and Alpine Research 44, 469–482. doi:10.1657/1938-4246-44.4.469

Mackelprang, R., Waldrop, M.P., DeAngelis, K.M., David, M.M., Chavarria, K.L., Blazewicz, S.J., Rubin, E.M., Jansson, J.K., 2011. Metagenomic analysis of a permafrost microbial community reveals a rapid response to thaw. Nature 480, 368–371. doi:10.1038/nature10576

Mikan, C.J., Schimel, J.P., Doyle, A.P., 2002. Temperature controls of microbial respiration in arctic tundra soils above and below freezing. Soil Biology and Biochemistry 34, 1785–1795.

Mondav, R., Ben J Woodcroft, Kim, E.-H., McCalley, C.K., Hodgkins, S.B., Crill, P.M., Chanton, J., Hurst, G.B., VerBerkmoes, N.C., Saleska, S.R., Hugenholtz, P., Rich, V.I., Tyson, G.W., 2014. Discovery of a novel methanogen prevalent in thawing permafrost. Nature Communications 5, 1–7. doi:10.1038/ncomms4212

Moorhead, D.L., Sinsabaugh, R.L., 2006. A theoretical model of litter decay and microbial interaction. Ecological Monographs 76, 151–174.

Morris, B.E.L., Herbst, F.-A., Bastida, F., Seifert, J., Bergen, von, M., Richnow, H.-H., Suflita, J.M., 2012. Microbial interactions during residual oil and n-fatty acid metabolism by a methanogenic consortium. Environmental Microbiology Reports 4, 297–306. doi:10.1111/j.1758-2229.2012.00333.x

Movasaghi, Z., Rehman, S., Rehman, I.U., 2008. Fourier Transform Infrared (FTIR) Spectroscopy of Biological Tissues. Applied Spectroscopy Reviews 43, 134–179. doi:10.1080/05704920701829043

Murrell, J.C., Jetten, M.S.M., 2009. The microbial methane cycle. Environmental Microbiology Reports 1, 279–284. doi:10.1111/j.1758-2229.2009.00089.x

Parton, W.J., Schimel, D.S., Cole, C.V., Ojima, D.S., 1987. Analysis of factors controlling soil organic matter levels in Great Plains grasslands. Soil Science Society of America Journal 51, 1173–1179.

Rivkina, E., Shcherbakova, V., Laurinavichius, K., Petrovskaya, L., Krivushin, K., Kraev, G., Pecheritsina, S., Gilichinsky, D., 2007. Biogeochemistry of methane and methanogenic archaea in permafrost. FEMS Microbiol Ecol 61, 1–15. doi:10.1111/j.1574-6941.2007.00315.x

Roden, E.E., Jin, Q., 2011. Thermodynamics of microbial growth coupled to metabolism of glucose, ethanol, short-chain organic acids, and hydrogen. Applied and Environmental Microbiology 77, 1907–1909. doi:10.1128/AEM.02425-10

Santrucková, H., Bird, M.I., Kalaschnikov, Y.N., Grund, M., Elhottova, D., Šimek, M., Grigoryev, S., Gleixner, G., Arneth, A., Schulze, E.-D., Lloyd, J., 2003. Microbial characteristics of soils on a latitudinal transect in Siberia. Glob Change Biol 9, 1106–1117.

Schaefer, K., Zhang, T., Bruhwiler, L., Barrett, A.P., 2011. Amount and timing of permafrost carbon release in response to climate warming. Tellus B 63, 165–180. doi:10.1111/j.1600-0889.2011.00527.x

Schädel, C., Schuur, E.A.G., Bracho, R., Elberling, B., Knoblauch, C., Lee, H., Luo, Y., Shaver, G.R., Turetsky, M.R., 2014. Circumpolar assessment of permafrost C quality and its vulnerability over time using long-term incubation data. Glob Change Biol 20, 641–652. doi:10.1111/gcb.12417

Schimel, J.P., Weintraub, M.N., 2003. The implications of exoenzyme activity on microbial carbon and nitrogen limitation in soil: a theoretical model. Soil Biology and Biochemistry 35, 549–563. doi:10.1016/S0038-0717(03)00015-4

Schmidt, M.W.I., Torn, M.S., Abiven, S., Dittmar, T., Guggenberger, G., Janssens, I.A., Kleber, M., Kögel-Knabner, I., Lehmann, J., Manning, D.A.C., Nannipieri, P., Rasse, D.P., Weiner, S., Trumbore, S.E., 2011. Persistence of soil organic matter as an ecosystem property. Nature 478, 49–56. doi:10.1038/nature10386

Sistla, S.A., Asao, S., Schimel, J.P., 2012. Detecting microbial N-limitation in tussock tundra soil: Implications for Arctic soil organic carbon cycling. Soil Biology and Biochemistry 55, 78–84. doi:10.1016/j.soilbio.2012.06.010

Sistla, S.A., Schimel, J.P., 2012. Stoichiometric flexibility as a regulator of carbon and nutrient cycling in terrestrial ecosystems under change. New Phytol 196, 68–78. doi:10.1111/j.1469-8137.2012.04234.x

Tarnocai, C., 1993. Sampling frozen soils, in: Carter, M.R. (Ed.), Soil Sampling and Methods of Analysis. Lewis Publishers, Boca Raton, pp. 755–765.

Tarnocai, C., Canadell, J.G., Schuur, E.A.G., Kuhry, P., Mazhitova, G., Zimov, S., 2009. Soil organic carbon pools in the northern circumpolar permafrost region. Global Biogeochem. Cycles 23, GB2023. doi:10.1029/2008GB003327

Treat, C., Natali, S., Ernakovich, J., Iversen, C., Lupascu, M., McGuire, A.D., Norby, R., Chowdhury, T.R., Richter, A., Santruckova, H., Schadel, C., Schuur, T., Sloan, V., Turetsky, M., Waldrop, M., 2014. Controls on CH4 and CO2 production from permafrost soil carbon under saturated conditions. Glob Change Biol.

Tveit, A., Schwacke, R., Svenning, M.M., Urich, T., 2012. Organic carbon transformations in high-Arctic peat soils: key functions and microorganisms 7, 299–311. doi:10.1038/ismej.2012.99

Uhlířová, E., Santrucková, H., Davidov, S.P., 2007. Quality and potential biodegradability of soil organic matter preserved in permafrost of Siberian tussock tundra. Soil Biology and Biochemistry 39, 1978–1989. doi:10.1016/j.soilbio.2007.02.018

Vaughan, D.G., Comiso, J.C., Allison, I., Carrasco, J., Kaser, G., Kwok, R., Mote, P., Murray, T., Paul, F., Ren, J., Rignot, E., Solomina, O., Steffen, K., Zhang, T., 2013. Observations: Cryosphere (No. 5). Cambridge University Press, Cambridge, United Kingdom and New York, NY, USA.

Wachinger, G., Fiedler, S., Zepp, K., Gattinger, A., Sommer, M., Roth, K., 2000. Variability of soil methane production on the micro-scale: spatial association with hot spots of organic material and Archaeal populations. Soil Biology and Biochemistry 32, 1121–1130.

Waldrop, M.P., Wickland, K.P., White, R.I., Berhe, A.A., Harden, J.W., Romanovsky, V.E., 2010. Molecular investigations into a globally important carbon pool: permafrost-protected carbon in Alaskan soils. Glob Change Biol 16, 2543–2554. doi:10.1111/j.1365-2486.2009.02141.x

Walker, T.W., Syers, J.K., 1976. The fate of phosphorus during pedogenesis. Geoderma 15, 1–19.

Weintraub, M.N., Schimel, J.P., 2003. Interactions between carbon and nitrogen mineralization and soil organic matter chemistry in arctic tundra soils. Ecosystems 6, 129–143. doi:10.1007/s10021-002-0124-6

Wieder, W.R., Bonan, G.B., Allison, S.D., 2013. Global soil carbon projections are improved by modelling microbial processes. Nature Climate Change 3, 909–912. doi:10.1038/nclimate1951

Chapter 6: Conclusion

The primary objective of my dissertation was to evaluate the vulnerability of permafrost C to decomposition from different perspectives: soil organic matter chemistry, taxonomic and functional diversity of the permafrost community, and biogeochemistry. My two earliest studies (chapters 2 and 3) were observational, where I took a natural history approach to describe the chemical properties of permafrost soil and the bacterial diversity of the permafrost. In my two later chapters (chapters 4 and 5), I assayed the response of microbial functional diversity and permafrost biogeochemistry to increased temperatures. I set out to answer these four questions:

(1) What is the chemical make-up of the organic matter in permafrost, and how is it similar or different from the soils in the seasonally thawed active layer?
(2) Do abiotic factors structure the permafrost and the active layer microbial communities similarly?
(3) How will microbial community function respond to a changing temperature regime?
(4) When permafrost thaws, what mechanisms control whether CO_2 or CH_4 is produced?

In chapter 2, investigating the chemistry of the organic matter, MidIR spectroscopy revealed there is more chemically labile C in the organic active layer than the top of the permafrost (0-15 cm below the maximum active layer thaw), which in turn has more labile C than the mineral active layer and deeper permafrost (16-30 cm). The top of the permafrost often was more similar in quantity and type of compound to the organic than the mineral active layer, indicating that compounds have either been preserved in the top of the permafrost or introduced

(e.g. through cryoturbation, diffusion, syngenetic permafrost formation), confirming previous findings in incubation studies showing that permafrost organic matter is more or equally able to be decomposed than active layer organic matter. All the soils showed evidence of processed material, but the compounds are different between the organic active layer and the permafrost and mineral active layer soils.

In chapter 3, investigating the factors shaping the diversity and community structure of permafrost bacterial communities, I found that diversity and structure were different between the permafrost and active layer. Relationships between richness and community structure with depth and soil C suggest that both environmental filtering and historical legacy dictate the current permafrost community. Permafrost is a fundamentally different environment than the active layer, and therefore harbors a microbial community distinct from the active layer.

In chapter 4, investigating the functional diversity of the permafrost microbial community, I found that growth rates of permafrost microbial communities were less than or equal to the organic active layer at every incubation temperature (1, 10, and 20 °C), including the 1 °C incubation temperature. All communities increased their growth rates with temperature, indicating that the highest incubation temperature (20 °C) was below their temperature optima. The organic active layer used more substrates than the permafrost and mineral active layer microbial communities at every incubation temperature, and the number of substrates used increased with temperature for the permafrost and mineral active layer. These results indicate that permafrost microbial communities may not be active immediately following thaw. However, changes in community composition or additional permafrost warming will increase the functional capabilities of permafrost microbes to decompose the C stored in those soils.

In chapter 5, investigating the mechanisms controlling CO_2 and CH_4 production from thawed permafrost, I observed that although of a much smaller magnitude, CH_4 production was more variable than anaerobic CO_2 production. Drake et al (2009) proposed that anaerobic metabolism terminating in methanogenesis should be viewed akin to a cellular network of pathways required to transform plant inputs to CH_4, which they termed "intermediary ecosystem metabolism". Methanogens, as the agents of the terminal step, can be outcompeted for energy by anaerobes higher on the redox ladder or be substrate limited, both of which limit methanogenesis. In my study, I found evidence for both limitations to methanogenesis. I propose that the variability in CH_4 observed can be attributed to the many processes required by a consortium of anaerobic microorganisms to enable methanogenesis, and that this complexity needs to be considered when estimating CH_4 production rates.

Implications for the vulnerability of permafrost C

The amount of C released over the course of the growing-season-length incubation at the field-relevant post-thaw incubation temperature of 1 °C was up to around 1% of the total soil C (anoxic: 0.08-1.06%; oxic: 0.13-0.63%), but was an average of 0.3%. Assuming a 10 cm thaw depth[2], the amount of C released annually could be roughly equal to the size of the United States C sink (Hurtt et al., 2002). CO_2 was the dominant gas under both oxic and anoxic conditions, however once corrected for its global warming potential (25 times over 100 years), CH_4 made up an average of 7% (0.6-25%) of the gaseous losses at 1 °C. Therefore, understanding the

[2] To make this calculation, I assumed that 75% of the total permafrost C stock of 1672 Pg (Tarnocai et al., 2009) was in the top 1 m of the soils and that the permafrost C is distributed evenly in the top meter (on average across the globe). I then assumed the average C loss of 0.3% to calculate the C lost from the top 0-10 cm of permafrost in one growing season.

mechanisms of both CO_2 and CH_4 production will help us to predict GHG flux from this unique and rapidly changing system.

My dissertation work revealed a hierarchical structure to the environmental, chemical, and biological on whether CO_2 or CH_4 are produced when permafrost organic matter is degraded (Fig. 6.1). Firstly, whether soils are saturated or drained dictates whether an oxic or anoxic path is followed (Fig. 6.1 a and b). After the environmental control, organic matter chemistry and the microbial community dictate the rates of GHG production. In the oxic production of CO_2 (Fig. 6.1 a), the microbial community is the more likely limiter of GHG production because the organic matter in the top of the permafrost seems to be chemically labile (chapter 2) and readily decomposable at 15 °C (chapter 5). The permafrost bacterial community, on the other hand, exhibited low functional diversity at 1 °C (chapter 4). In addition, in chapter 3, I identified that the microbial taxonomic diversity was reduced by both a historical and environmental filter, and that the permafrost had a lower bacterial taxonomic diversity than might otherwise be expected from its high C content. I hypothesize that GHG production at field relevant temperatures from thawed permafrost under oxic conditions is limited by the microbial community rather than by the recalcitrance of the organic matter (chapters 2 and 5; Lee et al., 2012; Waldrop et al., 2010). This suggests that the environmental filter imposed on the microbial community selected a community of survivors and not those necessarily capable of growth at low temperatures (Price and Sowers, 2004) or that psychrophiles were not members of the historical species pool. Shi et al (1997) proposed that under the oligotrophic conditions in permafrost, rates of evolution are diminished, which could also explain why the microbial community in permafrost is not well adapted for psychrophilic conditions.

Along the CH_4 production pathway (Fig. 6.1 b), organic matter lability, substrate supply and the activity of anaerobes plays an important role in GHG production (chapter 5), suggesting that anoxic GHG production is controlled by dynamics of a consortium of anaerobes. The lability of the organic matter is correlated to CH_4 production (Fig. 5.12; Hodgkins et al., 2014; Lupascu et al., 2012; Schädel et al., 2014; Treat et al., 2014), but this control is likely indirect through its controls on other anaerobes. Methanogenesis is the terminal step in the anaerobic oxidation of organic matter, and thermodynamics constrain the activity of methanogens when redox conditions favor other anaerobes (Lovley et al., 1994). In chapter 5, I found evidence that the activity of other anaerobes limited CH_4 production (Figs. 5.3 and 5.7). Thus, considering the activity of the entire anaerobic community could aid in our predictions of CH_4 production from permafrost, particularly in areas of fluctuating redox, such as thermokarst slumps and the banks of thaw ponds.

In addition to microbial community and organic matter controls on GHG production, negative feedbacks, such as mineral protection of organic matter and increased plant productivity, could also reduce the impact of permafrost C on the climate. Soil aggregation is limited in permafrost soils due to frozen conditions and cryoturbation, reducing the physical protection of organic matter from decomposition in permafrost soil (Xu et al., 2009). Despite this, matrix stabilization may contribute to the protection of organic matter in permafrost, but little is known in this area. A few fractionation studies have been performed and reveal that 50-80% of the organic matter is protected on clay-sized particles (Dutta et al., 2006; Xu et al., 2009), which is similar to the amount of C protected by mineral interactions in temperate soils (Christensen, 2001). Kawahigashi et al (2006) found that Gellisols were better at sorbing dissolved organic C than Inceptisols, so the site-specific history of the formation of permafrost

will affect the ability of the mineral matrix to protect organic matter, and will therefore play a large role in the vulnerability of permafrost C. By fitting a 3-C-pool model to incubation data, Schädel et al (2013) found that only 16% of the organic matter in shallow permafrost was able to cycle rapidly. They attributed the protection of the remaining C to chemistry (C:N ratio), but it is also possible that it is due to matrix protection since clay-protected organic matter generally has a low C:N ratio (Kleber et al., 2007). Despite the potential for mineral stabilization of organic matter in permafrost, degradation of the unprotected 20-50% of such a large C pool would still release considerable C into the atmosphere. In addition, permafrost has a low clay content relative to temperate soils and the ability of the matrix to protect organic matter is known to saturate (Stewart et al., 2008). Future studies should test the ability of the mineral matrix to protect organic matter at thawed temperatures to determine whether the organic matter is truly mineral protected or whether the seemingly high proportion of protected C in fractionation studies is due to the clustering of organic molecules at low temperatures.

CO_2 fertilization and increased nutrient availability could result in more C sequestration through shifts in aboveground community composition (Elmendorf et al., 2011; Ernakovich et al., 2014) or increased productivity of the extant community (Natali et al., 2011; Schuur et al., 2009). However, whether sites will act as a sink or source for C following permafrost degradation is uncertain and depends on the balance between plant inputs and heterotrophic respiration. For example, Natali et al. (2011) found that increased plant productivity following experimental degradation of permafrost resulted in greater ecosystem C sequestration relative to controls. However, permafrost thaw also resulted in increased microbial respiration during the winter season, which exceeded plant C gains in the summer (Natali et al., 2014). In addition, Schuur et al. (2009) found that this imbalance between microbial respiration and plant

productivity can increase with the time since permafrost degradation, causing sites of permafrost degradation to become large C sources to the atmosphere. Thus, the ability of increased plant productivity to negate C losses due to permafrost thaw is unlikely.

The complexity of the interactions between the "ancient" C stored in permafrost and the modern, living components of permafrost ecosystems has inhibited our deep understanding of these systems. My dissertation work is among the first studies to link biology and chemistry in detail, and as these types of studies increase in number and inform models, our ability to predict the vulnerability of permafrost C to decomposition will advance. However, as if often the nature of detailed and mechanistic work, my study was performed at only one site; future work linking biology and chemistry should be studied in permafrost with different temperature regimes, age, and organic matter content. Multi-disciplinary teams, such as those in the "Permafrost Carbon Research Coordination Network" and "Next Generation Ecosystem Experiment", and meetings, such as the International Permafrost Association's "International Conference on Permafrost (ICOP)" series, have increased the understanding of the system, and continued efforts will shed light on more of the system. These collaborative efforts are at the forefront of integrating experimental parameters into permafrost C and Earth system models, which will enable better forecasting of permafrost degradation and C losses.

Figures

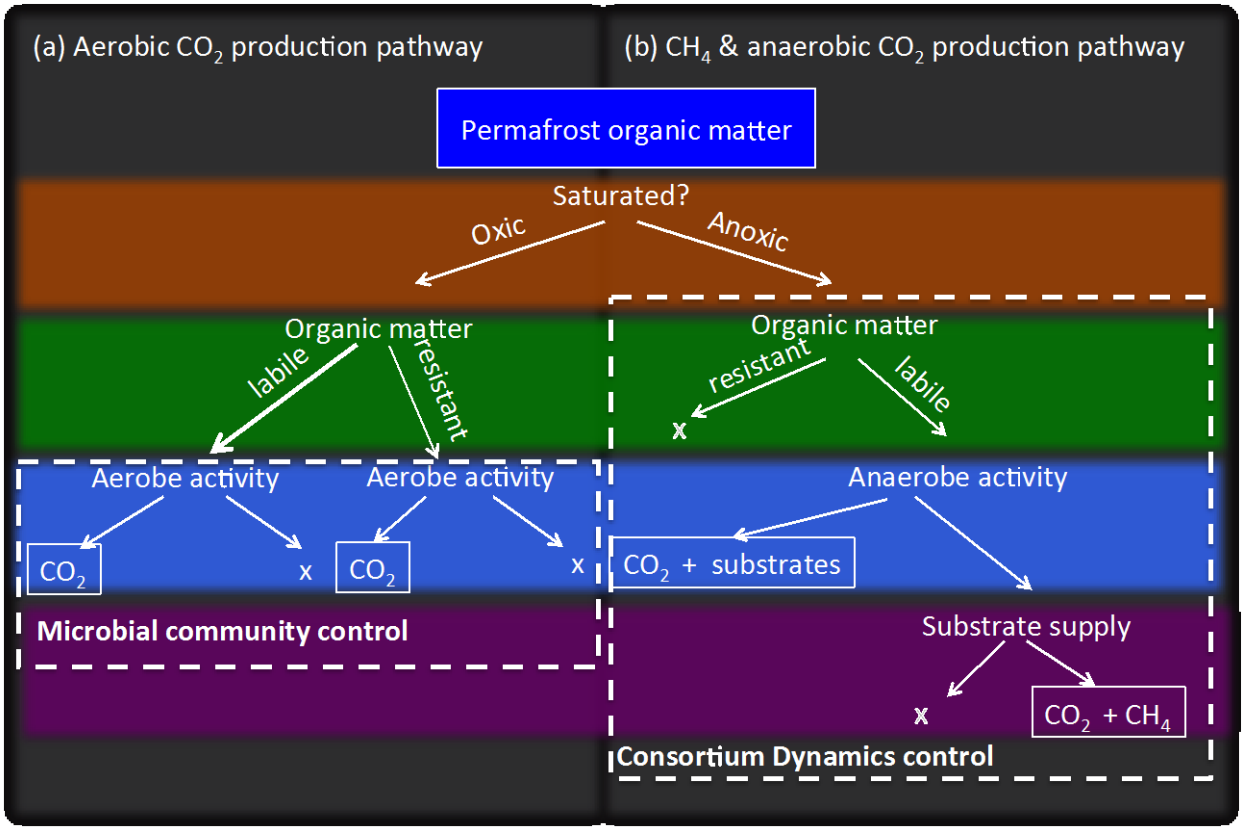

Figure 6.1. Hierarchical factors controlling GHG from thawed permafrost soil.

References

Christensen, B.T., 2001. Physical fractionation of soil and structural and functional complexity in organic matter turnover. European Journal of Soil Science 52, 345–353.

Drake, H.L., Horn, M.A., Wüst, P.K., 2009. Intermediary ecosystem metabolism as a main driver of methanogenesis in acidic wetland soil. Environmental Microbiology Reports 1, 307–318. doi:10.1111/j.1758-2229.2009.00050.x

Dutta, K., Schuur, E.A.G., Neff, J.C., Zimov, S.A., 2006. Potential carbon release from permafrost soils of Northeastern Siberia. Glob Change Biol 12, 2336–2351. doi:10.1111/j.1365-2486.2006.01259.x

Elmendorf, S.C., Henry, G.H.R., Hollister, R.D., Björk, R.G., Bjorkman, A.D., Callaghan, T.V., Collier, L.S., Cooper, E.J., CORNELISSEN, J.H.C., Day, T.A., Fosaa, A.M., Gould, W.A., Grétarsdóttir, J., Harte, J., Hermanutz, L., Hik, D.S., Hofgaard, A., Jarrad, F., Jónsdóttir, I.S., Keuper, F., Klanderud, K., Klein, J.A., Koh, S., Kudo, G., Lang, S.I., Loewen, V., May, J.L., Mercado, J., Michelsen, A., Molau, U., Myers-Smith, I.H., Oberbauer, S.F., Pieper, S., Post, E., Rixen, C., Robinson, C.H., Schmidt, N.M., Shaver, G.R., Stenström, A., Tolvanen, A., Totland, Ø., Troxler, T., Wahren, C.-H., Webber, P.J., Welker, J.M., Wookey, P.A., 2011. Global assessment of experimental climate warming on tundra vegetation: heterogeneity over space and time. Ecology Letters 15, 164–175. doi:10.1111/j.1461-0248.2011.01716.x

Ernakovich, J.G., Hopping, K.A., Berdanier, A.B., Simpson, R.T., Kachergis, E.J., Steltzer, H., Wallenstein, M.D., 2014. Predicted responses of arctic and alpine ecosystems to altered seasonality under climate change. Glob Change Biol n/a–n/a. doi:10.1111/gcb.12568

Hodgkins, S.B., Tfaily, M.M., McCalley, C.K., Logan, T.A., Crill, P.M., Saleska, S.R., Rich, V.I., Chanton, J.P., 2014. Changes in peat chemistry associated with permafrost thaw increase greenhouse gas production. Proc. Natl. Acad. Sci. U.S.A. doi:10.1073/pnas.1314641111

Hurtt, G.C., Pacala, S.W., Moorcroft, P.R., Caspersen, J., Shevliakova, E., Houghton, R.A., Moore, B., 2002. Projecting the future of the U.S. carbon sink. Proceedings of the National Academy of Sciences 99, 1389–1394. doi:10.1073/pnas.012249999

Kawahigashi, M., Kaiser, K., Rodionov, A., Guggenberger, G., 2006. Sorption of dissolved organic matter by mineral soils of the Siberian forest tundra. Glob Change Biol 12, 1868–1877. doi:10.1111/j.1365-2486.2006.01203.x

Kleber, M., Sollins, P., Sutton, R., 2007. A conceptual model of organo-mineral interactions in soils: self-assembly of organic molecular fragments into zonal structures on mineral surfaces. Biogeochemistry 85, 9–24. doi:10.1007/s10533-007-9103-5

Lee, H., Schuur, E.A.G., Inglett, K.S., Lavoie, M., Chanton, J.P., 2012. The rate of permafrost carbon release under aerobic and anaerobic conditions and its potential effects on climate. Glob Change Biol 18, 515–527. doi:10.1111/j.1365-2486.2011.02519.x

Lovley, D.R., Chapelle, F.H., Woodward, J.C., 1994. Use of dissolved h2 concentrations to determine distribution of microbially catalyzed redox reactions in anoxic groundwater. Environ. Sci. Technol. 28, 1205–1210. doi:10.1021/es00056a005

Lupascu, M., Wadham, J.L., Hornibrook, E.R.C., Pancost, R.D., 2012. Temperature sensitivity of methane production in the permafrost active layer at Stordalen, Sweden: a comparison

with non-permafrost northern wetlands. Arctic, Antarctic, and Alpine Research 44, 469–482. doi:10.1657/1938-4246-44.4.469
Natali, S.M., Schuur, E., Webb, E.E., Pries, C.H., 2014. Permafrost degradation stimulates carbon loss from experimentally warmed tundra. Ecology 95, 602–608.
Natali, S.M., Schuur, E.A.G., Rubin, R.L., 2011. Increased plant productivity in Alaskan tundra as a result of experimental warming of soil and permafrost. J Ecology 100, 488–498. doi:10.1111/j.1365-2745.2011.01925.x
Price, P.B., Sowers, T., 2004. Temperature dependence of metabolic rates for microbial growth, maintenance, and survival. Proceedings of the National Academy of Sciences 101, 4631–4636. doi:10.1073/pnas.0400522101
Schädel, C., Schuur, E.A.G., Bracho, R., Elberling, B., Knoblauch, C., Lee, H., Luo, Y., Shaver, G.R., Turetsky, M.R., 2014. Circumpolar assessment of permafrost C quality and its vulnerability over time using long-term incubation data. Glob Change Biol 20, 641–652. doi:10.1111/gcb.12417
Schuur, E.A.G., Vogel, J.G., Crummer, K.G., Lee, H., Sickman, J.O., Osterkamp, T.E., 2009. The effect of permafrost thaw on old carbon release and net carbon exchange from tundra. Nature 459, 556–559. doi:10.1038/nature08031
Shi, T., Reeves, R.H., Gilichinsky, D.A., Friedmann, E.I., 1997. Characterization of viable bacteria from Siberian permafrost by 16S rDNA sequencing. Microb Ecol 33, 169–179.
Stewart, C.E., Paustian, K., Conant, R.T., Plante, A.F., Six, J., 2008. Soil carbon saturation: evaluation and corroboration by long-term incubations. Soil Biology and Biochemistry 40, 1741–1750. doi:10.1016/j.soilbio.20
Tarnocai, C., Canadell, J.G., Schuur, E.A.G., Kuhry, P., Mazhitova, G., Zimov, S., 2009. Soil organic carbon pools in the northern circumpolar permafrost region. Global Biogeochem. Cycles 23, GB2023. doi:10.1029/2008GB003327
Treat, C., Natali, S., Ernakovich, J., Iversen, C., Lupascu, M., McGuire, A.D., Norby, R., Chowdhury, T.R., Richter, A., Santruckova, H., Schadel, C., Schuur, T., Sloan, V., Turetsky, M., Waldrop, M., 2014. Controls on CH4 and CO2 production from permafrost soil carbon under saturated conditions. Glob Change Biol.
Waldrop, M.P., Wickland, K.P., White, R.I., Berhe, A.A., Harden, J.W., Romanovsky, V.E., 2010. Molecular investigations into a globally important carbon pool: permafrost-protected carbon in Alaskan soils. Glob Change Biol 16, 2543–2554. doi:10.1111/j.1365-2486.2009.02141.x
Xu, C., Guo, L., Ping, C.-L., White, D.M., 2009. Chemical and isotopic characterization of size-fractionated organic matter from cryoturbated tundra soils, northern Alaska. J. Geophys. Res. 114, G03002. doi:10.1029/2008JG000846